THE DEVELOPMENT OF GLYCOSAMINOGLYCAN COATINGS FOR MESENCHYMAL STEM CELL-BASED CULTURE APPLICATIONS

A Dissertation
Presented to
The Academic Faculty

By

Jennifer Lei

In Partial Fulfillment
Of the Requirements for the Degree
Doctor of Philosophy in the
Interdisciplinary Bioengineering Program and
George W. Woodruff School of Mechanical Engineering

Georgia Institute of Technology
May 2016

THE DEVELOPMENT OF GLYCOSAMINOGLYCAN COATINGS FOR MESENCHYMAL STEM CELL-BASED CULTURE APPLICATIONS

Approved by:

Dr. Johnna S. Temenoff, Advisor
Department of Biomedical Engineering
Georgia Institute of Technology

Dr. Todd C. McDevitt
Department of Bioengineering and Therapeutic Sciences
Gladstone Institutes of Cardiovascular Disease

Dr. Edward A. Botchwey
Department of Biomedical Engineering
Georgia Institute of Technology

Dr. William L. Murphy
Department of Biomedical Engineering
University of Wisconsin-Madison

Dr. Robert E. Guldberg
School of Mechanical Engineering
Georgia Institute of Technology

Date Approved: January 15, 2016

Dedicated to my loving family:
My Mom, who is supportive and caring,
My Dad, who is the smartest goofball I know,
And to Sam and Tim, who will always be there for me.

TABLE OF CONTENTS

ACKNOWLEDGEMENTS

This work would not have been possible without the guidance and help of my advisor and my committee members. First and foremost, I would like to thank Johnna for accepting me into her lab back when I was a young, naïve, and very confused graduate student. I didn't have a clear grasp on what I wanted to do or know how to do it and Johnna's guidance and mentoring immensely helped shape me into a better scientist and engineer. She has taught me how to perform research with depth and meaning that has large implications for improving current technologies, which gave me a great sense of achievement and pride in what I was doing. Johnna also always opens up her home to us every year for the annual lab party, where I get my fix of good Mediterranean food and Alon's desserts. I will most certainly miss those good times. I would also like to thank Dr. Bill Murphy and his student Nhi Le, whom we collaborated with on the research performed in Aim 3. Nhi provided the peptide sequence used and helped get me started with using it for my experiments. Dr. Murphy provided great insight into the results observed and always had a great outlook on where this work could take us. Every year at SFB, we would meet to go over any updates and it was always refreshing to talk to him and hear all the ideas he had about the exciting research we were performing. I would also like to thank Dr. Todd McDevitt, who accepted me into the NSF IGERT Stem Cell Biomanufacturing training grant when I first joined Tech. Learning from him through courses and meetings taught me a great amount about the stem cell field. Lastly, I would like to thank Dr. Ed Botchwey and Dr. Bob Gulberg. They always encouraged me to take a step back and think about the bigger picture of my research and how it can improve the field of bioengineering. That was always very helpful because I often got too focused on

the details of the work, therefore, it was always a good reminder to think about their perspective and make me think about not only the details but also the bigger picture.

Other faculty members I would like to thank include Dr. Andres Garcia and Dr. Brani Vidakovic. I was able to work with Dr. Garcia when I was on the NIH Cell and Tissue Engineering training grant through journal clubs and monthly meetings. He is an awesome supporter of the BioE graduate students and always pushed us to complete our work in time and perform good science. Dr. Brani is, in my mind, the master of statistics and always has answers for how to perform appropriate analysis on the data we collected. Statistics has been a hot topic of contention in the field and I greatly appreciate having an expert on our side to help peruse through the complicated inner works of analysis.

I would also like to thank members of the BioE, BME and IBB staff that allow for research to even be possible at Georgia Tech. Chris Ruffin was one of the first people I met during my recruitment weekend and it was always my pleasure working with him during my time with BGSAC. He always had a huge smile on his face every time I saw him and was always so helpful in managing our program. Laura Paige has been a great coordinator for the BioE program and her help with everything paperwork-related and program-related has made my life so much easier in these past couple months. I am extremely grateful for her support and encouragement and am so happy she is around to make the BioE program as great as it can be. To the BME staff of DeWayne Robertson and Sally Gerrish, I will cherish all the fun moments we've had during my time at Tech. I would like to thank DeWayne for keeping me hydrated while working and letting us steal his drinking water all the time, but also would like to thank him for making sure the building doesn't burn down. I would like to thank Sally for her support and

encouragement. It has been my pleasure working with her on the Biotech Career Fair Committee over the many years. Lastly, to Andrew Shaw and Aqua Asberry, I would like to thank them for making sure our core facilities are always running smoothly and working properly. Their help and advice about how to use the confocal microscopes or cryostat have helped me immensely through the years.

I would like to also acknowledge all the members of the Temenoff Lab. I have had the unique opportunity to be able to work with almost all the members of the lab. Upon joining, I was able to learn from Derek, Peter, Jeremy, Taymour, Sharon and Yong. They were always willing to take time to answer my questions and help me with how to do everything and anything in lab. We also fostered our little lab family through delicious hot pot or pizza dinners that were not only delicious but always hilarious times because we'd be laughing so hard all the time. As lab members graduated and moved on, Song was a great resource, friend, graduate student that helped me with not only science but life problems in general. She always had great advice to help me through any problem. I cherish the times that we had driving and staying at UGA with our sheep and horse adventures. I would also like to thank Tobias, Melissa, Torri, Liane, Jennifer and Elda. Tobias and his odd and hilarious humor always made us laugh and his extensive knowledge of chemistry and polymer synthesis that proved extremely helpful during troubleshooting times. Melissa helped me troubleshoot all of our MSC culture problems and was also a very good friend. Torri (hai, I know you're reading this) and I were able to work together for the majority of my time in lab. She has helped me with so many problems in lab, been a great listener (during our walks home) and provided great feedback and insight to my research. I am thankful to have her as a labmate and friend

and I know she will do great things in the future because of her drive and passion for science. Liane has provided so much joy and hilarity to our lab. Her silly abbreviations and noobish ways are always entertaining and she also has been very encouraging and supportive these past couple months. I know that the lab will be in good hands with her taking over in the next couple years. I would like to thank Elda for helping me with some of my experiments in the past year since she has joined, she is a fast learner that made my life easier with large experiments and I would also like to thank Jennifer who coordinates so much in our lab these days. Without her, our lab move would not have been possible. I have been very fortunate to work with and learn from such bright and motivated lab mates these past years. I would also like to thank some other Georgia Tech friends, Dr. Patricia Pacheco, Dr. Lauren Priddy, Dr. Ashley Allen, Dr. Alex Caulk, Dr. Jenna Wilson, Amy Clark, Alex Schudel, Nate Rohner, and Marian Hettiaratchi. Without them, I wouldn't have had fun adventures at happy hour, playing Frisbee golf on campus, going to football games, doing monthly brewery run, and all the good times at conferences.

I would also like to thank my friends in Atlanta, who I consider my regional family. To Germ, Tay Tay, Song and Suever, we always found time during our busy days to grab dinner or go to trivia or go on hiking and camping adventures. All those times we spent just hanging out always helped relieve stress and made me laugh. To Stephen (and Pico), Katie, Allison, Alex, Kate, Baby Kev, Megan, Laura, Chris, Allen, Vanessa, and Gus Gus, whether we were just grabbing drinks and watching games, playing soccer/football/softball, going on ski trips or camping or hiking, or just any general shenanigan we were getting into, I always had so much fun and felt so relaxed when we hung out and I thank all of them for their friendship and laughter. Finally, to the FitWit

community that kept me healthy and in shape, I would like to thank them for always being great trainers and people to just work out with. It has been a great stress reliever to be able to run around or do burpees at the end of a busy work day.

I would also like to thank my friends from home that I have been friends with since 2nd grade and my friends from University of Maryland. To Lyd, Liz, Anna, Rachel, Jill, Monica and Aishat, they have been the best friends I could ask for and are always there to listen if I need to talk. I would like to thank them for their support and encouragement through the years.

Lastly, I would like to thank my family. My sister, Sam and her husband, Tim have been extremely supportive through the years. Regardless of the situation, they are always willing to help. Before taking quals, my sister knew that I was very stressed out and sent me a nice gift card for some retail therapy. As silly as that sounds, it was very thoughtful and her support has always meant so much to me. Tim has been a welcome addition to our family and is one of the nicest people I know. He is always offering his help in looking at my resume or trying to network and find contacts for me for future job opportunities. They are both extremely thoughtful and I love that I can call them my family. My mom and dad are probably the coolest people I know and are also supporting and loving. My mom always makes sure I'm doing okay and have such great advice for anything going on in my life. My dad is also an engineer and is the reason why I became interested in this field in the first place. He is the goofiest but smartest person I know, and I admire and thank him for everything he has done for me. This dissertation is dedicated to my family for all their love and support.

LIST OF TABLES

LIST OF FIGURES

LIST OF ABBREVIATIONS

3D	Three dimension
BA	Binding area
BLA	Biologics License Application
BMP-2	Bome morphogenic protein-2
COMP	Cartilage oligomeric matrix protein
CS	Chondroitin sulfate
DMEM	Dulbecco's Modified Eagle's Medium
ECM	Extracellular matrix
EDC	1-ethyl-3-(3-dimethylaminopropyl)carbodiimide hydrochloride
FBS	Fetal bovine serum
FDA	Food and Drug Administration
FGF-2	Fibroblast growth factor-2
FITC	Fluorescein isothiocyanate
GAG	Glycosaminoglycan
GDF	Growth differentiation factor
H&E	Hematoxylin and Eosin
Hep	Biotinylated heparin
Hep-	Biotinylated desulfated heparin
HEPpep	Heparin binding peptide
HGF	Hepatocyte growth factor
HIF-1α	Hypoxia-inducible factor-1α
HoBT	Hydroxybenzotriazole

HSC	Hematopoietic stem cells
HSPG	Heparin sulfate proteoglycans
HUVEC	Human umbilical vein endothelial cells
IDO	Indoleamine 2,3-dioxygenase
IGF	Insulin growth factor
IHC	Immunohistochemical
IL-6	Interleukin-6
INF-γ	Interfueron-γ
LPL	Lipoprotein lipase
MCP-3	Monocyte-specific chemokine-3
MLEC	Mink lung epithelial cell
MSC	Mesenchymal stem cell
NF-κB	Nuclear factor kappa-light-chain-enhancer of activated B cells
NMR	Nuclear magnetic resonance
PAI-1	Plasminogen activator inhibitor-1
PDGF	Platelet derived growth factor
PEG	Poly (ethylene glycol)
PGE2	Prostaglandin E2
PPARγ	Peroxisome proliferator-activated receptors-γ
PVA	Poly (vinyl alcohol)
RT-PCR	Real time-Polymerase chain reaction
SDF-1	Stromal cell-derived factor-1
SLeX	Sialyl-Lewis X

STC-1	Stanniocalcin-1
Sulfo-NHS	N-hydroxysulfosuccinimide
TGF-β1	Transforming growth factor-β1
TNF-α	Tumor neocrosis factor-α
TSG-6	Tumor necrosis factor-inducible gene-6
TZD	thiazolidinediones
VEGF	Vascular endothelial growth factor

SUMMARY

Mesenchymal stem cells are multipotent cells that have the ability to differentiate down multiple lineages as well as secrete trophic and anti-inflammatory factors. These qualities make MSCs a promising cell source for cell-based therapies to treat a variety of injuries and pathologies. Biomaterials are often used to control and direct stem cell behavior by engineering a desired environment around the cells. Recent research has focused on using the naturally derived sulfated glycosaminoglycan (GAG), heparin as a biomaterial due to its negative charge and ability to sequester and bind positively charged growth factors. Engineering a heparin coating that can mimic the native heparan sulfate proteoglycan structure found at cell surfaces can be used as a novel platform to present GAGs to cells to direct cell behavior. The overall goal of this dissertation was to develop GAG-based coatings on MSC spheroids in order to study the role of heparin and its derivatives on MSC culture applications.

To investigate the role of heparin in coating form on MSC behavior, the ability of the coating to sequester positively charged growth factors was characterized. Given the role of sulfation in the negative charge density of heparin and growth factor interactions, a desulfated heparin coating was develop and used to examine how presentation of coatings with native and no sulfation levels could potentiate response to growth factors in the surrounding environment. Additionally, heparin and growth factor binding in coating presentation was explored to develop a novel platform to assemble MSC-based microtissues. Together these studies provided valuable insight into a novel approach to direct cell behavior by engineering a coating that harnesses heparin interactions with the surrounding environment.

CHAPTER 1

INTRODUCTION

1.1 Motivation

Mesenchymal stem cells (MSCs) are multipotent cells commonly obtained from bone marrow and adipose tissue that have the ability to differentiate down bone, cartilage, muscle, marrow, tendon/ligament and connective tissue lineages [1]. Additionally, MSCs have the ability to secrete trophic and anti-inflammatory factors that can promote angiogenesis, modulate extracellular matrix (ECM) remodeling, modulate immune cell activation or suppression and promote cell recruitment [1-4]. These qualities make MSCs a promising cell source for cell-based therapies to treat a wide range of pathologies. Currently, MSCs are being used in 374 clinical trials that aim to treat diseases and injuries that involve bone/cartilage, heart, neural, kidneys, lung, liver tissues and autoimmune pathologies [5, 6]. Although the number of clinical trial has increased 3-fold since 2011, approximately 90% of these trials remain in Phase 1 or 2 and no Food and Drug Administration (FDA)-approved Biologics License Applications (BLAs) for MSC-based products currently exist [5].

To improve current therapies, recent research efforts have employed using MSC formed into aggregates as a platform for MSC-based treatments. The benefits of MSC aggregates have been shown in preclinical studies, in which administration of three-dimensional (3D) MSC aggregates in a porcine model have improved cell retention survival and integration in myocardial transplantation [7]. Additionally, in *in vitro* studies, MSC aggregates have shown to possess enhanced ability to differentiate down

osteogenic and adipogenic lineages as well as secrete trophic and anti-inflammatory factors [8]. Because single cell administration of MSCs often result in low engraftment, MSC aggregates can also be formed into microtissues as a means increase retention of cells upon delivery to a site of injury [9, 10]. Additionally, since the adherent MSCs are formed into 3D aggregates with cell-cell contacts with each other, they can be cultured in dynamic systems that are amenable for large scale processing [11]. While MSC aggregates have promising potential for future cell based-therapies, it has been shown that when aggregated, MSCs have limited proliferative capacity [12, 13]. Therefore, although this aggregated culture platform is amenable for scale up processes, its ability to support cell expansion is limited [14]. Additionally, due to the 3D organization of the densely packed cells together in an aggregate, the resulting microenvironment is biochemically and molecularly heterogeneous and the cells on the interior of the aggregate may not be exposed to the same nutrients or factors as the cells at the surface of the aggregate [15]. Efforts to improve upon these strategies to overcome these limitations may lead to the development of future MSC aggregate-based therapies.

To address limitations that exist in MSC aggregate culture, biomaterials can be used as a method to control and direct behavior by engineering a desired environment around the cells. Recent research has focused on using naturally derived glycosaminoglycans (GAGs) as a biomaterial for tissue engineering and drug delivery applications [16, 17]. Heparin, the most sulfated GAG, has anti-coagulant activity, plays a role in organizing basement membrane and can act as a coreceptor to bind and sequester positively charged growth factors, cytokines, and chemokines and enhance ligand-receptor signaling [18]. Engineering of a heparin coating that can mimic the native

heparin sulfate proteoglycan structure found at cell surfaces can be used as a novel platform to present GAGs to cells to direct cell behavior. Because it is known that interactions with growth factors is dependent on the sulfation pattern present [19, 20], there is an opportunity to examine how non-native sulfation patterns can play a role in potentiating growth factor signaling and response in MSCs. In addition to modulating growth factor response with heparin-derived coatings, there is also an opportunity to alter cell behavior by exploiting heparin's ability to bind positively charged growth factors. By taking advantage of this property, molecular interactions could then be translated to not only direct cellular response to growth factors in the surrounding environments, but also direct cell behavior in microtissue assembly. The role of heparin and its derivatives in coating form on cell response and culture has not been previously examined and can provide insight into novel techniques to develop effective MSC-based therapies. The engineering of the immediate cells microenvironment at its surface can be used to enhance and direct cell fate and behavior in many different applications for tissue engineering MSC based therapies.

1.2 Research Objectives

The objective of the research presented in this dissertation was to develop heparin-based coatings on MSC spheroids in order to study the role of heparin and its derivatives on MSC culture for the improvement of stem cell-based therapies. To develop an understanding of this novel approach to control cell behavior, MSCs were coated with heparin and its ability to sequester positively charged protein and the subsequent cellular response was examined. Given the importance of sulfation in the negative charge density

of heparin, a platform was developed to explore its role in growth factor interaction through the desulfation of heparin. These materials were used to examine how presentation of coatings with native and no sulfation levels could potentiate the mitogenic response to the growth factor fibroblast growth factor-2 (FGF-2) and the chondrogenic response to transforming growth factor beta-1 (TGF-β1) and subsequently cell proliferation and differentiation, respectively. Additionally, to explore other usages of these coatings, the interactions between heparin and a peptide sequence presenting the specific binding site found on FGF-2 (HEPpep), was explored to develop a novel platform to assemble MSC-based microtissues. The goal of these studies was to provide insight into the presentation and interaction of heparin that alter stem cell behavior regarding proliferation, differentiation or aggregation. The **central hypothesis** of this research was that engineering heparin-based coatings would allow for the ability to direct cell behavior in MSC spheroids by regulating the response to the surrounding cues (growth factors or peptide interactions) in the environment. The characterization and effects of this heparin coating on cell surfaces within MSC spheroids was explored in the following three specific aims:

Hypothesis I: Using a layer-by-layer method will facilitate coating MSC spheroids with heparin and subsequently a bioactive heparin binding growth factor.

Specific Aim I: Develop and characterize a multilayer heparin coating for biomolecule presentation to human MSC spheroids.

MSCs have been used as cell therapies to aid in regeneration of a variety of injured tissue. Moreover, MSCs aggregated into small spheroids have enhanced anti-

inflammatory properties over single MSCs grown in monolayer [21]. However, MSC-based therapies may be rendered ineffective due to lack of control over cell fate after introduction into a complex or harsh injured environment. We aimed to develop a heparin coating for MSC spheroids to potentially allow for simultaneous delivery of both cells and a soluble factor to direct cell differentiation. Heparin, a negatively charged glycosaminoglycan that can sequester and release positively charged proteins, was grafted onto cell surfaces through deposition of biotin and avidin as intermediate layers. Fluorescent imaging provided characterization of heparin coatings at different concentrations, confirmation of a loaded protein and effects on cell viability within the MSC spheroid. Additional characterization was performed through a particle exclusion assay to examine heparin coating effects on the native pericellular matrix of MSCs, through a monocyte anti-inflammatory coculture assay to reveal heparin coating effects on MSC spheroid anti-inflammatory properties, and through a mink lung epithelial cell line bioactivity assay to determine the bioactivity of TGF-β1 loaded onto coated cell surfaces.

Hypothesis II: A fully sulfated heparin coating will result in higher cell number in response to FGF-2 and to greater chondrogenic differentiation in response to TGF-β1 in MSC aggregates, compared to a desulfated heparin coating and a noncoated control, due to stronger electrostatic interactions with the positively charged growth factor within the vicinity of the cells.

Specific Aim II: Determine response of human MSC aggregates to growth factors in the culture media after coating with heparin of high and low sulfation levels.

MSC micromass culture has been traditionally used to study chondrogenic differentiation, however, recent interest in smaller MSC aggregates (500-1000 cells) with smaller diameters has increased because of their ability to be used as injectable therapies treatment of cartilage injuries and disease [22]. Although MSC spheroids can be a promising platform for effective cell-based therapies, the challenge of lack of proliferation in spheroid culture may hinder the scale-up of aggregate systems. Additionally, due to the 3D structure of formed aggregates, exogenous growth factors supplemented to the culture medium may not be exposed the entire cell population, especially the cells found on the interior of the aggregate. The incorporation of sulfated GAGs, like heparin, can be used as a potential vehicle to promote growth factor availability due to the negatively charge that local electrostatic interaction with positively charged proteins. Additionally, because the interaction between heparin and its growth factors depends on the presence of the negatively charged sulfate groups, desulfation of the GAG can modulate the interaction with a positively charged protein. Therefore, the objective was to characterize heparin MSC coatings of two different sulfation levels (native sulfation and fully desulfated) and study the effect of these coatings on MSC response in the presence of two different growth factors supplemented to the culture media. To evaluate the coating effect, MSC aggregates were coated with either heparin or desulfated heparin and then cultured in serum-free media containing FGF-2 or TGF-β1. Over 14 days *in vitro*, cell number was determined using a DNA assay, and over 21 days *in vitro*, cell morphology was characterized using histological staining and chondrogenic differentiation was evaluated using quantitative reverse transcription polymerase chain

reaction (RT-PCR) and immunohistochemical (IHC) staining for chondrogenic extracellular (ECM) components.

Hypothesis III: MSC spheroid building blocks coated with HEPpep and heparin will assemble due to the specific interaction between the peptide sequence and the GAG to form microtissue constructs with different cell populations.

Specific Aim III: Determine effect of HEPpep and heparin cell coating on MSC spheroid microtissue assembly in a dynamic culture system.

Another application of MSCs is their use in microtissues as either an *in vitro* model system or *in vivo* tissue repair replacement [23, 24]. Formation of these microtissues can be performed by using a "bottom-up" method, in which smaller building blocks of multiple cell types are assembled together to construct a larger tissue. To recapitulate complex structure of tissues, multiple cell types are often incorporated in specific spatial confirmations that mimic both homotypic and heterotypic cell interactions found in native tissues. The objective of this study was to investigate the use of HEPpep and heparin coatings on MSC spheroids assembly to form multi-cellular microtissues in a dynamic suspension culture system. It was envisioned that HEPpep coated spheroids would interact and assemble with heparin coated spheroids to form multi-cell type constructs in dynamic culture. First, HEPpep and heparin coatings and their effect on cell viability of MSC spheroids were characterized. Additionally, the specificity of these coatings was assessed by culturing together spheroids coated with different peptide sequences and GAGs for 24 hours. Finally, system parameters such as ratio of cell populations and surface area availability were varied to observe effects on assembly of

HEPpep coated and heparin coated spheroids and their interactions within the system by measuring assembled construct size, composition and interfacial area between two populations over the course of 3 days.

1.3 Significance and Scientific Contributions

The studies in this dissertation provide significant insight into the role of a novel presentation of the naturally derived GAG, heparin in coating form on MSC spheroid culture. Using a layer-by-layer technique, a method to graft heparin and subsequently facilitate protein sequestration onto cell surfaces was developed. The new technology of a heparin cell coating provides a new platform to present both GAGs and a sequestered growth factor to cells. The released growth factor from the heparin coating can also signal to surrounding environments, demonstrating that this heparin coating can also act as a carrier to deliver a therapeutic growth factor in addition to the stem cells to help regeneration and repair tissues.

In addition to the establishment of a heparin coating, the use of biotin and avidin as intermediate layers allow for the grafting of other biotinylated species on cell surfaces, therefore, other heparin derivatives, such as desulfated heparin can also be coated onto cell surfaces. The versatility of this system enabled investigating the effects of GAG species with native and no sulfation levels on cell surfaces and how it potentiates the response of the aggregated cells to the growth factor in the environment, specifically, MSC proliferation and chondrogenic differentiation. Desulfation of heparin provided insight into how coatings of different sulfation patterns can promote response to positively charged growth factors to ultimately direct cell behavior. These studies

provided evidence that pairings of different GAGs and growth factors can be used to tailor a MSC response to target and treat different pathologies. The knowledge gained in these studies, in turn, may advance the development of novel cell based therapies that modifies stem cell response using a combination of growth factors and GAG sulfation patterns for effective usage in a specific application.

Finally, the development of heparin and HEPpep coatings reveal insights into heparin and heparin binding peptide interactions that can be utilized to self-assemble microtissues from small building blocks in a dynamic culture system. By simply culturing heparin coated and HEPpep coated spheroids together in one system, the specific interaction between the coatings on each cell population can be exploited to promote assembly to form a population of microtissues containing multiple cell types. This platform provides insight into a novel technique to assemble microtissuses in one system under dynamic culture by harnessing the interactions that can be engineered at cell surfaces. This research highlights that a GAG-based coating for MSC spheroids can be used for different culture applications, ranging from proliferation to differentiation to microtissue formation. Together these findings represent a novel technology that modulates molecular interactions at cell surfaces through exploitation of the heparin binding properties to direct cell behavior.

CHAPTER 2

BACKGROUND AND LITERATURE REVIEW

2.1 Mesenchymal Stem Cells

2.1.1 Mesenchymal Stem Cell-Based Therapies

Adult bone marrow contains multipotent progenitor cells referred to as mesenchymal stem cells (MSCs) [1]. In the bone marrow, MSCs are isolated from the mononuclear layer after separation by density gradient centrifugation. These cells are cultured in media containing fetal bovine serum to allow for the MSCs to adhere to tissue culture plastic, exhibiting a fibroblast-like morphology [25]. Population doubling time is dependent on donor and playing density, however, these cells divide rapidly and are relatively easy to expand in culture [4, 26, 27]. This cell type exhibits two important qualities that make them a promising source for cell-based therapies. First, MSCs are able to differentiate into numerous mature cell types, such as those from bone, cartilage, muscle, bone marrow stroma, tendon and ligament, fat, dermis, and connective tissues [1, 2, 26, 28]. Therefore, this cell type is able to regenerate multiple tissues through the practices of tissue engineering. Second, MSCs also secrete a broad spectrum of trophic factors that can be classified as immunoregulatory and proangiogenic [1, 3, 29, 30]. These factors can be harnessed to promote a microenvironment in diseased or injured tissue that is favorable for repair and regeneration.

Since MSCs can differentiate into end-stage cell types, they have been used in tissue engineering practices to reform and regenerate tissues in tissue-specific biomaterials or when implanted into different tissue sites [1, 2, 4, 5, 26]. When cultured

in the correct environments containing lineage specific cues either by seeding on scaffolds, introducing growth factor cues or mechanical cues, MSCs can respond and begin to mature into the tissue specific cell type and produce tissue specific extracellular matrix (ECM) [31]. Typically, MSCs are characterized by their ability to different down three main lineages: osteogenic, adipogenic and chondrogenic [32-36]. Each pathway is achieved by culture under different conditions *in vitro*. To induce osteogenic differentiation in MSC, cells are cultured in the presence of dexamethasone, ascorbic acid and β-glycerol phosphate [35, 37, 38]. The master osteogenic transcription factor Runx2, activates and regulates osteogenesis as the targeted signaling pathway for growth factors such as TGF-β1, bone morphogenic proteins (BMPs), Wingless type (Wnt) and Hedgehog, all of which have been shown to induce bone differentiation [39-41]. Assessment of osteogenic different in MSCs is typically performed by measuring alkaline phosphatase (ALP) activity, gene expression of Runx2, collagen I and ALP, protein production of collagen I and ALP, and mineralization of calcium deposits over the course of 21 or 28 days [12, 35, 37-39, 42].

Adipogenic differentiation in MSCs is achieved by culture in the presence of insulin, isobutylmethylxanthanine, dexamethasone and hydrocortisone over the course of 3 weeks [43-45]. The transcription factor, peroxisome proliferator-activated receptors-γ (PPARγ) is known to be a master regulator of promoting adipogenesis and represseing osteogenesis in MSCS [42]. The binding of PPARγ to various ligands, including long fatty acid chains and thiazolidinediones (TZDs) induce the transactivation of the transcription factor [46]. Additionally, studies using PPARγ deficient mice have demonstrated increased bone mass and decreased fat storage [47]. Adipogenic

differentiation in MSCs is typically measured by gene expression analysis of PPARγ and lipoprotein lipase (LPL), as well as, Oil Red O staining for fatty deposits over the course of 21 days [43, 44].

For chondrogenic differentiation, MSCs are typically formed into pellets of aggregates of approximately 250,000 cells, to recapitulate embryonic limb bud development of high cell density environments [48-50]. Chondrogenic culture media contains dexamethasome, ascorbate acid, sodium pyruvate, insulin-transferrin-selenous acids and the growth factor TGF-β1 or TGF-β3 [49-53]. Other factors that have been implicated in inducing chondrogenic differentiation include the growth factors BMP-6 and insulin growth factor-1 (IGF-1) and mechanical stimulation in the form of dynamic compression [54, 55]. It is also known that activation of the transcription factor Sox9 can regulate the expression of downstream signaling molecules that result in the expression of chondrocytic markers, such as collagen II and aggrecan [53, 56, 57]. Additionally, MSC chondrogenesis is also accompanied with expression of cartilage oligomeric matrix protein, fibromodulin, and deposition of sulfated glycosaminoglycans [48, 52].

Other differentiation pathways, such as myogenesis and tendonogenesis in MSCs have also been achieved via *in vitro* culture. Myogenesis has been induced by culturing MSCs in media containing platelet derived growth factor-BB (PDGF-BB) and TGF-β or culturing MSC on bladder derived ECM [58, 59]. The smooth muscle cell phenotype has been characterized by measuring expression and deposition of collagen IV, desmin and myosin [59]. Tenogenic differentiation has been induced by culturing MSCs in environments undergoing mechanical strain and in the presence of growth differentiation factor (GDF) proteins [46]. The expression of the transcription factor, scleraxis, has been

used as an early marker of tendon lineage commitment [60, 61]. Other measurements of the protein collagen I and collagen III, as well as the expression of tenascin-C, biglycan and decorin, molecules all present in native tendon tissue, have been examined to determine tendon differentiation [60-62].

In addition to differentiation, when subjected to biochemical or mechanical cues, MSCs can also secrete specific bioactive factors that create an environment favorable for regeneration and repair [1]. This environment containing trophic factors can promote activity that inhibits scarring, inhibit apoptosis, stimulate angiogenesis, and stimulate mitosis of tissue intrinsic stem cells [63]. MSCs and conditioned medium from MSCs in growth have shown do have strong immunosuppressive effects by inhibiting T-cell recognition and proliferation and tumor necrosis factor-α (TNF-α) and interferon-λ (INF-γ) production [64-66]. MSCs also secrete anti-inflammatory cytokines, such as interleukin-6 (IL-6) and IL-8 that can alter antigen-presenting maturation, induce T-cell unresponsiveness, and suppress the secretion of inflammatory molecules by activated monocytes [28, 30, 67-69].

In the NIH clinical trial database, there are 374 registered clinical trials using MSCs [6]. Over the past 4 years, there has been a 3-fold expansion over the existing number; however, the distribution of the number of trials by phase has remained the same, with the majority of them in Phase 1 or 2 [5]. Additionally, of the Phase 3 trials , 3 have reported completion with results that have shown that MSCs are safe in treatment of myocardial infarction, cartilage defects and spinal cord injury (clinicaltrials.gov) [70]. One Phase 4 study that uses allogeneic umbilical cord blood MSCs is currently recruiting patients to treat aplastic anemia [6]. These trials are currently MSC clinical trials include

treatments for bone, cartilage, and heart, diabetes, lung and liver organ regeneration, and repair of neurodegenerative disease and injury [5]. Some limitations in MSC-based therapies are the donor and tissue source diversity, manufacturing diversity in culture parameters (serum, oxygen tension, cryopreservation), and the lack of a standard characterization of MSCs [5, 71].

2.1.2 Mesenchymal Stem Cell Aggregates

Although MSCs have canonically been defined as plastic adherent cells, it was revealed that 2D culture can alter the native phenotype after multiple passages and extended expansion [8, 11]. Using conventional *in vitro* culture techniques of tissue culture plastic substrates, MSC eventually lose their ability to self-renew, replicate, form clonal colonies and differentiate into the numerous lineages after successive passages and often before adequate cell numbers for transplantation is obtained [72, 73]. This has led to recent studies examining MSCs assembled into tightly packed clusters of 500-100,000 cells to mimic an *in vivo* microenvironment and better preserve MSC phenotype and innate properties [8, 14, 74]. The formation of the 3D aggregates have shown to enhance regenerative properties, such as differentiation potential and secretion of trophic factors, as well as improve cell retention, survival and integration in animal models [11, 75-78].

Recent studies have shown that 3D aggregate culture can enhance the differentiation potential of MSCs. While pellet culture has long been used to induce chondrogenic differentiation from MSCs [76], recent studies have also revealed that human bone marrow MSCs formed into aggregates exhibit a 2-5-fold increase in osteogenic gene expression of osteocalcin, osteopontin, ALP and Runx2 when compared

to MSCs cultured in 2D [78, 79]. Additionally, aggregate form increased Oil red O staining and adipogenic gene expression of PPAR-γ, LPL and aP2 3-fold in MSCs when compared to 2D monolayer [79]. When cultured in aggregate form, it has been demonstrated that cell-cell contacts can improve adipogenic and osteogenic differentiation through increased gap junction or cadherin signaling. In chondrogenic differentiation, the widely used micromass culture provides cell-cell contacts that are required to activate Notch signaling to initiate chondrogenesis [8]. ECM protein secretion of collagen, fibronectin and laminin also appears to increase when MSCs are cultured in 3D clusters, which can also help regulate differentiation potential of MSCs [80]. Overall, the increased differentiation potential and ECM production can enhance cell survival and the therapeutic effect in wound healing and tissue repair [81].

Another advantage of MSC aggregate culture is the enhanced secretion of anti-inflammatory and proangiogenic factors [21, 28, 82]. It was shown that the enhanced secretion of the anti-inflammatory cytokine TNF-α stimulated gene protein-6 (TSG-6) by MSC aggregates was a major mechanism in the beneficial effects of MSC administration in mice with myocardial infarctions [83, 84]. Additionally, MSC aggregate containing between 50k-250k cells can increase secretion of prostaglandin E2 (PGE2), which in turn can modulate macrophage response [82]. Anti-inflammatory effects were also observed with small MSC spheroids containing 200-1000 cells, in which immunomodulatory factors secretion of PGE2, transforming growth factor- β1 (TGF-β1), IL-6 and indoleamine 2,3-dioxygenase (IDO) activity was greater when compared to MSCs cultured in monolayer [85]. Other trophic factors that are secreted in elevated amounts when MSCs are cultured in high density clusters include vascular endothelial growth

factor (VEGF), fibroblast growth factor-2 (FGF-2), hepatocyte growth factor (HGF), CXCR4, monocyte chemotactic protein-3 (MCP-3), stromal cell derived factor (SDF-1) and angiogenin [11, 83, 86]. Combined, these qualities elicit strong interest in the field of culturing and utilizing MSCs in aggregate form for potential therapeutic regimens.

Compared to single cell administration, MSC aggregates offer numerous advantages to improve low retention and engraftment in preclinical animal studies [8]. These advantages include having upregulated secretion of trophic and anti-inflammatory factors that enhance therapeutic efficacy, secreting factors and producing ECM to create a microenvironment that protects the cells in a cytotoxic injury site, and improving cell adhesion and retention due to the increased cell-cell contacts and ECM production [78, 87, 88]. These characteristics have contributed to MSC aggregates demonstrating positive outcomes in multiple animal in vivo models of regenerating bone and cartilage, wound healing, neoangiogenesis and cardiac transplantation [76].

Various methods and culture platforms have been used to generate and study MSC aggregates. Formation methods include self-assembly on nonadherent or treated surfaces, hanging drop, forced aggregation, and microfabrication or microwells. Nonadherent or low-attachment surfaces culture MSCs in suspension so that the cells spontaneously adhere to each other forming 3D aggregates [8]. Although this method is easy to implement in the laboratory, formed aggregates are typically in variable size, low viability and low efficiency [12, 89]. In surface treated methods, typically, MSCs are seeded on a positively charged membrane, such as chitosan, that do not support substrate adhesion; therefore MSCs adhere to each other to form aggregates [90, 91]. Cell aggregation in the hanging drop method occurs when MSCs are suspended in separate

droplets and cultured on an inverted surface, during which, cells form a sphere in the apex of the drop [92]. During forced aggregation, cells are spun down into separate wells in a 96-well plate and allow cells to attach to each other [93]. Lastly, microwells typically seed cells in an array of micropatterned wells to separate small aggregates or micropatterned regions that are nonadherent to promote self-adherence [77, 94]. These methods utilize spatial confinement or mechanical forces to increase cell-cell contacts to control for aggregate size and cellular composition [95]. The formation of MSC spheroids used in the experiments of this dissertation was performed by using the commercialized microwell product, AggreWells^{TM}. This platform has shown to support cell viability in high through manner through control of initial aggregate size and aggregate cell number [11, 96].

For culture of formed aggregates, the use of dynamic cultures via rotary orbital shakers or spinner flasks have shown to minimize aggregate fusion, improved nutrient delivery and increased MSC viability [97, 98]. Bioreactor systems such as stirred tank, rotating wall, and perfusion bioreactors, have also been used to cultivate MSC aggregates for long term periods [98]. The dynamic setting appeared to enhance their biological function, and supported increased secretion of factors such as VEGF, HGF and FGF-2 from MSCs [6, 8, 99]. For clinical applications, high doses of cell numbers (on the order of 10^9 per administration) are typically required; therefore bioreactor systems that provide homogenous environment with control over parameters such as oxygen tension, pH and nutrient feeding are utilized [100]. However, when aggregated, the proliferation potential of MSC aggregates is rather limited and increased compaction has been observed during prolonged culture [14]. It is believed that proliferation is inversely

related to aggregate size due to diffusion limitations, thus large aggregates have reduced proliferation potential when compared to smaller aggregates. Additionally, regardless of size, due to the 3D environment in a tightly packed and dense cluster, the resulting MSC microenvironment is biochemically and molecularly heterogeneous [101, 102]. Further studies are needed to both understand the mechanisms behind the limited proliferation capacity, as well as develop methods and techniques to improve it in MSC aggregates.

2.1.3 Mesenchymal Stem Cell Chondrogenesis

During development, MSCs proliferate and differentiate into chondrocytes secreting cartilage ECM. These chondrocytes can undergo hypertrophy during the final stage of development and produce proteins necessary for calcification in the subchondral bone [103]. Because chondrocytes have low proliferation capacity and low metabolic activity, MSCs are of high interest as a promising source of cells for cartilage tissue engineering.

MSC chondrogenic differentiation has been achieved by culturing cells in the presence of growth factors from the TGF-β superfamily, ascorbate and dexamethasone [104]. Traditional methods of chondrogenesis have mimicked embryonic limb bud development in high cell density pellet culture because a key factor in successful differentiation down a chondrogenic lineage is presence of cell condensation, which is also a natural progression observed during cartilage formation *in vivo* [105-107]. Common markers for chondrogenic differentiation include ECM markers collagen II, aggrecan, and cartilage oligomeric matrix protein (COMP), as well as the Sox9 transcription factor [51, 108, 109]. Glycosaminoglycan deposition is also observed to

increase during *in vitro* pellet culture as MSCs differentiate down a chondrogenic lineage [49, 106, 107, 110]. While large aggregates have been used to study this process, one limitation includes the formation of undifferentiated or necrotized central core, leaving only the outside layer of cells to undergo differentiation [21]. This has led more recent studies to focus on the use of smaller MSC aggregates for a platform for tissue engineering for cartilage restoration [111].

Additional studies have shown that MSCs can also differentiate when cultured on scaffolds or hydrogels [112-114]. Both natural and synthetic scaffolds, such as collagen II, silk/chitosan, poly(lactic-co-glycolic) acid or poly(epsilon-caprolactone), have all supported MSC chondrogenic differentiation, seen through upregulation of cartilage specific ECM gene markers and GAG deposition [112, 113, 115]. Additionally, implantation of these MSCs on scaffolds has shown evidence of *in vivo* cartilage regeneration in rabbit and caprine models [115, 116].

MSCs have also been cultured in hydrogels containing naturally derived ECM or synthetic polymers [51, 117-120]. MSCs encapsulated in 3D network of collagen II, a major component of hyaline cartilage, has been shown to increase expression of Sox9, collagen II, aggrecan and COMP in a time dependent manner when cultured in the presence of TGF-β1 and dexamethasone [51]. Similarly, when MSCs were encapsulated in collagen I hydrogels, which is clinical used for matrix-based autologous chondrocyte transplantation, and cultured in the presence of TGF-β1 or BMP-2, MSCs exhibited distinct, chondrocyte-like cell morphology, sulfated proteoglycan-rich ECM and collagen II deposition was detected [119]. Gene expression for collagen II, collagen X, and aggrecan were also all upregulated [119]. In synthetic hydrogels that incorporate collagen

mimetic peptides into a poly (ethylene glycol) (PEG) network, MSCs exhibit enhanced secretion of cartilage specific ECM when compared to PEG only hydrogels [117, 118]. This has also been observed when MSCs are cultured in chondroitin sulfate (CS) containing hydrogels, in which cells in CS-based bioactive hydrogels supported aggregation of cells and expressed increased expression of cartilage gene markers such as Sox9 and aggrecan [120]. Overall, the use of different hydrogel networks has shown to support *in vitro* chondrogenic differentiation in MSCs, indicating that the surrounding cell-ECM environment around MSCs can play a role in guiding MSC fate.

Another method to induce chondrogenic differentiation in MSCs is by subjecting them to dynamic compressive loading [121-123]. This mechanical stimulation recapitulates the *in vivo* knee environment that supports cyclic loading at the joint. It has been observed that MSCs seeded in agarose hydrogels and subjected to 10-20% strain lead to significantly greater proteoglycan synthesis and produced constructs with greater mechanical strength when compared to agarose gels that were not loaded [121-123]. It has been speculated that the dynamic compression regimen facilitates the diffusion of growth factors, such as TGF-β1, throughout the entire construct [124]. Culturing MSCs in a load bearing environment in *in vitro* systems can be utilized as a preculture technique to induce chondrogenic differentiation prior to implantation for cartilage tissue repair.

Lastly, in *in vitro* systems, chondrogenic differentiation of MSCs can also be enhanced by hypoxic culture (< 5% O_2), during which gene expression markers of Sox9, aggrecan, collagen I and II and X were upregulated in comparison to MSCs cultured in normoxic conditions (21% O_2) [125]. It is suggested that exposure to hypoxic conditions results in the translocation of the transcription factor hypoxia-inducible factor-1α (HIF-

1α) from the cytosol to nucleus and can upregulate the expression of cartilage-related genes in MSCs [126]. Given that cartilage tissue resides in low oxygen environments, HIF-1α has also been implicated in maintaining chondrocyte phenotype and preventing hypertrophy of differentiated cells [127].

2.1.4 Mesenchymal Stem Cell-Containing Microtissues

Microtissues that exhibit complex physiological microenvironments can readily be used as a building material for *in vivo* tissue repair or can be implemented as an *in vitro* tissue model [74, 128-130]. They often require the assembly of multiple cell types to better mimic realistic tissue structure. Cell-cell contacts between different cell populations are important in microtissues because they can provide contact dependent signals between cells and can provide cues to induce cells to perform a certain function and properly organize to better recapitulate specific niche environments [131].

Microtissue models can recapitulate tumor microenvironments for drug screening and have been typically executed in cellular arrays or microfluidic devices that provide a means to culture cells in either two-dimensions or three-dimensions. These arrays are used to study effects of different conditions, such as drug dosage, on the resulting cellular response, such as viability, to determine safety and toxicity [132]. In more complex systems, tissue matrix arrays that combine extracellular matrix (ECM) and cells can be used to investigate cell function, such as proliferation and differentiation, in response to different environments. Such approach enables high-throughput analysis of many factors to determine optimal conditions to achieve a desired cellular response [129, 133, 134].

For tissue repair purposes, assembled 3D microtissues aim to exhibit similar characteristics as the complex physiological microenvironments for efficient integration, both functionally and morphologically, with the defect tissue [9, 74, 130]. For example, cardiac spheres formed from aggregating cardiomyocytes and cardiac muscle tissue has been used to form contractile constructs that can be implanted for treatment of myocardial infarctions [23]. Microtissues are advantageous in tissue repair applications because they are not as prone to clearance compared to single cells and can produce proangiogenic factor that enable pre-vascularization or induce angiogenesis post implantation, ultimately, can improve engraftment when delivered [128].

MSCs have been extensively used in numerous microtissue applications, including cartilage, hepatic, vascularized tissues and bone marrow niches [23, 130, 135-137]. For cartilage tissue engineering, it has been shown that MSCs cultured with chondrocytes results in constructs that decreased deposition of collagen X, a marker for MSC hypertrophy, increased glycosaminoglycan (GAG) deposition and higher Young's modulus and dynamic moduli when compared to constructs without MSCs [107, 138]. The presence of the progenitor cells also have been shown to prevent dedifferentiation and maintain functional phenotype in chondrocytes. For hepatocyte culture, microtissues containing MSCs and hepatocytes have results in maintenance of the functional phenotype of the hepatocytes, as seen through urea and albumin secretion [139-141]. Additionally, the use of MSCs cultured in 3D can further improve hepatocyte phenotype, and ultimately can be used in strategies for liver regeneration and bioartificial liver-assist devices [142, 143]. In vascularized tissue, MSC and cardiomyocyte can be formed into small myocardial spheroids that secrete VEGF and support vascularization in injured

myocardial tissue [23, 128]. Implantation of these contractile constructs has been shown to improve function in myocardial infarction models in a number of animal models and ongoing clinical trials. Due to their numerous usages, MSCs can be used in many different microtissue applications.

To assemble microtissues with multiple cell types, previous methods have used encapsulation in hydrogels, scaffold-free technologies and microfluidic devices. Hydrogel encapsulation has been used to control organization of cell populations by encapsulating different cell types into separate sections of a hydrogel or seeding all cell types in a mixed population in one single hydrogel [144-146]. Hydrogel microtissues have been used to examine the cross talk and interactions between MSC, osteoblast and adipocyte populations cultured in different regions [145]. Additionally, a hybrid hydroxyapatite and alginate hydrogel containing chondrocytes has been developed to form osteochondral constructs that can support the formation of a calcified cartilage-like matrix for the interfacial tissue engineering between bone and cartilage [147].

The other option of scaffold-free technologies uses centrifugation or gravity to force cells into aggregate form. Multiple cell types are typically mixed together and cultured together in one aggregate [148, 149]. Scaffold-free microtissues containing small spheroids of different cell types as the building block can also be formed by the incorporation of magnetic microparticles that direct the assembly of spheroids upon application of a magnetic field [150]. Aggregated microtissues have previous been used to form hepatocyte tissue containing hepatocytes and fibroblasts or cardiospheres containing cardiomyocytes and MSCs [9, 10].

Lastly, microfluidic systems have been used to form high throughput arrays of small microtissues [24, 129, 151-154]. Spatial organization of different cell types is typically achieved by introducing different cell types into the small specialized devices sequentially to allow for each cell type to interact ad bind with each other [24, 134, 155, 156]. This platform facilitates control over the formation of the construct and culture parameters of media exchange and flow rate and can ultimately resemble a complex and accurate *in vivo* tissue environment [153, 154].

2.2 Heparin

2.2.1 Glycosaminoglycans

Glycosaminoglycans (GAGs) are a class of lineage polysaccharides that are found throughout the entire human body and located on cell surfaces, inside cells and in the ECM [157, 158]. Their functions include maintaining hydrostatic pressure by osmotically attracting water in cartilage, regulating cell function by controlling growth factors at cell surface proteoglycans, as well as acting as co-receptors to modulate biological environment at cell surfaces or in the ECM [159]. Sulfated GAGs, such as heparin, heparin sulfate, chondroitin sulfate, dermatan sulfate, and keratin sulfate bear negative charge throughout its repeating disaccharides [158]. Non-sulfated GAGs, such as hyaluronic acid, also exists as the GAG with the lowest net negative charge [160]. GAGs can attract and bind positively charged proteins through both electrostatic interactions, as well as carbohydrate specific sequences [161]. Based on their multiple functions and ability to bind proteins, GAGs have been used as a biomaterial for controlled delivery of growth factors for improvement of a variety of diseases [162-164].

2.2.2 Heparin Structure and Biosynthesis

Heparin is a linear GAG polymer composed of repeating iduronic acid and glucosamine units [158, 165]. It contains the highest amount of N- and 2-O sulfate groups as well as numerous carboxyl groups, making it the most highly negatively charged polysaccharide structure. Heparin molar mass can range from 3-30 kDa, with an average around 15 kDa. Each disaccharide unit contains approximately 2.7 sulfate groups, located at the 6-O or N- position on the glucosamine unit and 2-O position on the iduronic unit [20].

Heparin is structurally similar to its proteoglycan counterpart, heparan sulfate (HS) [20, 166]. Heparin is typically found in mast cell granules and HS is present in many tissues and located on cell surfaces or in the ECM as a part of the proteoglycans perlecan and agrin [167, 168]. Both heparin and HS play a role in cell adhesion, protein storage and can interact with numerous growth factors [169]. Biosynthesis of heparin begins with non-sulfated polysaccharides attached to a protein core. Then, sulfotransferases couple sulfate groups to the repeating subunits and proteases eventually release heparin from the protein core, resulting in the free floating form of heparin utilized in clinical and biomaterial applications [170].

2.2.3 Heparin-Protein Interactions

Heparin is clinically used as an anti-coagulant and is of great pharmacological importance in hemostasis due to its ability to interact with antithrombin [19, 20]. This protein is a member of the serpin family of proteases, many of which are known to also

bind heparin. This binding causes a conformational change in the protein and enhances the rate at which it inactivates thrombin and Factor Xa [171]. Additionally, the heparin chain acts as a template that can bring together antithrombin and thrombin physically to facilitate the inhibition. Studies have shown that only 5 sugar residues in heparin actually bind to antithrombin with high affinity [172]. This interaction with antithrombin provides a basis for heparin's anti-coagulant activities [171].

Heparin is also known to interact with many different families of growth factors, including FGFs, HGFs, VEGF, insulin-like growth factor binding proteins, and TGF-β [20, 166]. Summarized here are the protein interactions observed with FGF-2 and TGF-β1, as these are the growth factors used throughout this dissertation. The well-known interaction between heparin and FGF has been used in chromatography technologies to purify the growth factor due to their strong affinity [173]. FGF-2 has a very high affinity for heparin and has potent mitogenic activity in cells that express the corresponding FGF receptor [173]. Cell surface HS is known to bind both FGF-2 and the FGF-2 receptor to facilitate the formation of a ternary complex and promote dimerization of the ligand-receptor complex [174]. Both the binding and mitogenic response is greatly stimulated by heparin or HS [175]. Similar to the interaction with antithrombin, binding of heparin to the protein requires a small portion of the overall polysaccharide chain, in which the binding sequence for FGF-2 consists of a pentassachride [176]. However, a longer oligosaccharide containing 10 units is required to trigger biological mitogenic response [175]. Within this binding site, only one N- and the 2O- sulfate group on the adjacent iduronic acid are required to bind the growth factor [174, 176, 177]. Unlike the antithrombin interaction, no conformation change occurs upon binding, which is

consistent with the idea that heparin serves to dimerize the FGF-2-FGF-2 receptor complex to activate the subsequent signaling pathway. It has been shown that the removal of those sulfate groups, decreases the affinity for the growth factor and the mitogenic response is no longer stimulated when desulfated forms of heparin are present [178]. This interaction demonstrates the importance of the sulfate groups and contributions of the electrostatic interaction to the binding and signaling capacity of heparin. Heparin complexation has also been shown to protect growth factors from enzymatic degradation or denaturation [179-182]. This results in increased bioactivity and a stronger mitogenic response by cells, such as MSCs, fibroblasts and HUVECs, when exposed to FGF-2 in the presence of heparin [180, 183]. This response can be due to the protection from proteolytic degradation which results from heparin binding or the requirement that binding of heparin is necessary for binding to the cell surface receptor [184]. Overall, heparin binding plays an important role in FGF-2 bioactivity and signaling.

Heparin is also known to interact with the growth factor TGF-β1 [185-187]. Traditionally known as protein that induces chondrogenesis in MSCs, TGF-β1 has also been identified as a heparin-binding protein. Heparin is can bind to TGF-β1 near the N-terminal along the β-strand loop, a position that is also close in proximity to the receptor binding site [186, 188]. It has been shown that sulfated HS in the liver can potentiate the activity of TGF-β1, indicating that there is no competition between the GAG binding site and receptor binding site [188]. Recent studies have also identified that interaction between heparin and TGF-β1 requires the presence of the N- and 6O-sulfate groups [186]. However, upon desulfation at these positions, downstream signaling molecules of TGF-β1 (Smad2/3) in human MSCs were not decreased compared to fully sulfated

heparin treatment [186]. This demonstrates that the specific sulfate groups along the polysaccharide chain required for binding are the same as those required for signaling by TGF-β1 [186].

2.2.4 Heparin Binding Peptides

FGF-2 binding to cell surface receptors requires interactions with heparin sulfate [189]. A specific peptide sequence derived from the heparin binding site on FGF-2 has been identified and can be used to selectively sequester heparin from standard fetal bovine serum [190]. The result of this heparin sequestration facilitated cell to growth factor interaction that enhanced human MSC proliferation via FGF-2 binding and human MSC differentiation via BMP-2 binding [191, 192]. This heparin and heparin binding peptide interaction can be exploited in systems that require cell adhesion and cell-material interactions to control cell behavior.

The heparin binding site isolated from FGF-2 has previously been identified as the sequence Lys-Arg-Thr-Gly-Gln-Tyr-Lys-Leu (KRTGQYKL) [193]. This peptide sequence (HEPpep) has been utilized in form of a self-assembled monolayer able to sequester heparin from standard fetal bovine serum [191]. Sequential exposure to a solution containing the growth factor FGF-2 resulted in the binding of FGF-2 onto HEPpep assembled surfaces. Furthermore, it has been shown that the surface containing the sequestered heparin is able to amply FGF-2 mediated HUVEC proliferation [191]. Heparin binding peptides and other shorting peptide sequences, such as an integrin-binding peptide, have been employed in self assembled monolayer arrays to screen MSC behavior in response to multiple peptide presenting surfaces and media conditions [194,

195]. It was observed that the heparin binding peptide can support MSC adhesion and osteogenic differentiation (measured through ALP activity) [194].

2.3 Heparin Containing Biomaterials

2.3.1 Heparin Biomaterials Applications

Due to its biological effect in culture with multiple growth factors, its interactions can be harnessed as heparin is incorporated into biomaterial applications. Additionally, due to its binding ability, heparin can be used as a carrier for sequestration and controlled release of growth factors to promote angiogenesis and bone regeneration. It can be presented in multiple forms, either by incorporation into hydrogels and microparticles, or presentation onto thin film surfaces. Given its binding characteristics, heparin based materials can be a great candidate for emerging applications that aim to regenerate and repair tissue.

2.3.2 Growth Factor Delivery

Due to the strong interaction that exists between heparin and positively charged growth factors, heparin based systems are often used to deliver and release growth factors to targeted sites of interest [163, 196]. Collagen scaffolds have previously been modified heparin and pre-adsorbed with FGF. It was observed that heparin containing scaffolds exhibit enhanced proliferation of HUVECs and can sustain release of the protein for up to 40 days, compared to collagen scaffolds without heparin released all loaded FGF by day 15 [197]. Additionally, when heparin has been incorporated into fibrin gels, it was observed that the FGF release rate decreased compared to fibrin-only gels, indicating that

heparin can promote sustained release of FGF [196, 198]. Additionally, when implanted into ischemic hind limb in mice, it was observed that FGF-2 loaded heparin containing fibrin gels resulted in reduced muscle fibrosis and inflammatory and enhanced neovascularization, compared to non-heparin containing controls [196, 198]. Growth factor release from heparin has been utilized as a means to deliver therapeutic biomolecules to areas of injury for tissue regeneration.

It has also been shown that desulfation of glycosaminoglycans can result in changes of the negative charge, and ultimately can have effects on protein interactions [165, 178, 199, 200]. For heparin, desulfation can be performed through chemical modification using solvolytic processes to selectively desulfated certain groups or fully desulfate to remove all groups [201]. Figure 2.1 provides a schematic of the heparin ring structure and identifies the sulfate groups that can be removed as a result of desulfation. Desulfation can be advantageous for *in vivo* applications in that the removal of certain sulfate groups can reduce the anti-coagulation property of heparin, and thus not inhibiting clotting when necessary [201].

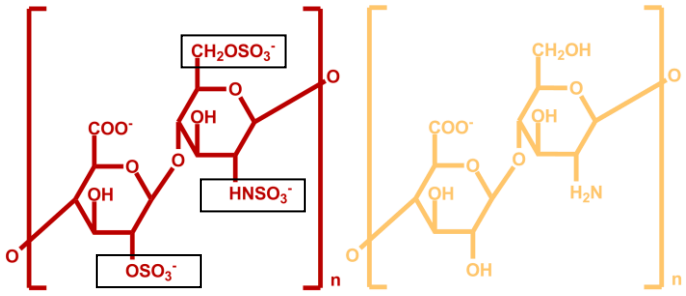

Figure 2.1 Heparin and desulfated heparin structure. Schematic adapted from [165].

Heparin systems that have been selectively or fully desulfated have shown that incorporation of these materials into PEG hydrogel systems have resulted in different

release kinetics of the growth factor, VEGF over time [202]. It was observed that cumulative VEGF release after 96 hours was greatest when using a fully sulfated heparin derivative. Additionally, when this hydrogel was implanted in diabetic mice, fully desulfated heparin hydrogels containing VEGF appeared to promote wound angiogenesis, seen through larger areas of granulation tissue and greater amounts of CD31 positive cells [202]. Additionally, it has also been shown that a fully desulfated heparin containing hydrogel can support greater cumulative FGF-2 release [164]. Taken together, desulfation provides a platform to control growth factor presentation from heparin containing systems by altering release kinetics.

2.3.2 Ultrathin Films

Heparin ultrathin films can be grafted onto surfaces using layer-by-layer deposition of anionic and cationic electrostatic interactions [203-206]. This layering deposition procedure can be repeated multiple times to control for the thickness of the surface film and has utilized polymers such as poly (ethyleneimine), poly (allylamine), or proteins such as fibronectin, or other polysaccharides such as chitosan and dextran [203-206]. Layering of heparin on surfaces has been used on medical devices, such as coronary stents, to enhance strength and blood compatibility, and to accelerate the re-endothelialization and healing process once deployed [204, 206]. Heparin ultrathin films also have the ability to deliver growth factors that have been sequestered or loaded onto surfaces for release once implanted [205]. Heparin ultrathin films have typically been used on titanium or other metal surfaces because it has been shown that the polycationic layer involved often results in cell toxicity and death [207].

2.3.2 Hydrogel Incorporation

Heparin can be incorporated into hydrogels via physical crosslinking or covalent crosslinking [16, 17]. As a biomaterial platform, hydrogels can support the culture of encapsulated cells as well as potentially protect from the surrounding environment, which allowing for diffusion of the required nutrients [208]. Heparin containing hydrogels have demonstrated the ability to act as a drug delivery carrier or a culture platform to promote stem cell differentiation [208-210]. Physical crosslinking of heparin occurs as a result of entanglement between or noncovalent interactions with the polymer chains [16]. Physical entanglement can provide a means to deliver a hydrogel with release of heparin that can act as an anti-coagulant. Free radical polymerization or Michael-type addition can also be used to form hydrogels containing methacrylate modified heparin [16, 210].

Heparin-functionalized poly ethylene glycol (PEG) hydrogels have demonstrated the ability to sequester FGF and release it in a controlled manner over the course of 5 weeks after the initial burst. Additionally, hydrogels loaded with FGF also has shown to enhance encapsulated human MSC growth. Additionally, sustained release of VEGF has been shown to induce proliferation of human umbilical vein endothelial cells (HUVECs) as well as support capillary formation *in vitro* systems over the course of 2 weeks [211]. For stem cell differentiation, MSCs cultured in heparin containing hydrogels and osteogenic differentiation cues can increase ALP product and osteopontin and collagen I gene expression over the course of 5 weeks, compared to non-heparin controls [209, 212]. Additionally, chondrocytes cultured in heparin containing hydrogels without exogenous growth factors or chondrogenic components support effective redifferentiation

and production of GAGs and ECM proteins within a week [213]. Transplantation into a rabbit knee partial thickness defect also demonstrated cartilage regeneration superior to non-heparin and chondrocyte containing hydrogels [213]. Overall, incorporation of heparin in hydrogels can promote cell adhesion, proliferation and differentiation, as well as support sustained local delivery of growth factors. However, although hydrogels are a promising platform for tissue engineering applications, some limitations include the use of extra radical initiators that can potentially be cytotoxic to encapsulated cells, and the excess void space of the material which can increase the required volume of the delivered therapeutic.

2.3.3 Microparticles

Microparticle incorporation into 3D aggregates is another approach to present heparin to stem cells. Microparticles are able to load growth factors with minimal excess material due to the high surface area to volume ratio of this platform [183]. This ability presents a potential method to deliver growth factor to cells that are located closer in proximity to the core of an aggregate to overcome diffusional barriers [214]. Finally, incorporation of microparticles into stem cell aggregates has shown to modulate pluripotent stem cell differentiation [111, 214, 215]. Heparin containing microparticles have been shown to efficiently bind growth factors including BMP-2, VEGF and FGF-2. Additionally, microparticles loaded with BMP-2 also exhibit sustained bioactivity and support prolonged release when compared to soluble BMP-2 delivery [216].

2.4 Cell Surface Engineering

2.4.1 Cell Surface Modification

Surface modification of cells with natural and synthetic polymers is another method to present biomaterials to control cell behavior [207]. The introduction of function and bioactive molecules at the cell surface can be used to add biological function, such as blood compatibility, controlling cell transplantation by masking surface antigens to increase graft efficiency and controlling interactions with the surrounding environments [207]. Cell surface modifications can be used to study cell-cell interactions as well as control stem cell lineages for regenerative medicine.

MSC surface engineering has previously been used to chemically attach cell adhesion molecules to cell surfaces to improve homing efficiency to specific tissues [217]. Improving homing efficiency can provide an approach to infuse MSCs to local environments that target injured tissue sites that are difficult to access, thus overall increasing efficacy of the delivered therapeutic cells [30]. To achieve this, sialyl Lewis^X (SLeX) moiety, a cell rolling ligand, has been grafted onto surface of MSCs without compromising MSC viability adhesion proliferation and differentiation potential [218]. The SLeX engineered MSCs exhibit rolling response *in vitro* on substrates coated with P-selection that are superior to noncoated MSCs [217, 219]. This indicates that harnessing interactions that control cell adhesion at cell surfaces, this strategy can be used to potentially target P-selectin expression endothelium at sites that exhibit inflammation [218].

To attach cell adhesion molecules onto cell surfaces, this method uses a stepwise layer-by-layer deposition of first, a sulfonated biotinylated N-hydroxy-succinimide

(NHS) that targets and covalently attaches to cell surface amines [220]. This is followed by the addition of streptavidin that binds to the biotin on cell surfaces, and lastly, attachment of the final biotinylated ligand that promotes cell adhesion to the targeted substrate [217, 219]. This system has been shown to efficiently graft molecules onto cell surfaces without adverse impact on the native MSC phenotype.

Other methods to modify cell surfaces have used hydrophobic interactions with amphiphilic polymers [221-224]. These polymers, such as PEG-conjugated phospholipids or poly(vinyl alcohol) bearing a hydrophobic side alkyl side chains (PVA-alkyl), can be spontaneously anchored into the lipid bilayer of cell membranes and can be controlled by the length of the alkyl chain, or the molecule's hydrophobicity [221-224]. This occurs without compromising the integrity of the cells, however, over time, it has been seen that PEG-lipids gradually disappear from the cell surfaces without uptake inside the cells [221, 222]. This technique has previously been used to mask cell surface markers on pancreatic islet cells and increase engraftment for treatment of type I diabetes [221, 222].

Another method to modify cell surfaces employs electrostatic interactions layering anionic and cationic polymers [225-228]. Some polymers used include poly-L-lysine, poly(ethyleneimine), poly(styrene sulfate) and poly (allylamine hydrochloride) [225, 226, 228]. Using layer-by-layer technique alternating between positively charged and negatively charged layers results in the ability to control surface presentation at the outermost layer as well as surface thickness [226]. While this technique is simple, most polycations, such as poly-L-lysine are cytotoxic and can severely damage cell membrane [207].

2.4.2 Heparin Cell Coating

Using the previously mentioned layer-by-layer strategy, heparin can also be grafted onto cell surfaces, as is observed with pancreatic islets [229-232]. This strategy utilizes the electrostatic interaction with between the intermediate streptavidin or avidin layer that is positively charged to bind the negatively charged heparin. Additionally, heparin can similarly be biotinylated to attach to the avidin layer. Heparin grafted onto pancreatic islets can be used for numerous applications [220, 229, 230, 233, 234]. First, a heparin coating can be used to prevent the instant blood mediated inflammatory reaction during islet transplantation, thus protecting the delivered cells to increase engraftment efficiency [230]. It has also been used to anchor VEGF onto pancreatic islet surfaces to stimulate angiogenesis and anchor thrombomodulin to regulate thrombosis and inflammation upon islet transplantation for type 1 diabetes treatment [229, 232]. Utilizing these interactions to modulate inflammation and the surrounding environments has been beneficial for developing pancreatic islet treatments that can increase engraftment efficiency and promote vascularization [229, 230]. Prior to the work presented in this thesis, heparin has not previously grafted onto MSC surfaces, thus presenting an opportunity to examine the effects of GAG coatings and how exploiting those interactions can be utilized to control MSC behavior.

CHAPTER 3

CHARACTERIZATION OF A MULTILAYER HEPARIN COATING FOR BIOMOLECULE PRESENTATION TO HUMAN MESENCHYMAL STEM CELL SPHEROIDS[1]

3.1 Introduction

Mesenchymal stem cells (MSCs) have been used as a cell therapy to regenerate injured tissue and treat inflammation resulting from a wide range of pathologies such as cardiovascular disease, myocardial infarction, osteoarthritis, brain and spinal cord injury, diabetes, Crohn's disease and graft versus host disease [2, 3]. These multipotent adult progenitor cells are capable of differentiating into bone, cartilage, fat, muscle, tendon/ligament, and other connective tissue cell types, which can be mediated through local soluble factors and/or mechanical stimulation [1]. In addition to their differentiation capacity, MSCs have the ability to secrete cytokines and growth factors that can promote angiogenesis, modulate extracellular matrix (ECM) remodeling, affect immune cell activation or suppression (immunomodulation) and promote cell recruitment [1-4]. Recently, there is growing evidence that, when aggregated into spheroids, MSCs have enhanced anti-inflammatory properties over single MSCs grown in monolayer [21]. These anti-inflammatory effects are useful in treating inflammatory pathologies and regulating the damage that can be caused by inflammation in an acute injury.

[1] Portions of this chapter were taken from Lei, J., McLane, L., Curtis, J.E., Temenoff, J.S. (2014). "Characterization of a multilayer heparin coating for biomolecule presentation to human mesenchymal stem cell spheroids." *Biomaterials Science*. 2: 666- 673. DOI:10.1039/C3BM60271K

Upon injection or placement into an injured environment, MSCs are able to respond to the milieu surrounding them and secrete the appropriate mediators to repair the tissue or begin to differentiate to a tissue-specific cell type [4, 29]. However, MSC-based therapies may be rendered ineffective due lack of control over cell fate upon administration into a complex, pathological environment. Further compounding the problem is the fact that that the injured environment may contain many proteases or highly inflammatory molecules that can harm the injected cells [235].

Controlled differentiation of stem cells has been achieved by cell seeding on scaffolds that mimic the architecture and mechanical properties of native extracellular matrix in tissues in the presence of soluble factors.[236] However, fibrous scaffolds do not retain ECM secreted by cells, which can limit their ability to fully repair tissue [237]. Additionally, processing that requires specialized equipment to synthesize scaffold materials (i.e. electrospinning) make this method difficult to scale up for cell therapies. Finally, scaffold-based technologies cannot be utilized as a minimally invasive injectable treatment, and thus, require a full surgical implantation for cell delivery [237, 238].

Another method of controlled differentiation is by encapsulating cells in injectable hydrogels [209, 239, 240]. Hydrogels can be functionalized to be biodegradable, contain motifs that drive differentiation, and provide a 3D environment that can retain secreted extracellular matrix molecules [239]. However, limitations of using a hydrogel system include the polymerization requirement that typically involves an extra radical initiator that could potentially be cytotoxic to encapsulated cells, the excess void space of the material which increases the required volume injected and the

lack of temporal and spatial control of degradation, which may be required for full tissue integration [241].

In response to these shortcomings, we aim to develop a thin, conformal coating method for MSC spheroids to allow simultaneous injection of both cells and a therapeutic agent to a site of injury. This system uses multilayer deposition of biotin and avidin to graft heparin onto cell surfaces [230, 234]. Heparin is a negatively charged glycosaminoglycan that can sequester and release positively charged proteins [242]. It has been used as an anti-coagulant, as a drug delivery system and as a component of hydrogels to help drive differentiation in multiple cell types, including MSCs and embryonic stem cells [243-245]. It is envisioned that the negative charge on this coating will allow for preloading of a growth factor of interest to both guide stem cell differentiation, as well as release the loaded biomolecule to facilitate local tissue repair. These coating layers are advantageous over using scaffolds or bulk hydrogels for guiding cell fate because of their simple assembly through nontoxic interactions (i.e. noncovalent, electrostatic) and precise tuning of thickness, composition and permeability, ultimately allowing for control over coating degradation (and concomitant biomolecule release) [246-248]. Moreover, such cell coating technologies would greatly enable injectable therapies, as there is no excess material that needs to be delivered with the cells. Toward developing this coating methodology, the objectives of this study were to characterize the coating and loaded protein via fluorescence microscopy and a particle exclusion assay, determine cell viability after coating, investigate MSC anti-inflammatory properties after coating, and determine the bioactivity of a growth factor (TGF-β1) loaded on cell surfaces.

3.2 Methods

3.2.1 Cell culture

MSCs derived from bone marrow aspirates were obtained from The Texas A&M Health Sciences Center. Cryopreserved MSCs were thawed and expanded in alpha Minimum Essential Medium (α-MEM, Mediatech, Herndon, VA) containing 16.5% fetal bovine serum (FBS, Atlanta Biological, Atlanta, GA), 2 mM L-glutamine (Mediatech), 100 units/mL penicillin and 100 µg/mL streptomycin (Mediatech). Media was changed every 2-3 days until 80% confluent and used at passage 3 or 4. Human THP-1 monocytes (ATCC, Manassas, VA) were expanded in RPMI 1640 (Mediatech) containing 10% FBS, 2 mM L-glutamine, 100 units/mL penicillin and 100 µg/mL streptomycin and 0.05 mM 2-β-mercaptoethanol (Sigma, St. Louis, MO). Media was replaced every 4 days until seeding in co-culture systems. Mink lung epithelial cells (MLECs, ATCC) were thawed and expanded in Dulbecco's Modification of Eagle's Medium (DMEM) with 4.5 g/mL glucose, 10% FBS, 2 mM L-glutamine and 200 µg/mL Geneticin® (G418, Gibco, Grand Island, NY). Media was exchanged ever 2-3 days until cells were at 80% confluent and used at passage 29.

3.2.2. MSC spheroid formation

To make spheroids, cells were forced into aggregation via centrifugation.[249] Briefly, a single cell suspension (3-6 x 10^6 cells/mL) was added to AggreWell™ agarose microwell inserts (400 µm wide wells; ~6000 wells/insert) and centrifuged (200 rcf; 5 minutes) to aggregate cells within the microwells. After 24 hours, MSC aggregates were rinsed from the microwells and cultured thereafter either encapsulated in a 1.5% alginate

layer (approximately 3 mm thick) crosslinked in 100 mM calcium chloride contained in 10 cm petri dish (Corning, Tewksburg, MA) for up to 14 days or in rotary orbital suspension culture for up to 3 days to inhibit agglomeration of individual aggregates (approximately 1500 spheroids/10 mL media/petri dish; 65 rpm for rotary suspension only).

3.2.3 Multilayer coating and subsequent cell viability

MSCs and MLECs were cultured until 80% confluent and lifted using 0.05% trypsin (Mediatech). Cells were washed in phosphate buffered solution (PBS, Life Technologies, Grand Island, NY) 2 times and then modified with heparin by multilayer assembly of biotin and avidin layers [230, 234]. Cells were first cultured in 4 mM EZ-Link Sulfo-NHS-LC-Biotin (Pierce, Rockford, IL) in PBS, followed by 0.5 mg/mL avidin in PBS (Life Technologies, Carlsbad, CA), and lastly in 5 μg/mL, 1 mg/mL or 5 mg/mL biotin-conjugated heparin in PBS. Each incubation step was performed in an Ultra-Low Attachment Surface plate (Corning) for 30 minutes at 37ºC. For imaging studies, cells were incubated in a biotin-heparin solution that has been tagged with AlexaFluor 633 (Invitrogen). To load coated surfaces with a protein after the heparin layer, cells were incubated for 30 minutes in a 90 μg/mL fluorescein isothiocyanate (FITC)-tagged histone (Sigma) solution for imaging studies or 3 ng/mL or 3 μg/mL TGF-β1 (Peprotech, Rocky Hill, NJ) solution for MLEC luminescence studies. Once multilayer deposition of all layers was complete, all cells were washed in PBS and formed into spheroids (500 or 1000 cells/spheroid) as previously described. Spheroids were stained with LIVE/DEAD solution (1 μM calcein AM and 1 μM ethidium

homodimer-1) to assess cell viability. Images were taken using a Zeiss LSM 700 LSM confocal microscope and channels were merged and projections were flattened in ImageJ (NIH, Bethesda, MD).

3.2.4 Particle exclusion assay

To characterize the pericellular matrix (PCM), 3 μm passivated (covalently modified with methoxypolyethylene glycol amine) polystyrene microspheres (Life Technologies, supplied by Curtis laboratory) were used in a particle exclusion assay on a monolayer of MSCs [250]. Beads with diameter size of 3 μm are of the same order of magnitude in size as other particles excluded by the pericellular matrix, as seen in previous experiments.[250] MSCs were seeded at 500 cells/cm^2 on 12 mm glass coverslips and cultured for 24 hours. Cells were then modified via multilayer deposition with 5 mg/mL biotin-heparin as described above and then suspended in PBS. Control samples were handled identically, but not treated with the multilayer coating. After coating, 20 μL of the bead solution and 180 μL of PBS were added to a custom imaging mold (Teflon) containing seeded MSCs. Beads were allowed to settle for 10 minutes. Bright field imaging was performed using a using a Zeiss LSM 700 LSM confocal microscope. The effective thickness of the PCM was measured as a separation between the beads and cell surface and was measured using ImageJ (3 measurements per cell).

3.2.4 Monocyte anti-inflammatory co-culture assay

To examine anti-inflammatory effects of spheroid culture with and without coating, MSCs were co-cultured with LPS-activated human monocytes [21, 251, 252]. MSCs were coated and formed into spheroids as previously described and cultured in rotary orbital suspension for 3 days. MSC monolayer and 1000-cell spheroids (coated and

noncoated) were then indirectly co-cultured with THP-1 monocytes in a 12-well transwell system (Corning) at a ratio of 100,000 MSCs to 400,000 THP-1 monocytes. All cells were suspended in RPMI 1640 media. Monocytes were activated by addition of lipopolysaccharide (LPS, 400 ng/mL) to the media. After 16 hours, MSC monolayer and spheroid supernatant was collected and tumor necrosis factor (TNF)-α levels were quantified via ELISA (R&D Systems, Minneapolis, MN).

3.2.5 Mink lung epithelial cell luminescence assay

MLECs were used as a reporter cell line to study the effects of the coating on TGF-β1 signaling to cells. MLECs were coated with heparin at the concentration of 5 mg/mL and then loaded with TGF-β1 at the concentrations of 0 ng/mL, 3 ng/mL and 3 μg/mL by incubating heparin-coated cells in TGF-β1 solutions for 30 minutes, similar to the previously discussed coating experiment. Noncoated controls were also exposed to TGF-β1 at the previously mentioned concentrations using identical methods. After coating and growth factor loading, all cells were formed into aggregates (500 cells/aggregate) using the technique previously described. At 24 hours, cells were transferred to a 96-well plate (150,000 cells/well) and ONE-GloTM Luciferase Assay buffer was added to each well using manufacturer's protocols. Luminescence was measured using a plate reader (BioTek Synergy H4 Hybrid Multi-Mode Microplate Reader, Winooski, VT). Simultaneously, to study bioactivity of released protein, supernatant from aggregates was also collected 24 hours after aggregate formation. 100 μL aliquots of each supernatant sample suspended over noncoated MLECs plated in monolayer at 50,000 cells/cm^2 in a 96-well plate and cultured for 24 hours. The following

day, 100 μL of ONE-GloTM Luciferase Assay buffer was added according to manufacturer's protocols and luminescence levels were measured using a plate reader (BioTek).

3.2.6 Statistical analysis

All values were reported as mean + standard deviation. For statistical analysis, one or two factor analysis of variance (ANOVA) was used to determine statistical significance of groups, and Tukey's post hoc multiple comparison test with significance set at $p<0.05$ indicated a significance between individual samples. Analysis was performed using Minitab (v.15.1, State College, PA).

3.3 Results

3.3.1 MSC spheroid coating

MSCs were successfully coated by using a multilayer technique with deposition of biotin and avidin to graft molecules of interest (heparin and a protein) onto their surfaces and subsequently formed into spheroids (Figure 3.1). Using a dimethyl methylene blue assay, it was seen that biotinylated heparin was 90.2% $\pm$ 3.9% sulfated when compared to native heparin. Additionally, nuclear magnetic resonance analysis revealed that the sugar structure was 53% conjugated with biotin at the carboxyl groups.

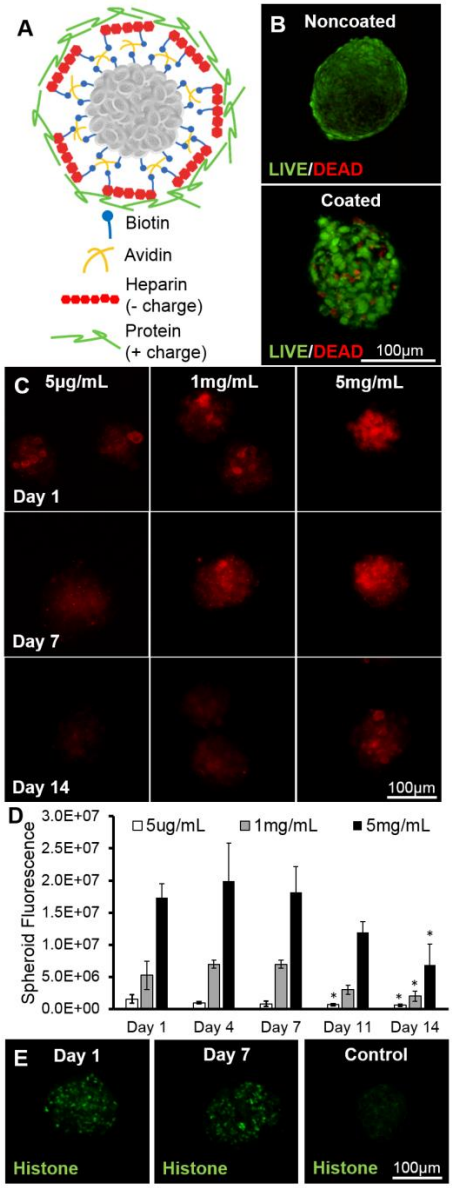

Figure 3.1.Characterization of heparin coating and histone loading via layer-by-layer deposition on cell surfaces. (a) Schematic of coating. (b) High cell viability in both coated and noncoated spheroids as visualized with flattened image of LIVE/DEAD staining. (c) Flattened images of Alexafluor 633-tagged heparin coating at 5 μg/mL, 1 mg/mL and 5 mg/mL coating concentrations over 14 days. (d) Quantification of fluorescence/spheroid from tagged heparin over 14 days. (e) FITC-histone loaded on heparin-coated cells at day 1 (left) and day 7 (middle) and non-heparin coated control cells at day 1 (right). *Statistically different from day 1 levels at the same concentration; $p < 0.05$; $n = 10–12$.

The viability of the resulting coated spheroids does not appear to be affected when compared to the viability of noncoated spheroids, as most of the cells in the aggregates in all cases were with calcein dye, indicating that the cells are live (Figure 3.1B). A higher initial coating concentration results in more heparin being grafted to cell surfaces throughout the entire spheroid when compared to spheroids coated with heparin at a lower concentration, seen by fluorescent quantification via image analysis (Figure 3.1C&D). Heparin fluorescence decreases over 14 days, resulting in approximately a 40% loss of heparin from all three groups when compared to the amount of heparin found on surfaces at day 1 (Figure 3.1D). After coating, a model positively-charged protein, histone (~19 kDa, pI = 8.5), tagged with FITC, was loaded onto spheroid cell surfaces. It was seen that histone was present on cell surfaces at day 1 and remained up to day 7. Without the intermediate biotin and avidin layers, heparin was not grafted to cell surfaces, resulting minimal protein loading on cell surfaces (Figure 3.1E).

3.3.2 Particle exclusion assay

Many cell surfaces are decorated with surface bound hyaluronan (a long, linear glycosaminoglycan) that acts to densely aggregate native proteoglycans (aggrecan, versican) that possess a very high negative charge. This hierarchical assembly of bottlebrushes of bottlebrushes anchored to the cell surface makes up the PCM [253, 254]. We performed a particle exclusion assay to determine if the native PCM is altered after multilayer coating of cell surfaces. Immediately after coating MSCs in monolayer (day 0), there was no PCM observed around coated cell membranes, as evidenced by the lack of separation between the beads and cell membrane, as opposed to the noncoated MSCs in which a PCM thickness of approximately 6 μm thick was observed (Figure 3.2A). 24

hours after coating (day 1), coated samples still did not indicate the presence of any PCM, while noncoated samples remained similar to the previous day.

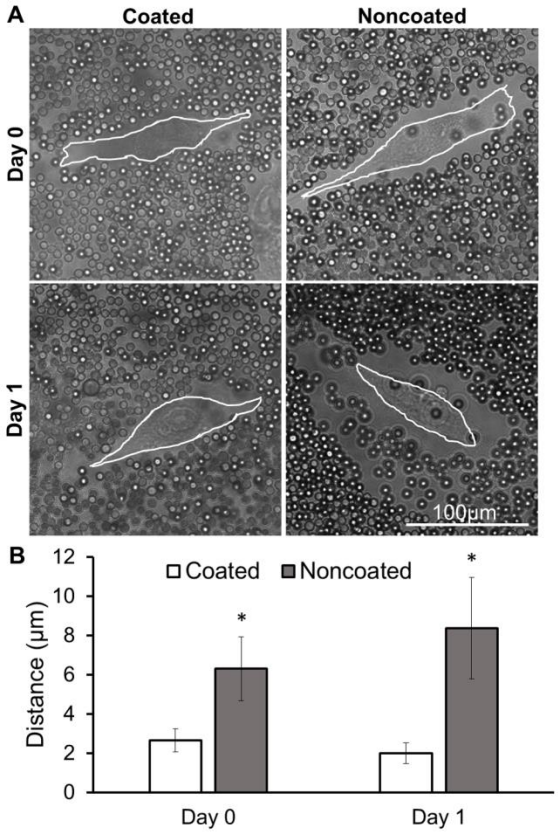

Figure 3.2 Particle exclusion analysis of coated and noncoated MSCs. (a) Phase images of coated and noncoated MSCs in monolayer with 3 µm passivated polystyrene microspheres. White lines outline cell surfaces. (b) Quantification of PCM thickness (distance between cell surface and microsphere layer). *Statistically different from coated samples on the same day; $p < 0.05$; $n = 18$.

Both immediately after coating and 24 hours after coating, noncoated samples had a significantly thicker PCM than coated samples (Figure 3.2B).

3.3.4 Monocyte anti-inflammatory co-culture assay

In this experiment, the effects of the heparin coating on MSC spheroid anti-inflammatory properties were studied through a monocyte co-culture assay. Both

noncoated and coated spheroids were able to attenuate the level of secreted TNF-α from LPS-activated monocytes significantly more than MSCs seeded in monolayer,

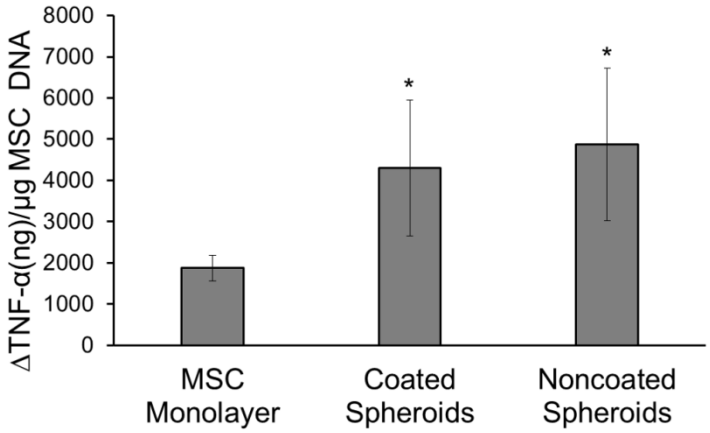

Figure 3.3 Degree of attenuation of TNF-α secretion by LPS-activated monocytes in co-culture with MSCs in monolayer, coated MSC spheroids, or noncoated spheroids (reported as a change from levels of TNF secreted from activated monocytes not in co-culture with MSCs divided by MSC amount in each culture as determined by picogreenTM assay). *Statistically different from MSC monolayer; $p < 0.05$; $n = 5$.

as seen by greater changes in TNF-α levels normalized to MSC DNA content (Figure 3.3). No difference was seen between the two spheroid groups.

3.3.5 TGF-β1 bioactivity (MLEC assay)

To study the biological activity of a protein localized to cell surfaces via heparin coating, MLECs were used as a biological reporter of loaded TGF-β1 activity. MLECs are a cell type that has been transfected with a luciferase reporter gene fused to plasminogen activator inhibitor-1 (PAI-1), which is expressed in response to TGF-β1. It has been seen that TGF-β1 activity results in a dose-dependent increase in the quantified luciferase activity [255]. First, it was seen that MLECs can be coated with heparin and formed into aggregates using the previously utilized methods, without having detrimental effects on cell viability (Figure 3.4A&B). When heparin was not present, there is minimal protein localized to cell surfaces (Figure 3.4C), however, when the heparin layer was

present, a positively charged model protein (histone) was observed on the surfaces of the cells (Figure 3.4D). Noncoated MLECs exhibited a dose-dependent response to

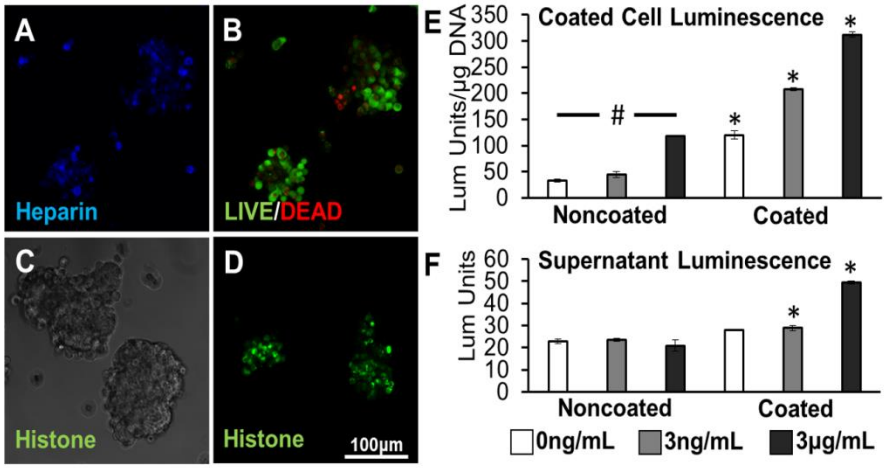

Figure 3.4 Coated MLEC aggregates loaded with TGF-β1. (a) Flattened image of Alexafluor 633-tagged heparin coating on MLEC aggregates after layer-by-layer deposition of biotin and avidin. (b) High cell viability in coated aggregates as visualized with flattened image of LIVE/DEAD staining. (c) No FITC-tagged histone is observed on control MLEC aggregates without heparin coating (phase image). (d) Flattened image of FITC-tagged histone loaded on heparin-coated aggregates. (e) Luminescence response of noncoated and coated MLEC aggregates after loading. (f) Luminescence response resulting from released supernatant from noncoated and coated MLEC aggregates collected 24 hours after TGF-β1 loading and aggregate formation. *Statistically different from noncoated samples at the same concentration; #statistically different from all other concentration samples within the same coating treatment; $p < 0.05$; $n = 4$.

TGF-β1 exposure. Coated MLECs had significantly higher luminescence reported when compared to noncoated samples at each loading concentration after 24 hours (Figure 3.4E). In a second bioactivity assay, supernatant collected from noncoated and coated MLEC aggregates 24 hours after protein loading was suspended over a different set of MLECs plated in 96-well plates. Supernatant collected from all noncoated spheroid groups 24 hours after formation elicited a low level of luminescence response that was not significantly different from each other. However, supernatants taken from TGF-β1

loading concentrations of 3 ng/mL or 3 μg/mL elicited a luminescence response significantly higher than their noncoated counterparts (Figure 3.4F).

3.4 Discussion

In this study, a multilayer assembly technique was applied to form a conformal coating of heparin on MSCs, with the ultimate goal of grafting a biomolecule of interest on cell surfaces that may control cell behaviors, such as differentiation. A similar technique has been used previously to graft unmodified heparin or thrombomodulin onto the surface of pancreatic islets to prevent blood-mediated inflammation or coagulation upon injection into the bloodstream [230, 234]. We have used a modification of this system to sequester a protein of interest onto the surface of cells that may act as a stimulus to guide cell fate after delivery. In this method, biotin is functionalized with a NHS group that targets cell surface amines. The grafted biotin can then bind avidin with high affinity and specificity. In the following layer, while heparin can electrostatically interact with the positively charged avidin, heparin has also been further functionalized with a biotin group that can interact with the presented avidin with higher affinity. As the outer layer, heparin's highly negative charge, resulting from the presence of multiple sulfate groups, facilitates the sequestration of positively charged biomolecules via electrostatic interactions [244].

The amount of heparin grafted on cells can be tuned by using different initial concentrations in solution. Given a fixed number of cells/spheroid, the coating concentrations chosen for this study represented levels that were below the theoretical saturation of heparin loaded onto the cell surfaces as a packed single layer (5 μg/mL),

close to saturation level (1 mg/mL), and well above saturation level (5 mg/mL) (calculations based on a cell diameter of 7.5 μm, cell surface area and heparin diameter of 10 nm) [256]. While it may be expected that the amount of heparin grafted would plateau near saturation at the 1 mg/mL concentration, the fact that increase in fluorescence beyond saturation concentration was observed (Figure 3.1C) suggests that multiple layers of heparin can be deposited onto the surface, perhaps mediated through both the avidin-biotin-heparin interactions and electrostatic interactions between avidin and heparin. These results indicate that it is possible to tune the amount of heparin that can be grafted to cell surfaces, and thus, ultimately control the amount of biomolecules being sequestered.

Over time, the heparin coating appeared to be removed from cell surfaces, as seen by lower levels of quantified fluorescence at later timepoints. While this loss could be attributed to several factors, we have observed that fluorescence of the same heparin coating in an acellular system does not decrease over time when placed in media (Supplemental Figure B.1). This leads us to believe that the loss of heparin is cell-mediated via secretion of enzymes that cleave heparin or via cell membrane turnover. Non-biotin-tethered heparin molecules could also be released due to diffusion into the surrounding media or exchange of ions with other charged molecules [257]. For all three concentrations, there was a 40% loss of heparin by day 14 when compared to the original amount on day 1. However, the rates of decrease were different, as a higher percentage of heparin was lost on earlier days for cells coated with 5 μg/mL, indicating that the kinetics of heparin loss are different depending on starting concentrations (Figure 3.1D). This discrepancy in release kinetics lends support to the idea of multiple heparin layers being

present when coated with a concentration above the theoretical saturation concentration, some of which may be less tightly bound through electrostatic interactions and therefore diffuses away from cell surfaces more quickly. To further characterize the heparin coating, the model protein, fluorescent histone, was used to image protein sequestration. Heparin coating facilitates the localization of a model positively charged protein, seen through imaging of histone, indicating that a biomolecule can be presented to MSCs via the heparin coating that may then act on to direct cell fate.

The PCM is composed predominantly of chondroitin sulfate-rich proteoglycans and hyaluronan. In its native form, the PCM can extend several microns from the cell surface and can play a role in cell interaction with the environment and cell adhesion [250, 254, 258]. It is important to study to presence of the PCM after the coating procedure to better understand what is being presented on the surface of the cells and how that may affect cell behavior [259]. The decrease in PCM thickness seen in coated cells compared to noncoated cells, observed in the particle exclusion assay, suggests that the coating procedure removed or collapsed (via crosslinking) the natural PCM found on cell surfaces.

It was also observed that, 24 hours after coating, an appropriate amount of time to allow the PCM to grow to its natural state in media [250], the native PCM did not grow back on coated cells (Figure 3.2B). This finding confirms that using our method, the resulting heparin coating can exist on cell surfaces for at least 1 day without being overwhelmed by the natural matrix, potentially allowing for control of what loaded biomolecules are presented to the cells during that time, while simultaneously

maintaining a high concentration of the loaded biomolecule near cell surface receptors for efficient signaling.

It has been shown that MSCs have anti-inflammatory properties and are able to act as modulators of lymphocyte [30, 260]. MSCs in spheroid form have enhanced anti-inflammatory characteristics when compared to single MSCs from monolayer culture [21]. The results from the co-culture experiments demonstrate the intrinsic anti-inflammatory properties of the MSCs are not affected during the coating process or by the coating itself as both spheroid samples exhibited enhanced properties over MSCs in monolayer (Figure 3.3). It has been shown that aggregation of MSCs results in the production of prostaglandin E2 (PGE2), tumor necrosis factor-inducible gene 6 protein (TSG-6) and stanniocalcin-1 (STC-1), molecules that can act on activated monocytes to decrease TNF-α secretion [252, 261]. PGE2 is a small molecule derivative of arachidonic acid and TSG-6 and STC-1 are large anti-inflammatory proteins (29 kDa and 25 kDa, respectively) that are not expected to penetrate through multilayers of negatively charged heparin [262-264]. However, in this assay, the highly negatively charged coating did not alter the MSC's ability to attenuate TNF-α production by monocytes, suggesting that sufficient anti-inflammatory signaling was still able to occur. On the other hand, clinical evidence has also shown that heparin administration has benefitted patients with pathologies that are associated with strong inflammatory response, such as asthma, ulcerative colitis and burns [265, 266]. A proposed mechanism of this anti-inflammatory property is inhibition of the transcription factor nuclear factor-κB (NF-κB) that promotes the expression of pro-inflammatory cytokines in monocytes [267]. Surprisingly, it was observed that a heparin coating on MSC spheroids does not increase the anti-

inflammatory properties in this study when compared to noncoated spheroids. A potential explanation is that heparin may not be released from cell surfaces in high enough concentrations after 3 days in culture to act on activated monocytes [267], or that the decrease in MSC anti-inflammatory secretion was compensated for by a direct anti-inflammatory effect of heparin, resulting in no overall change from noncoated spheroids. Further studies need to be performed to in order to fully study the effects of the heparin coating on changes to the anti-inflammatory secretome of MSC spheroids.

For this coating system to be effective in promoting cell differentiation, the protein must remain bioactive to act on cells or the surrounding environment. Therefore, after ascertaining that the coating was not deleterious to viability or anti-inflammatory properties of MSCs, we used a reporter cell line to study bioactivity of a growth factor (TGF-β1) sequestered to the heparin. MLECs are a cell line that is known to express PAI-1 in response to the specific presentation of TGF-β1 in the media or on cell surfaces. In these cells, the PAI-1 gene has been fused with a luciferase firefly reporter. Addition of TGF-β1 results in a dose-dependent increase of luciferase activity in the lysed cells, rendering this assay to be highly specific and sensitive [255, 268]. Utilizing the heparin coating, TGF-β1 was localized to the surfaces of MLECs and aggregates were formed with the coated cells (Figure 3.4A-D). When noncoated, aggregated MLECs were exposed to TGF-β1, the short term exposure during coating process resulted in a dose-dependent increase in luminescence, representing a cellular response to TGF-β1. This phenomenon reveals that aggregation of these cells does not impair their inherent response to TGF-β1 and that short term (30 minutes) exposure can activate luciferase expression.

While it is noted that the heparin coating itself, without TGF-β1 exposure, can upregulate luciferase activity (Figure 3.4E), it has not been previously studied if heparin directly affects the MLEC cell type. It is known that biotin (used in the coating procedure) can act as a coenzyme that is involved fatty acid synthesis, glucogenesis and catabolism of branched amino acids, but is unlikely to affect PAI-1 expression due to its specificity to TGF-β1 [269, 270]. When assaying the aggregates themselves, it is evident that the combination of TGF-β1 loading and heparin coating results in a luminescence response from the cells within the aggregate that is significantly higher than the luminescence response from noncoated samples and coated, non-loaded samples (Figure 3.4E) and that there are no effects of soluble heparin on activation of this cell line (Supplemental Figure B.2). While promising, further studies with a cell type that are not activated by the coating procedure are necessary to fully confirm the ability of the coating to facilitate signaling of a loaded growth factor to the cells.

With the coating present, the supernatant collected from coated aggregates that were loaded with either concentration of TGF-β1 can elicit a luminescence response from reporter MLECs that is significantly higher than noncoated samples treated at the same loading concentration (Figure 3.4F). These results provide evidence that presence of heparin may help preserve the bioactivity of the TGF-β1, as previous studies have shown that heparin complexes can protect proteins from enzymatic degradation and may potentiate presentation to its target receptor [244, 271, 272]. Such results are striking because in a control experiment, it was seen that when soluble heparin was present in the media during MLEC exposure to TGF-β1, luminescence response by the cells was significantly lower (Supplemental Figure B.3), suggesting that soluble heparin may not

preserve bioactivity of TGF-β1 in this assay and may even interfere with or inhibit signaling to the cells. Taken together, these data indicate that TGF-β1 can be released from the heparin coating in a bioactive form. This coating technique is advantageous over delivering soluble heparin with growth factors because the coating allows release over a longer period (in this case, at least 1 day), thus providing a sustained effect of preserving bioactivity of growth factors over time to interact with surrounding tissue. In contrast, the addition of soluble heparin will likely diffuse away and only have an effect immediately upon administration.

Based on these results, it is envisioned that the bioactive protein may be able to "signal out" to the neighboring cells and the surrounding environment to encourage regeneration, as well as potentially "signal in" and act on the cells to which it is sequestered to promote differentiation or other functions. Thus, this multifaceted system may be used to both prime cells for cell-mediated tissue regeneration and modulate the damaged tissue environment after implantation.

3.5 Conclusions

Through these studies, we have developed a multilayer coating system to graft heparin and facilitate protein sequestration onto cell surfaces. Results demonstrate that MSC spheroids can be coated without negatively affecting cell viability and anti-inflammatory properties. Positively-charged proteins bind preferentially to the coated cells and an assay with a reporter cell line suggests that TGF-β1 remains bioactive after sequestration and release. In the future, this simple and efficient method of presenting growth factors to stem cell aggregates may have significant implications in enabling local

signaling between transplanted cells and surrounding tissue post-injection. Moreover, the ease of the chemistries employed makes this technique amenable to attaching other bioactive molecules (antibodies, enzymes) to stem cell aggregate surfaces. As such, the methods presented here represent an exciting platform with sufficient flexibility to maximize the therapeutic effect of injected stem cells in ways that could be tailored to the needs of a particular pathology.

CHAPTER 4

RESPONSE OF HUMAN MSC AGGREGATES TO GROWTH FACTORS IS AFFECTED BY THE SULFATION LEVEL OF HEPARIN USED AS A CELL COATING

4.1 Introduction

Mesenchymal stem cells (MSCs) are currently being utilized in over 350 National Institute of Health-registered clinical trials treating pathologies ranging from graft versus host disease and diabetes to bone and cartilage injuries [5, 6]. Their ability to differentiate down multiple lineages and/or secrete trophic factors makes MSCs a promising cell source to regenerate tissue and treat a variety of diseases [1, 2, 162]. However, in these trials, one to five doses of 2,000,000-8,000,000 cells are required for administration; thus, for these multipotent cells to be a viable option, mass expansion is needed [6]. Additionally, for certain applications, precise control of differentiation of these multipotent cells is required to ensure that a homogenous cell population is delivered [4]. To achieve cell proliferation and differentiation, growth factors such as fibroblast growth factor-2 (FGF-2) and transforming growth factor-β1 (TGF-β1) can be employed. FGF-2 is a common mitogenic growth factor used to promote proliferation for multiple cell types, including MSCs, fibroblasts and endothelial cells and plays a crucial role in MSC self-renewal [273-276], while TGF-β1 is a growth factor typically used to induce chondrogenesis in MSCs [111].

In addition to growth factor supplementation, different MSC culture platforms can affect both MSC proliferation and differentiation. For example, pellet systems (25,000

cells) have traditionally been used to study chondrogenic differentiation of MSCs, however, recent interest in smaller MSC aggregates (500-1000 cells) with smaller diameters has increased because of their ability to be used as injectable therapies treatment of cartilage injuries and disease [79, 107, 277]. Additionally, it has been shown that MSCs aggregated into spheroid form ranging from 500-250,000 cells have the ability to attenuate inflammatory cytokine secretion and secrete higher levels of anti-inflammatory molecules when compared to their monolayer counterparts [21, 85]. Although MSC aggregates such as these seem like a promising platform for effective cell-based therapies, the challenge of lack of proliferation in spheroid culture may hinder the scale-up of MSC aggregate systems [14]. Additionally, due to the 3D structure of formed aggregates, exogenous growth factors supplemented to the culture medium may not be exposed the entire cell population, especially the cells found on the interior of the aggregate.

To address these potential limitations in MSC aggregate culture, incorporation of sulfated glycosaminoglycans (GAGs), such as heparin, within an aggregate can be used as a potential vehicle to promote growth factor availability due to the GAGs' high negative charge that facilitates local electrostatic interaction with positively charged proteins [16, 158, 178, 210, 278]. Such a concept would mimic the actions of heparin sulfate proteoglycans (HSPGs) typically found on the plasma membrane of a cell and within the ECM [19, 166]. HSPGs play a role in regulation of signaling factor activity and can act as co-receptors for various growth factor receptors to lower receptor activation or alter duration of the signaling reactions [19, 166]. Because the interaction between heparin and its growth factors depends on the presence of the negatively charged

sulfate groups, desulfation of the GAG can modulate the interaction with a positively charged protein [158]. Specifically, it has been seen that desulfation of heparin can affect affinity for FGF-2 and TGF-β1 and the growth factors' subsequent bioactivity [178, 186, 199], but it remains unclear what effects GAGs of different sulfation levels may have on aggregate cell culture with growth factor supplementation.

To incorporate GAGs into a 3D aggregate, we have previously developed and characterized a GAG cell coating that sequesters positively charged proteins onto cell surfaces [279]. We have shown that through layer-by-layer deposition of biotin and avidin, biotinylated heparin has been grafted onto cell surfaces at different concentrations without negatively affecting cell viability and inherent anti-inflammatory properties of MSC aggregates. When loaded onto aggregates of heparin-coated cells, TGF-β1 remains bioactive and has the ability to signal to surrounding cells upon release [279]. While characterization of this heparin coating has been performed, effects of a heparin coating on cell response to growth factors in long-term culture have not been explored. Moreover, because the electrostatic interactions between heparin and growth factors are necessary for binding and signaling, decreasing the sulfation level of the coating may provide insight into how these interactions can play a role in the subsequent cellular response.

Thus, the objective of this paper is to characterize heparin MSC coatings of two different sulfation levels (native sulfation and fully desulfated) and study the effect of these coatings on MSC response in the presence of two different growth factors supplemented to the culture media, as would be found in traditional cell culture approaches for stem cell therapies. To evaluate the coating effect, MSC aggregates were

coated with either heparin or desulfated heparin and then cultured in serum-free media containing FGF-2 or TGF-β1. Over 21 days *in vitro*, cell morphology was characterized using histological staining, cell number was determined using a DNA assay, and chondrogenic differentiation was evaluated using quantitative reverse transcription polymerase chain reaction (RT-PCR) and immunohistochemical (IHC) staining for chondrogenic extracellular (ECM) components. In these studies, we hypothesize that the strong electrostatic interaction between heparin and the positively charged growth factors in the vicinity of the cells will promote growth factor availability, and therefore, the fully sulfated heparin coating will result in higher cell number in response to FGF-2 and to greater chondrogenic differentiation in response to TGF-β1, compared to the desulfated heparin coating and a noncoated control.

4.2 Materials and Methods

4.2.1 Heparin derivative synthesis

Desulfation of heparin was performed using a previously published protocol [165]. Briefly, heparin was mixed at 5 mg/mL in methanol (VWR, Radnor, PA) containing 0.5% v/v acetyl chloride (Thermo Fisher Scientific, Grand Island, NJ). A methyl ester of heparin product was synthesized by acidic methanol treatment for 6 days. The product was dissolved in H_2O and precipitated in an excess of 95% ethanol on ice. The methyl ester product was then precipitated in ethyl ether (Thermo Fisher Scientific) and vacuum dried using lyophilization (-40ºC at 0.120 mmHg). Demethylation was performed by 0.1 M potassium hydroxide treatment for 24 hours to produce the final desulfated heparin, which was precipitated in ethanol and ethyl ether and vacuum dried via lyophilization. To produce biotinylated GAGs, heparin was dissolved in water at 2

mg/mL and conjugated with biotin by reacting N-(3-dimethylaminopropyl)-N′-ethylcarbodiimide (EDC) (Sigma Aldrich, St. Louis, MO), hydroxybenzotriazole (HoBT) (VWR) and biotin-hydrazide (Sigma Aldrich) at a molar excess compared to heparin of 0.4 for all reagents for four hours at pH5. Desulfated heparin was dissolved at 2 mg/mL and reacted with EDC, HoBT and biotin-hydrazide at a molar of 3:3:8, respectively, for four hours at pH 5. Each reaction solution was dialyzed for two days in 3500 MWCO dialysis tubing (Spectrum, Rancho Dominguez, CA) followed by flash freezing and vacuum drying via lyophilization for two days. All heparin products were stored at -20ºC.

4.2.2 Proton nuclear magnetic resonance (^{1}H NMR) characterization

^{1}H NMR was used to assess level of sulfation after solvolytic desulfation of heparin and used to determine conjugation efficiency following biotinylation of heparin derivatives. Approximately 5 mg/mL of each product was dissolved in deuterated water and ^{1}H NMR experimented were conducted on a Bruker Avance III 400 spectrometer at 400MHz. The resulting spectra were analyzed with ACD NMR Processor software (Version 12). Spectra can be seen in Appendix D.

4.2.3 MSC expansion

MSCs derived from human bone marrow aspirates were obtained from the Texas A&M Health Sciences Center. Cryopreserved MSCs from three different donors (2 males, 1 female; ages 22, 24 and 37) were thawed and expanded in α-Minimum Essential Medium (Mediatech, Herndon, VA) containing 16.5% fetal bovine serum (FBS, Atlanta Biological, Atlanta, GA), 2 mM L-glutamine (Mediatech), 100 units/mL penicillin and 100 μg/mL streptomycin (Mediatech) under normoxic conditions (37ºC, 5% CO_2 and

20% O_2) . Media were changed every 2–3 days until 80% confluence and were used at passage 3.

4.2.4 Cell coating, aggregate formation, and culture

After lifting with 0.05% trypsin (Mediatech), MSCs were washed in phosphate buffered saline (PBS, Life Technologies, Grand Island, NY) two times and then modified with a glycosaminoglycan by multilayer assembly of biotin and avidin layers, as previously described [279]. Briefly, cells were first cultured in 4 mM EZ-Link Sulfo-NHS-LC-Biotin (Pierce, Rockford, IL) in PBS, followed by 0.5 mg/mL avidin in PBS (Life Technologies, Carlsbad, CA), and lastly 5 mg/mL biotin-conjugated heparin (Hep) or biotin-conjugated desulfated heparin (Hep-) in PBS (Process outlined in Figure 1A). Each incubation step with cells was performed in a 24-well Ultra-Low Attachment Surface plate (Corning) for 30 minutes at 37°C on a rotary orbital shaker plate at 65rpm. Once cells were coated with their respective glycosaminoglycan layers, 2000 cells in 200 μL were pipetted into each well of a 5% Pluronic-coated 96-well V-bottom plate to form individual aggregates. Plates were spun down at 200 rcf to promote spheroid formation in serum free media composed of Dulbecco's Modified Eagle Medium, 1% nonessential amino acids, 1% antibiotic/antimycotic, 1% insulin, human transferrin and selenous acid premix (BD Biosciences, San Jose, Calif., USA) and 50 μg/ml ascorbate-2-phosphate (Sigma-Aldrich). Aggregates were cultured in serum free conditions in the V-bottom wells with either 10 ng/mL of FGF-2 (R&D Systems, Minneapolis, MN) for DNA content assay or 10 ng/mL or TGF-β1 (Peprotech, Rocky Hill, NJ) and 100 nM dexamethasone (Sigma-Aldrich) for chondrogenic differentiation assays. Aggregates for

chondrogenic differentiation were cultured under hypoxic conditions (37ºC, 5% CO2 and 3% O2 and N2).

4.2.5 Chromatography analysis of cell coating solutions

To quantify amount of GAG grafted to cell surfaces, supernatants were obtained immediately after GAG incubation of single cells prior to aggregate formation. Quantification of Hep or Hep- that was remaining in the supernatant was analyzed using a high-performance liquid chromatography system (Shimazdu, Columbia Maryland). Duplicate samples were run in a 150 mM magnesium sulfate and 10 mM Tris base buffer through a TSK-GEL G4000PWX1 column (Tosoh Bioscience, King of Prussia, PA) for 30 minutes at a flow rate of 1 mg/mL. Eluted samples were detected using a UV detector at the wavelength of 256 nM. GAG concentration in each sample was calculated using a standard of known concentrations ranging from 0.05 mg/mL-5 mg/mL for both Hep and Hep- polymers. The amount of Hep or Hep- grafted onto cells was normalized to the cell number for that coating group (n=3).

4.2.6 Histological staining

At appropriate timepoints, MSC aggregates were collected and washed with PBS to remove excess media. Aggregates were fixed in 10% neutral buffered formalin (Thermo Fisher Scientific) for 15 minutes and embedded in Histogel (Thermo Fisher Scientific) before subsequent incubation in increasing sucrose solution concentrations up to 15% under vacuum (–25 in Hg). Samples were then vacuum infiltrated with increasing concentrations of 20% sucrose:optimal cutting temperature compound solutions (4:1 to 1:2 volume ratios). After overnight infiltration, samples were embedded in optimal cutting temperature compound and frozen in mixture of dry ice and 100% ethanol [111].

Samples were stored at –80°C and cryosectioned at 10 μm thickness (Cryostar NX70; Thermo Fisher Scientific) prior to staining with hematoxylin & eosin (H&E).

4.2.7 DNA quantification

At appropriate timepoints, MSC aggregates were collected and washed with PBS three times to remove excess media. Aggregates were dissociated by incubation in 200 μL 0.05% trypsin for 20 minutes and mechanical disruption by pipetting. Samples were spun down at 6000 rcf and collected cells were washed with PBS 1x before storing in 500 μL of water containing 0.1% Triton-X100 (Sigma Aldrich) at -20ºC. Samples were subjected to three freeze-thaw cycles, in which samples were placed in a sonicating bath containing ice for 30 minutes, followed by freezing in the -80ºC freezer for 1 hour. Upon removal from the freezer, samples were thawed to room temperature for 30 minutes before repeating sonication and freezing cycle. Once samples were ready, DNA content was assayed using a CyQUANT® Cell Proliferation Assay (Life Technologies), according to manufacturer's protocol. Samples were read at excitation 485 nm, emission 525 nm by a plate reader (Biotek Synergy H4 Hybird Multi-Mode Microplate Reader, Winooski, VT) and DNA amount was determined using a standard curve of DNA. Data is reported as the DNA amount normalized to each group's initial amount at day 1 (n=8).

4.2.8 Gene expression analysis (RT-PCR)

Over the course of 21 days, MSC aggregates were collected for gene expression analysis and lysed with RLT lysis buffer (Qiagen, Hilden, Germany). Each sample (n=1) contained three individually cultured aggregates to provide enough RNA for analysis. Cell lysates were filtered with QIAshredder tissue homogenizer and RNA was extracted with RNAeasy kit (Qiagen). Reverse transcription was performed using SuperScript III

Reverse Transcriptase (Invitrogen) with Oligo$(dT)_{15}$ primers and nucleotides (Promega, Madison, WI). Primers were custom designed to target human mRNA for β-actin, 18s ribosomal protein, Sox9, collagen II, aggrecan, collagen I, collagen X, Runx2 and PPARγ2 (Table 1). Quantitative RT-PCR amplification for each gene was performed on a StepOnePlus System (Applied Biosystems, Carlsbad, CA) with SYBR Green Master Mix (Applied Biosystems). Raw amplification values were processed in LinReg software (v13.1, Amsterdam, Netherlands) to individually determine PCR efficiency and fold regulation relative to noncoated day 1 samples was determined for each sample with β-actin and 18s used as housekeeping gene controls (n=3-4).

Table 4.1. Human primer sequences for quantitative PCR.

Target	Marker		Primer Sequences (5'→ 3')	GenBank
β-actin	Housekeeping	F	GCAGTCGGTTGGAGCGAGCATCCCC	NM_001101
		R	TCCCCTGTGTGGACTTGGGAGAGGAC	
Ribosomal 18s	Housekeeping	F	CGATGGGCGGCGGAAAATAGCCTTTGC	NM_022551
		R	CAGTGGTCTTGGTGTGCTGGCCTCGG	
Sox9	Chondrogenic	F	GCGGAGGAAGTCGGTGAAGAACGGGCA	NM_000346
		R	TGTGAGCGGGTGATGGGCGGG	
Collagen II	Chondrogenic	F	ACCCCAATCCAGCAAACGTT	NM_001844
		R	ATCTGGACGTTGGCAGTGTTG	
Aggrecan	Chondrogenic	F	ACAGCTGGGGACATTAGTGG	NM_001135
		R	GTGGAATGCAGAGGTGGTTT	
Collagen I	Fibroblastic	F	GAAAACATCCCAGCCAAGAA	NM_000089
		R	GCCAGTCTCCTCATCCATGT	
Collagen X	Hypertrophic Chondrocyte	F	GGCCCAGCAGGAGCAAAGGG	NM_000493
		R	GTGGCCCGGTGGGTCCATTG	
Runx2	Osteogenic	F	GTGCAGAGTCCAGCAAAGGT	NM_199173
		R	AGCAGAGCGACACCCTAGAC	
PPARγ2	Adipogenic	F	TCCATGCTGTTATGGGTGAA	NM_015869
		R	GGGAGTGGTCTTCCATTACG	

4.2.9 Immunofluorescent staining for matrix molecules

Immunostaining for ECM deposition in cryosectioned samples was performed using primary monoclonal antibodies for collagen II, aggrecan, collagen X and collagen I (Abcam, Cambridge, UK; collagen X from Sigma Aldrich). Antigen retrieval was performed for all sections by incubating in 20 μg/ml proteinase K (Sigma-Aldrich) for 10 minutes at 37°C. Samples for aggrecan and collagen X immunostaining were deglycosylated with 0.75 U/ml chondroitinase ABC (Sigma-Aldrich) for 1.5 hours at 37°C. Samples were blocked with Image-iT FX signal enhancer (Life Technologies) and incubated with the primary antibodies overnight at 4°C (1:20 dilution for all primary antibodies). Secondary antibody binding with Alexa Fluor 488-conjugated goat polyclonal anti-mouse IgG (Molecular Probes, Carlsbad, California) at room temperature

for 1 hour (1:200 dilution). Lastly, samples were stained with Hoechst (Sigma-Aldrich) for 5 minutes at room temperature to visualize cell nuclei (n=12).

4.2.10 Statistical Analysis

Quantitative data was transformed to fit a normal distribution using Box-Cox transformations, followed by a one-way and two-factor analysis of variance with Tukey's post hoc multiple comparisons test ($p<0.05$) to determine statistical significance between samples in Minitab (v.15.1, State College, PA). Quantitative data are reported as mean $\pm$ standard deviation.

4.3 Results

4.3.1 Coating characterization on MSC aggregates

Using ^{1}H NMR analysis, it was confirmed that solvolytic treatment of heparin resulted in removal of all sulfate groups. Furthermore, post biotinylation conjugation, ^{1}H NMR also determined that both heparin and desulfated heparin species were both biotinylated with a conjugation efficiency of approximately 20%. Based on chromatography analysis, at a coating concentration of 5 mg/mL of both heparin species, $9.89x10^{-7}\pm1.37x10^{-7}$ mg GAG/cell of Hep and $8.53x10^{-7}\pm2.63x10^{-8}$ mg GAG/cell of Hep- was grafted onto cell surfaces.

4.3.2 Histological staining of MSC aggregates

H&E staining revealed that the morphology of coated aggregates is distinct from noncoated aggregates. MSCs within aggregates coated with Hep and Hep- exhibited rounded cell morphology (Figure 4.1B, black arrows). This behavior persisted through day 14, at which rounded cell morphologies were still observed. Coated aggregates

cultured in media containing the growth factors FGF-2 or TGF-β1 also exhibited similar rounded cell morphology that persisted through 14 days in culture (data not shown).

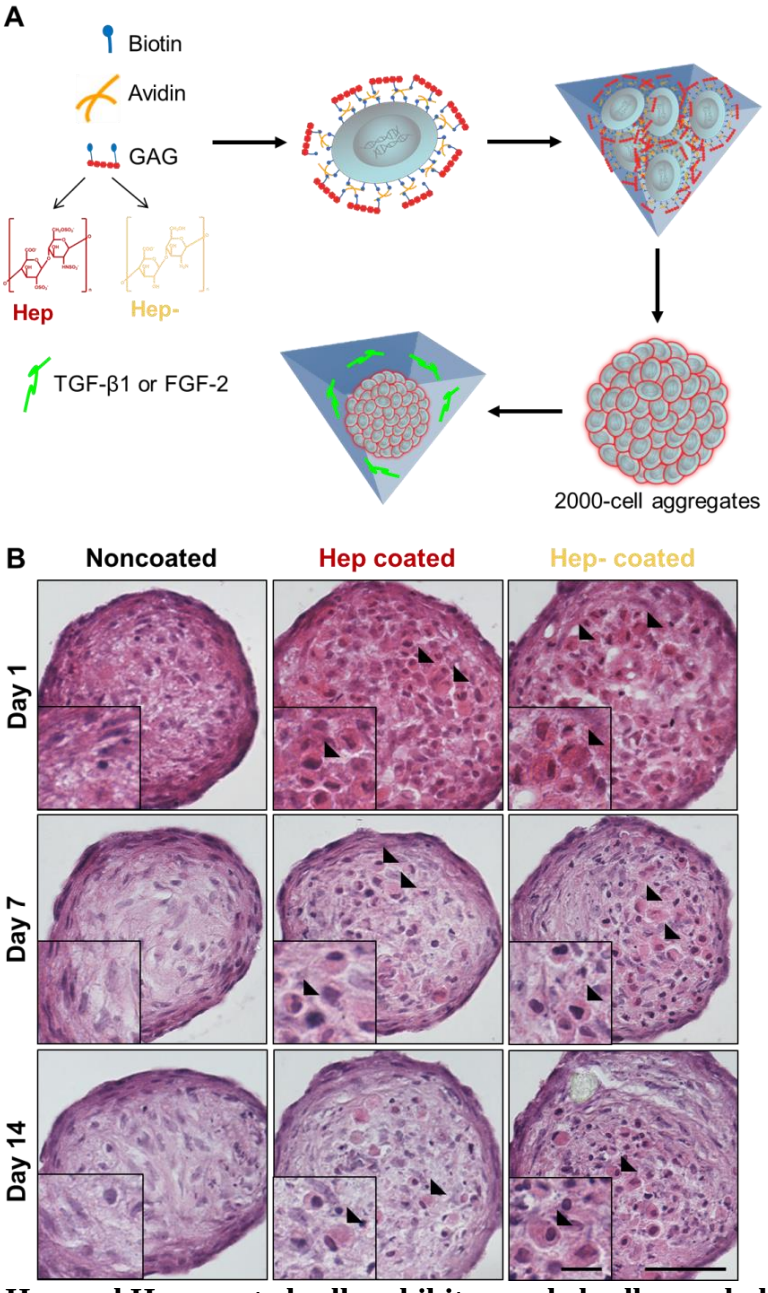

Figure 4.1. Hep and Hep- coated cells exhibit rounded cell morphology within aggregates. A) Schematic of layer-by-layer coating technology and MSC aggregate formation. B) H&E staining demonstrates rounded cell morphology observed in coated aggregates at day 1, 7 and 14. Arrowheads indicate cells with rounded morphology within the aggregate. Scale bar = 100µm, inset scale bar = 25µm, n=8.

4.3.3 Effect of GAG coatings on DNA content in MSC aggregates

DNA content assay of noncoated and coated aggregates revealed that the addition of FGF-2 caused an initial increase in DNA amount 7.2±1.9 fold for Hep coated aggregates, which was significantly higher than the other two groups (2.54±0.3 fold and 4.11±0.8 fold for Hep- and noncoated aggregates, respectively) at day 4 (Figure 4.2).

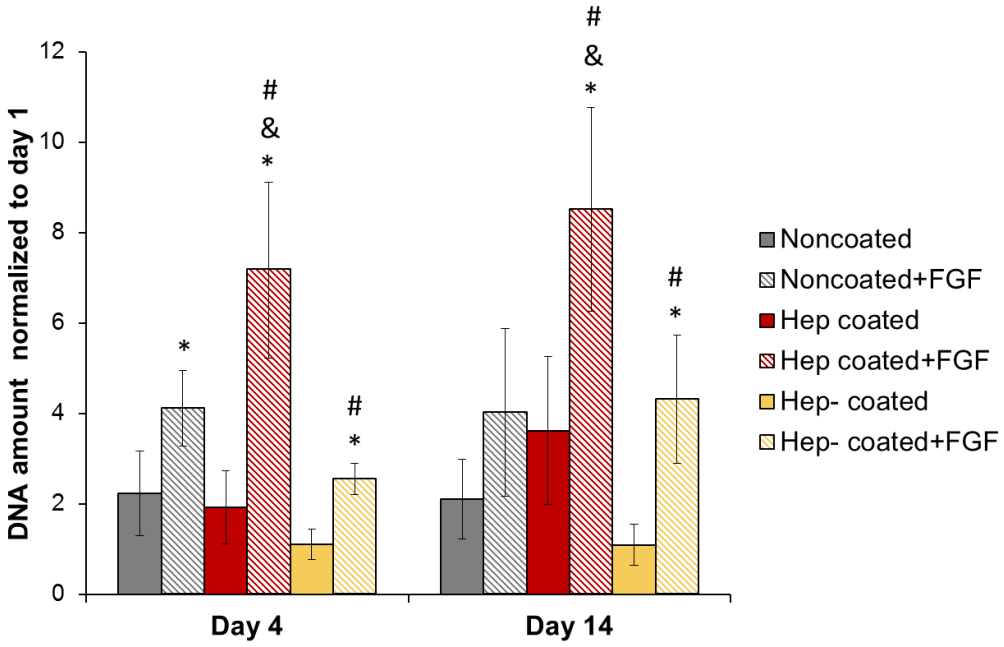

Figure 4.2. DNA content of Hep coated aggregates cultured with FGF-2 is significantly greater at day 4 and day 14 compared to other groups cultured with FGF-2. * indicates significant difference from respective coating group without FGF on same day; & indicates significant difference from noncoated and Hep- coated cultured with FGF on same day; # indicates significant difference from same group at day 1. Data reported as average mean ± standard deviation, $p<0.05$, n=8.

At day 14 with FGF-2 exposure, while noncoated aggregates only had a 2.1±0.9 fold increase in amount DNA, Hep coated aggregates increased 8.5±1.6 fold, and Hep- coated aggregates increased 4.3±1.4 fold, both of which were significantly higher compared to their respective group without FGF-2 and their respective group at day 1. At day 14, MSCs cultured without FGF-2 had DNA increases of 2.1±0.9 fold in noncoated

aggregates, 3.6±1.6 fold in Hep coated aggregates and 1.1±0.5 in Hep- coated aggregates, all of which were not significantly higher compared to their respective day 1 value.

4.3.4 Effect of GAG coatings on chondrocytic gene expression in MSC aggregates

Gene expression revealed that when noncoated and Hep and Hep- aggregates were cultured with TGF-β1 under hypoxia, MSCs from Hep- coated aggregates demonstrated an 86.5±7.5 fold upregulation of collagen II expression, which was significantly greater than the 37.7±10.6 fold increase for Hep coated aggregates and the 15.1±4.7 fold increase in noncoated aggregates at day 21 (Figure 4.3A). At day 14, collagen II expression in Hep- coated aggregates was significantly increased compared to noncoated aggregates, while this was not observed Hep coated aggregates. Aggrecan expression was significantly upregulated compared to the day 1 level at day 7 in Hep coated aggregates only (8.26±4.3 fold), however, it did not significantly increase further over time (19.3±5.4 fold at day 21). For Hep- coated aggregates, aggrecan expression was significantly upregulated (15.9±7.7 fold) only at day 21 (Figure 4.3B) and was not significantly different than the expression levels observed in Hep coated aggregates. Interestingly, Sox9 expression was not detected over the course of the 21 days for all samples (data not shown).

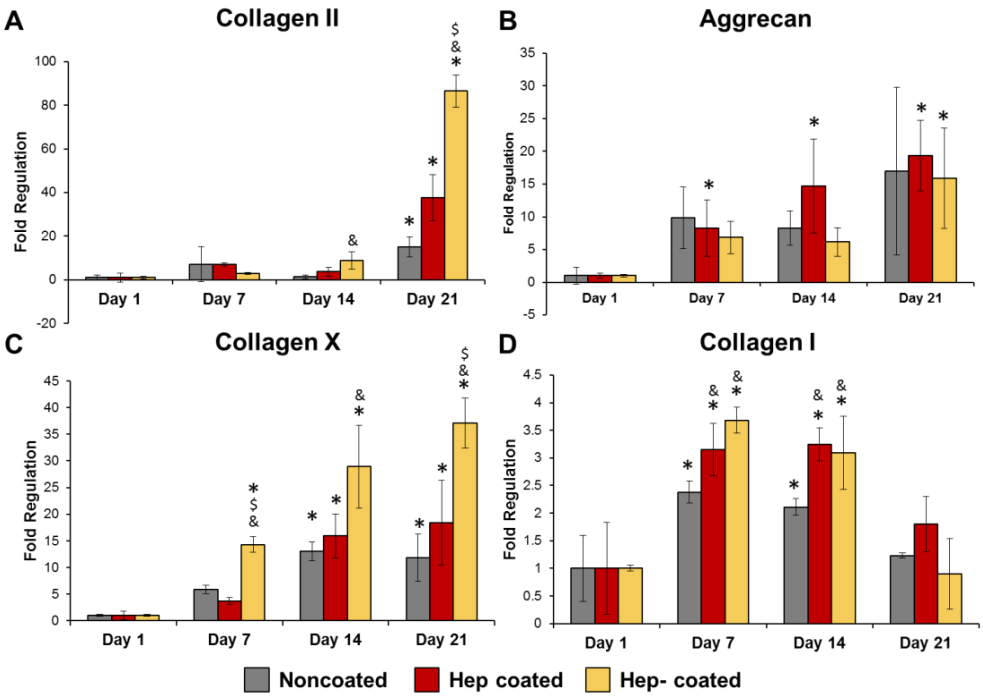

Figure 4.3. MSC aggregates coated with Hep- upregulate gene expression for collagens II and X compared to noncoated and Hep coated controls. Summary of gene expression for (A) collagen II and (B) aggrecan gene expression, markers for chondrocytic differentiation, (C) collagen X gene expression, a marker for chondrocyte hypertrophy and D) collagen I gene expression, a marker for fibroblast/fibrochondrocyte differentiation. * indicates significantly greater than respective coating group at day 1. & indicates significantly greater than noncoated on same day. $ indicates significantly greater than Hep coated on same day. Data reported as average mean ± standard deviation, p<0.05, n=3-4.

Collagen I expression, indicative of fibroblastic differentiation, initially increased by day 7 but by day 21 was only expressed at 1.2±0.1 fold in noncoated groups, 1.8±0.5 fold in Hep coated groups and 0.8±0.6 fold in Hep- group (Figure 4.3D), all of which were not significantly different from each other or compared to day 1. At day 7, Hep and Hep- coated aggregates had significantly upregulated expression of collagen I (3.14±0.5 fold and 3.68±0.2 fold, respectively) when compared to noncoated aggregates (2.37±0.2 fold). Collagen X expression, an ECM marker of hypertrophic chondrocytes, gradually increased over time for all groups but was significantly upregulated in Hep- coated

aggregates over both noncoated and Hep coated aggregates at day 21. Hep- coated aggregates exhibited a 37.1±4.7 fold upregulation on day 21 compared to an 18.4±8 fold regulation in Hep coated and 11.8±4.4 fold regulation in noncoated (Figure 4.3C). By day 14, all groups had significantly upregulated expression of collagen X compared to its respective day 1 level (13.1±1.8 for noncoated, 15.91±0.3 for Hep coated and 28.9±7.7 for Hep- coated), however, only Hep- coated aggregates exhibited significant upregulation compared to the other two groups at that timepoint and its day 1 level as early at day 7 (14.28±1.4 fold). No trends in expression levels were observed for Runx2, an osteogenic marker, and PPARγ2, an adipogenic marker, over time for all groups (data not shown).

4.3.5 Effect of GAG coatings on chondrocytic ECM deposition in MSC aggregates

Immunostaining was performed to visualize specific ECM component deposition. On day 14, coated groups exhibited similar levels of staining for collagen II and appeared slightly stronger compared to noncoated aggregates (Figure 4.4). This increase in deposition for coated groups was observed as early as day 14. Additionally, at day 14, there appeared to be increased aggrecan staining in all samples, however, at day 14 and 21, coated groups seemed to demonstrate stronger positive staining compared to noncoated samples (Figure 4.5). Positive staining for collagen X was obvious for all groups by day 14, at which time, differences could already be discerned between noncoated and coated aggregates. By day 21, Hep- coated aggregates exhibited pockets of pericellular collagen X, which was not observed for noncoated and Hep coated aggregates (Figure 4.6, insets). Collagen I staining was detected throughout all noncoated

and coated aggregates, however, the staining intensity was not observed to change over the course of 21 days within each group (Supplemental Figure B.8).

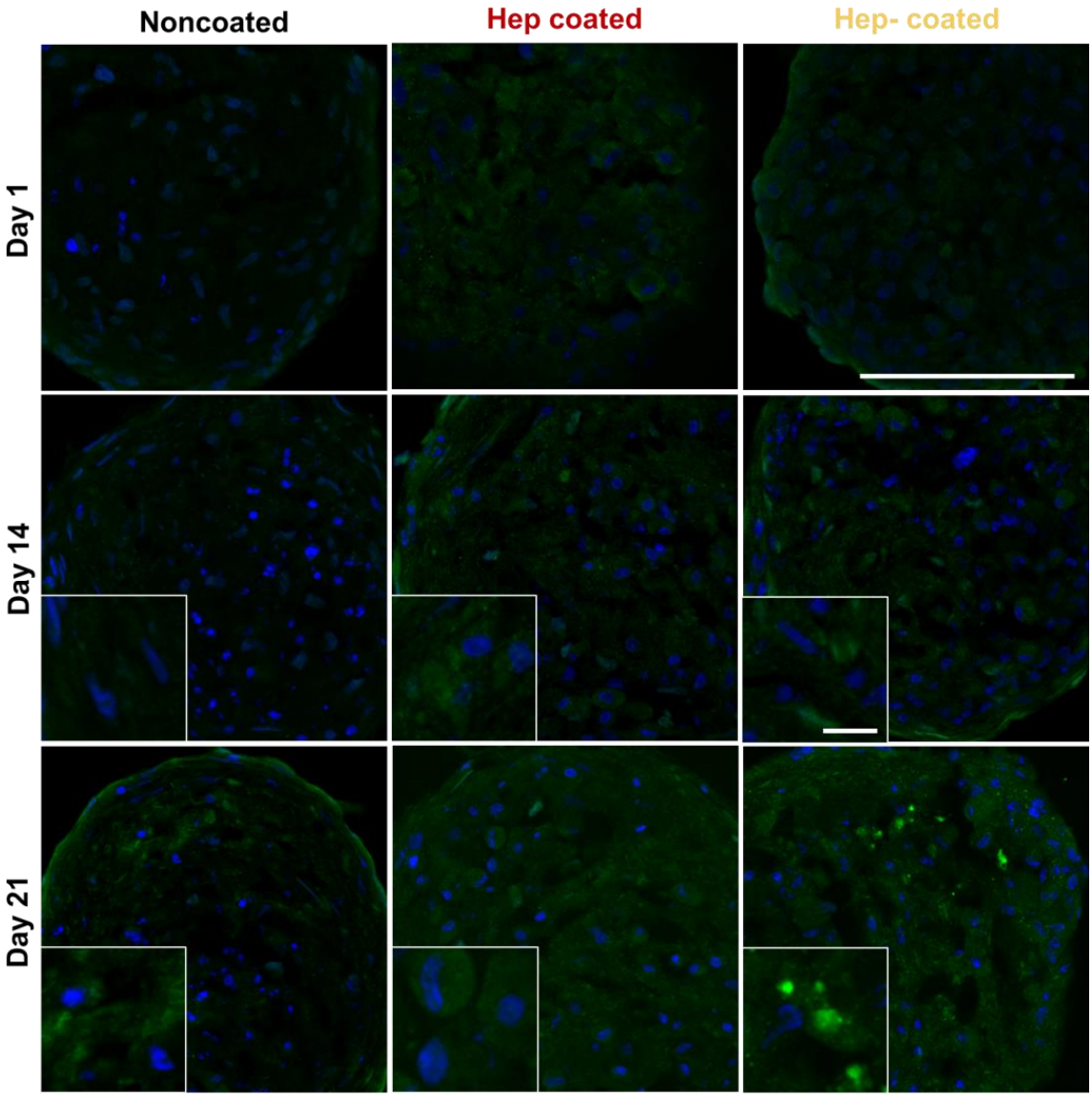

Figure 4.4. Positive immunofluorescent staining of collagen II observed over 21 days for all aggregates, however Hep and Hep- coated aggregates exhibited stronger staining compared to noncoated aggregates at day 21. Collagen II is seen in green and cell nuclei are stained blue. Scale bar = 100µm, inset scale bar = 10µm, n=12.

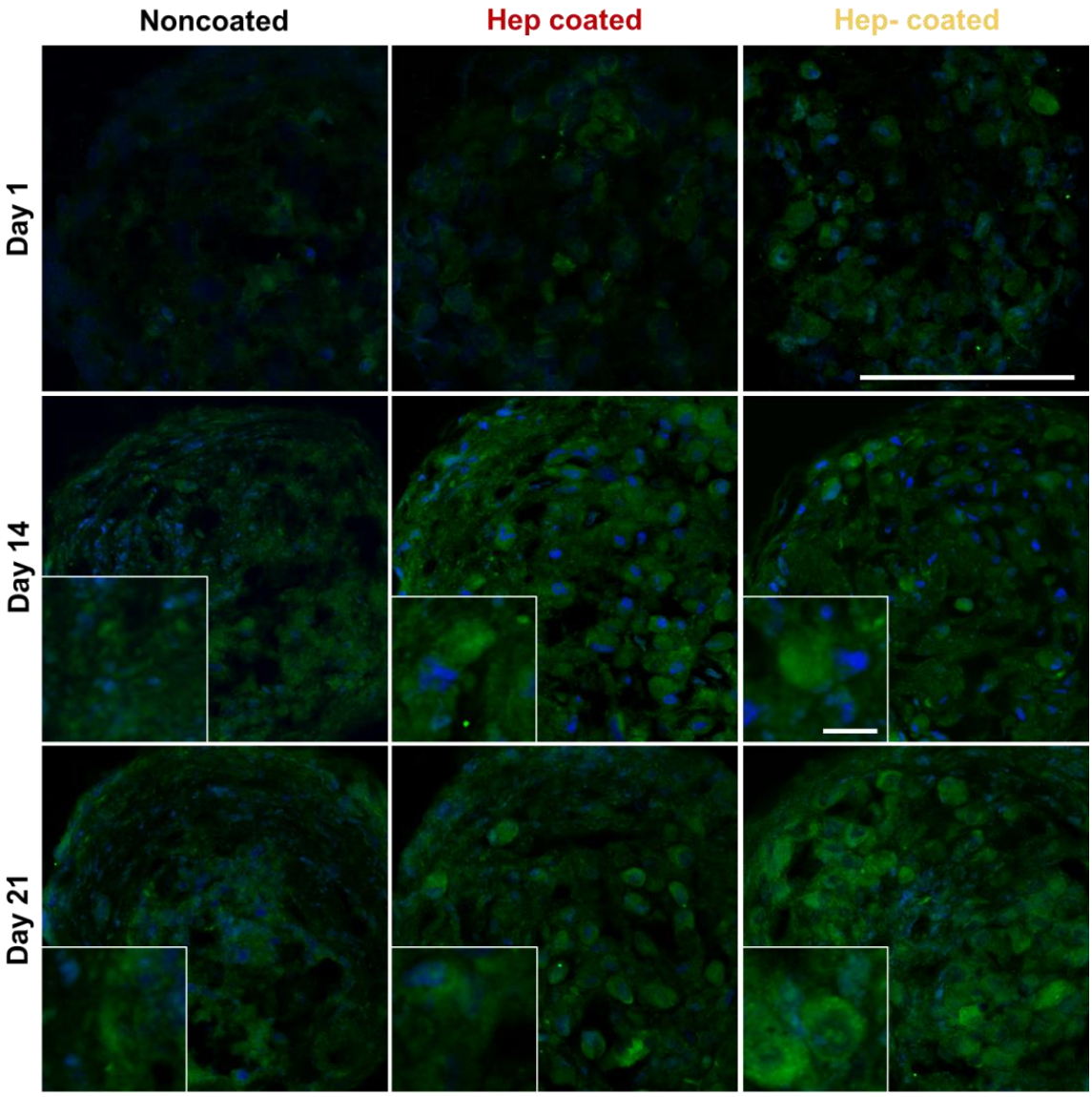

Figure 4.5. Positive immunofluorescent staining for aggrecan observed at day 14 for all aggregates. Aggrecan is seen in green and cell nuclei are stained blue. Scale bar = 100µm, inset scale bar = 10µm, n=12.

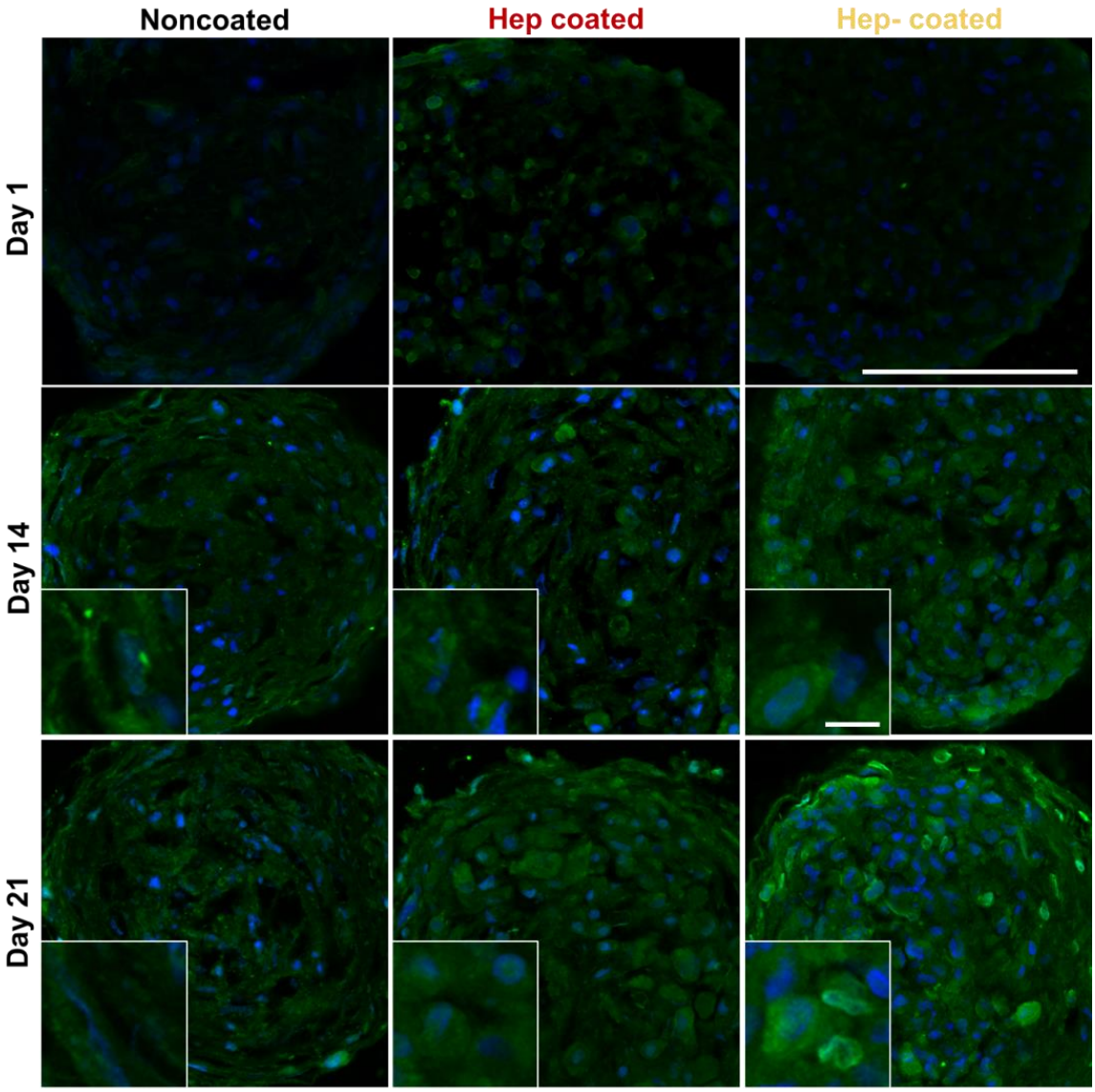

Figure 4.6. Positive immunofluorescent staining for collagen X observed at day 14 for all aggregates, and Hep- coated aggregates exhibited stronger staining compared to Hep coated and noncoated aggregates at day 21. Collagen X is seen in green and cell nuclei are stained blue. Scale bar = 100µm, inset scale bar = 10µm, n=12.

4.4 Discussion

In this study, we have demonstrated the ability to coat MSC surfaces with different heparin species (Hep and Hep-) using an established layer-by-layer technology. Via chromatography analysis, the same GAG concentration (5 mg/mL) in the coating

solution resulted in similar amounts of each heparin species grafted onto cell aggregates. Moreover, using confocal microscopy imaging, over time, both fluorescent coatings decreased at similar rates (Supplemental Figure B.4). Therefore, we believe that similar amounts of Hep or Hep- are grafted on cell surfaces within the aggregate at any timepoint and that the different effects observed between heparin species are thus not a result of differing amounts of GAGs present in the system.

After coating, H&E staining over time revealed rounded cell morphology within coated aggregates (Figure 4.1B). This phenomenon is specific to the presence of a GAG layer, as seen by the lack of rounded cell morphology in aggregates coated only with biotin and avidin (Supplemental Figure B.5). Additionally, when soluble heparin is introduced into the media, the morphology looks similar to that of the noncoated group (Supplemental Figure B.6A). While the mechanism is unknown, we conclude that Hep and Hep- coatings on cell surfaces can affect the organization and packing of the cells within the aggregate to produce the unique rounded cellular morphology observed in areas of the aggregate.

It is known that MSCs have limited proliferation capacity when cultured as aggregates in long-term suspension systems [8]. Because cell-based therapies require high dosages, developing a system that utilizes the mitogenic growth factor FGF-2 to improve proliferation may be necessary. Increased cell number over time was observed in MSC aggregates when both the Hep coating and FGF-2 were present in the system. Because heparin is known to preserve the bioactivity of FGF-2 [180, 182], it is possible that the presence of a Hep coating may simply be maintaining higher levels of active growth factor in the culture media. However, because this effect was not observed in

MSC aggregates cultured with FGF-2 and heparin added to the culture media (Supplemental Figure B.6B), the response of increased cell number is unique to the pairing of the cell surface presentation of heparin and the presence of the mitogenic growth factor.

FGF-2 signaling occurs when dimerization of the growth factor and cell surface receptor, facilitated by heparin interactions between the 2-O and N-sulfate groups and growth factor, occurs [20, 176, 280]. Thus, the presence of the Hep coating could facilitate the sequestration of FGF-2 within the aggregate, as well as could promote signaling through dimerization of the receptor, together resulting in the increased cell number observed in these studies (Figure 4.2). Similar results have been observed when heparin was immobilized onto 2D surfaces and cultured with exogenous growth factors found in serum. The cultured cells on this 2D system exhibited increased proliferation when compared to MSCs cultured on surfaces without heparin [191]. Additionally, when heparin is crosslinked into a 3D hydrogel and loaded with FGF-2, the encapsulated MSCs undergo increased angiogenesis and proliferation when compared to hydrogels not containing heparin and loaded FGF-2 [191, 281]. While the Hep- coating may still be able to sequester FGF-2 locally in the aggregate, due to an overall negative charge that exists because of the remaining carboxyl groups, it may lack the sulfate groups necessary for signaling of FGF-2 to cause cell proliferation [178], resulting in DNA content more similar to the noncoated controls in this system. Taken together, these results suggest that a heparin coating combined with mitogenic growth factors in the media may help address the reduced proliferation capacity and thus could be used as a system for expansion of

MSC aggregates for subsequent administration in cell-based therapies such as treating graft versus host or autoimmune diseases.

However, for other applications of MSCs, such as cartilage repair, cell expansion alone may not be sufficient, and systems that aim to differentiate MSCs down a chondrogenic pathway may be required to develop effective therapies. TGF-β1 is a potent growth factor known to induce chondrogenic differentiation [282]. Thus, the effects of our GAG coatings on the response of MSC aggregates to TGF-β1 in the media was examined to better understand how this system can be utilized for stem cell-based therapies to treat cartilage injury or disease. When coated and cultured in the presence of TGF-β1, Hep- coated aggregates exhibited more upregulation of the chondrogenic gene marker collagen II (nearly 90-fold) by day 21 compared to both noncoated and Hep coated aggregates, indicating that a Hep- coating can promote increased chondrocytic differentiation in MSC aggregates. Additionally, both noncoated and Hep coated aggregates had significantly higher collagen II expression at day 21 when compared to day 1, thus while the Hep coating may not promote high expression levels of collagen II, as seen with Hep- samples, it does not diminish the ability of the MSC aggregates to differentiation down a chondrogenic lineage. Overall increase in gene expression was matched by an apparent increase in staining for collagen II over time, however, intensity for the two coated groups looked similar at day 21 (Figure 4.4).

Gene expression for aggrecan, another chondrogenic ECM molecule, was upregulated in Hep coated aggregates at day 14, followed by upregulation in Hep- coated aggregates at day 21 (Figure 4.3B). In contrast, increase in aggrecan deposition was seen as early as day 14 for all groups (Figure 4.5) via immunostaining, and both types of

coated aggregates appeared to exhibit stronger positive staining for aggrecan at day 21, compared to noncoated aggregates. These inconsistencies can be attributed the transient gene expression of aggrecan in this system that could have been upregulated earlier than day 14, as was observed in another MSC and GAG platform from our laboratory [111]. The differences observed in gene expression and. immunostaining are somewhat similar to previous work in our laboratory with chondroitin sulfate microparticles incorporated in human MSCs aggregates, in which differences in aggrecan gene expression, but not immunostaining, were observed between groups treated with GAG vs. untreated [111]. This could be due, in part, to post-transcriptional regulation of ECM production that was not captured in the PCR results [283]. Although Sox9 expression was not detected in this system, it has been shown that collagen II expression is not correlated to levels of Sox9 expression in adult chondrocytes [284], and that Sox9 expression is a regulator of chondrogenic differentiation typically expressed early during the differentiation process [285]. Therefore, it may be possible that differentiation in this system is occurring during the 21 day culture time and end points earlier than day 7 may need to be performed to capture the initial upregulation of Sox9 expression.

While collagen I expression was upregulated for coated groups at day 7 and 14 and decreased by day 21 (Figure 4.3C), minimal differences in positive staining for ECM deposition was observed over time in each group (Supplemental Figure B.8). This discrepancy can be explained by the fact that the magnitude of fold regulation increase in the system (around 3-fold) may not be enough to elicit a visual increase in deposition of the ECM protein. Additionally, the level of collagen I expression and staining is consistent with what has previously been shown in our laboratory with this cell type

[111], and may be a result of basal-level production of this molecule throughout culture. When the collagen II/collagen I ratio, a measure used to assess chondrocytic differentiation in MSCs [286], was calculated, all aggregates exhibited an upregulation (18.2±3.23 fold for noncoated, 19.7±8.0 fold for Hep coated, 182.2±40-fold for Hep-coated) at day 21. While collagen I is expressed in this system, the increased ratio between collagen II to collagen I indicates that MSCs in this system are favoring a chondrocytic pathway, rather than a more fibroblastic pathway.

Expression of collagen X, a marker for MSC hypertrophic chondrogenic differentiation, increased over time for all groups, however, it was the greatest for Hep-aggregates by day 21 (Figure 4.3D). This was also observed in the staining for ECM deposition, in which bright pockets of pericellular collagen X were observed in Hep-coated aggregates on day 21 (Figure 4.6). Taken together, this indicates that coated MSC aggregates may become hypertrophic in our system, a result that has been previously observed in our laboratory [111, 200] and reported in other studies with human MSCs, including those with larger cell aggregates [106, 287]. This demonstrates that while many different platforms of MSC chondrogenesis exist, preventing hypertrophy remains a key challenge in cartilage tissue engineering, and additional culture methods, such as exposure to parathyroid hormones or co-culture with chondrocytes may be required to prevent hypertrophic differentiation during *in vitro* culture [105, 138, 288]. Although collagen X upregulation was measured in this MSC aggregate system, gene expression of other lineage markers, Runx2 (osteogenic) and PPARγ2 (adipogenic), were minimally changed or not expressed (data not shown), suggesting that those differentiation pathways were not favored in this system.

Although Hep coatings were seen to promote proliferation in response to the growth factor FGF-2 in MSC aggregates, upregulated chondrogenic marker expression was observed in Hep- coated aggregates in response to TGF-β1. It has previously been shown that the addition of GAG species with decreased sulfation level compared to heparin (such as hyaluronan and chondroitin sulfate) can activate or bind CD44, a cell surface receptor known to complex with the TGF-β1 receptor and activate downstream effector functions without the presence of TGF-β1 [289-291]. This demonstrates that multiple GAG species have potential to elicit TGF-β1 signaling in a manner that does not require binding between the GAG and growth factor. Another factor that can play a role when negatively charged GAGs are introduced is the change in osmotic swelling pressure within the aggregate. Previous studies have shown that increasing osmolarity can increase chondrogenic marker expression and matrix synthesis in MSC and progenitor cell systems undergoing chondrogenic differentiation [292, 293].

While these possibilities may play a role in the observed effects with the Hep- coating, it was seen that coated aggregates cultured without TGF-β1 did not exhibit chondrogenic differentiation (data not shown), suggesting that the effects observed are a result of the coating interacting with the chondrogenic growth factor to promote a cellular response. It has been shown that the 6-O and N-sulfate groups play a role in the interaction of heparin with TGF-β1, and upon desulfation of certain groups, the affinity for the growth factor decreases [186]. We speculate that in this coating system, the strong binding of TGF-β1 to heparin may have prevented growth factor interaction with its receptor, resulting in reduced chondrogenic effects when compared to Hep- coated MSCs. The effect of desulfation has also been observed in another system in our

laboratory, in which in the presence of TGF-β1, MSCs encapsulated in desulfated chondroitin hydrogels had significantly greater expression of collagen II, aggrecan and collagen X when compared to MSCs in natively sulfated chondroitin sulfate hydrogels [200]. This provides evidence that although the desulfated forms of different GAGs may have a lower affinity for TGF-β1, their effect on cellular response is not dictated by that binding interaction. While these results support the concept that GAG cell coatings can be used to improve the effect and presentation of growth factors in culture, it is important to consider that a "one GAG fits all" strategy may not be optimal for all MSC culture applications and that non-native sulfation patterns may have the capability to potentiate the activity of specific growth factors. Thus, our coating technology represents a versatile platform to design MSC culture systems with pairings of GAGs and growth factors that can be tailored to overcome specific challenges in scale-up and culture for MSC-based therapeutics.

4.5 Conclusion

These studies have demonstrated that GAG coatings have the ability to modulate growth factor interactions with MSC aggregates. By using layer-by-layer technology, biotinylated GAGs can be grafted onto cells within the MSC aggregate at similar amounts, thus enabling control over both the amount and sulfation level of heparin at cell surfaces. When cultured in the presence of the mitogenic growth factor FGF-2, natively-sulfated Hep coatings were able to increase cell number over the culture period of two weeks greater than both Hep- coated and noncoated aggregates. On the contrary, when cultured in the presence of the chondrogenic growth factor TGF-β1, Hep- coated

aggregates exhibited the greatest expression of collagen II and collagen X, gene markers for chondrogenic and hypertrophic differentiation. The finding that heparin coatings of two different sulfation levels can result in different responses to two distinct growth factors indicates that this novel cell coating platform that enables specific pairings of growth factors with GAG sulfation patterns could be a potent future means of modifying cell response during scale-up culture of stem cells for specific applications.

CHAPTER 5

DEVELOPMENT OF HEPPEP AND HEPARIN COATINGS FOR MSC SPHEROID MICROTISSUE ASSEMBLY

5.1 Introduction

Microtissues formed from smaller tissue constructs or cells have been used in both *in vitro* model and *in vivo* tissue repair applications [10, 129]. Microtissue models can recapitulate tumor microenvironments for drug screening and have been typically executed in cellular arrays or microfluidic devices that provide a means to culture cells in either two-dimensions or three-dimensions (3D). These arrays are used to study effects of different conditions, such as drug dosage, on the resulting cellular response, such as viability, to determine safety and toxicity. In more complex systems, tissue matrix arrays that combine extracellular matrix (ECM) and cells can be used to investigate cell function, such as proliferation and differentiation, in response to different environments. Such approach enables high-throughput analysis of many factors to determine optimal conditions to achieve a desired cellular response [129, 133, 134].

For tissue repair purposes, assembled 3D microtissues aim to exhibit similar characteristics as the complex physiological microenvironments for efficient integration, both functionally and morphologically, with the defect tissue [9, 74, 130]. For example, cardiac spheres formed from aggregating cardiomyocytes and cardiac muscle tissue has been used to form contractile constructs that can be implanted for treatment of myocardial infarctions [23]. Microtissues are advantageous in tissue repair applications because they are not as prone to clearance compared to single cells and can produce

proangiogenic factor that enable pre-vascularization or induce angiogenesis post implantation, ultimately, can improve engraftment when delivered [128].

Microtissues are also often composed of multiple cell types in order to better mimic the complex structure of tissues. For example, functional myocardial microtissues can be formed from a combination of fibroblasts and cardiomyocytes to produce a contractile tissue that recapitulates *in vivo* extracellular matrix (ECM) organization and blood vessel microtissues that are composed of layers of artery derived fibroblasts and umbilical cord vein endothelial cells can be configured into a microtissue that resembles the spatial structure of the *in vivo* artery [10]. With the complexity using multiple cell types, forming cell contacts of proper cell type and spatial organization can be crucial to properly mimicking an *in viv*o microenvironment. Such is the case when recapitulating the complex bone marrow niche that contains multiple cell types, such as hematopoietic stem cells (HSCs), MSCs and endothelial cells, to study HSC maintenance and proliferation [96, 294, 295].

Additionally, introducing multiple cell types into a microtissue structure requires an added factor of controlling interactions between the same cell types (homotypic cell interactions) and interactions between different cell types (heterotypic cell interactions). These cellular interfaces within a microtissue can provide contact-dependent signals between cells and can provide cues to induce cells to perform a certain function [131]. This has been shown during hepatocyte culture with mesenchymal stem cells (MSCs) or fibroblasts, during which, the combination of homotypic and heterotypic interactions between cell populations can affect the resulting hepatocyte function [139, 142, 148, 149, 296]. Specifically, increasing the heterotypic cell interaction between hepatocytes and

fibroblasts while maintaining homotypic cell interactions has been shown to increase albumin production and urea secretion and ultimately maintain functional hepatocyte phenotype [148, 149, 296]. Control over cellular contacts is an important factor in developing microtissues that properly mimic *in vivo* tissues.

To assemble microtissues with multiple cell types, previous methods have used encapsulation in hydrogels, scaffold-free technologies and microfluidic devices. Hydrogel encapsulation has been used to control organization of cell populations by encapsulating different cell types into separate sections of a hydrogel or seeding all cell types in a mixed population in one single hydrogel [144-146]. The other option of scaffold-free technologies uses centrifugation or gravity to force cells into aggregate form. Multiple cell types are typically mixed together and cultured together in one aggregate [148, 149]. Scaffold-free microtissues containing small spheroids of different cell types as the building block can also be formed by the incorporation of magnetic microparticles that direct the assembly of spheroids upon application of a magnetic field [150]. Lastly, microfluidic systems have been used to form high throughput arrays of small microtissues. Spatial organization of different cell types is typically achieved by introducing different cell types into the small specialized devices sequentially to allow for each cell type to interact and bind with each other [24, 134, 155, 156]. This platform facilitates control over the formation of the construct and culture parameters of media exchange and flow rate and can ultimately resemble a complex and accurate *in vivo* tissue environment [153, 154].

While these methods have all shown have the ability to produce multicellular microtissues, some aspects that are not addressed in these techniques include formation

of populations, the lack of self-assembly of the different cell populations, and production in dynamic culture. In encapsulation and scaffold-free technologies, formation is typically performed at a single microtissue scale, in which one hydrogel or one aggregate is produced. While microfluidic devices have the ability to produce multiple microtissues in a high throughput manner, the number formed is limited by the number of devices that need to be used. Therefore, current methods do not address assembly of microtissues at a larger population scale that can be achieved in culture system. Another shortcoming is that formation of microtissues with multiple cell types requiring physical placement of populations adjacent to each other or direction via an external driving force to bring cells together. These methods often require external biomaterials, such as hydrogels or microparticles, or specialized devices, such as microfluidic devices that support assembly. Finally, previous methods have all developed microtissues under static conditions. This can be a disadvantage because dynamic culture often provides the mixing and diffusion of nutrients and oxygen that can promote higher viability of the cells within the microtissue construct. Overcoming these shortcomings can result in the development of a platform for self-assembled microtissue that is amenable to future large scale bioprocessing culture, a property of microtissue assembly that has not previously been addressed.

Given limitations of microtissue assembly in current technologies, the overall goal of this study is to develop a platform that supports self-assembly of 3D microtissues containing multiple cell types in a dynamic suspension system. The introduction of a dynamic system facilitates the formation of multicellular microtissues in a novel system that can eventually be translated to large scale bioprocessing technologies. MSC

spheroids were as the starting building block material and the model cell type in these studies because this cell type has been extensively used in numerous microtissue applications, including cartilage, hepatic, vascularized tissues and bone marrow niches [23, 130, 135-137].

To achieve this self-assembly of microtissues, we utilized a cell coating that has been previously developed in this laboratory that uses layer-by-layer technology using biotin, and avidin to graft a biotinylated glycosaminoglycan (GAG), heparin, onto cell surfaces prior to formation of small spheroids [279]. Heparin is a negatively charged naturally derived polysaccharide that is known to interact electrostatically and specifically the positively charged growth factor fibroblast growth factor-2 [176, 280]. This binding site has been identified and has been synthesized into a short sequence known as a heparin binding peptide (HEPpep). It has been previously used in a self-assembled monolayer that is able to sequester heparin from culture media [152, 191]. The sequestration of heparin from serum then facilitates the binding of growth factors such as FGF-2, which subsequently directs behavior of the cells cultured on that surface.

We believe that this interaction between HEPpep and heparin can be exploited to control interactions between two different cell populations in a dynamic 3D culture system. Thus, the objective of this study is to investigate the use of HEPpep and heparin coatings on MSC spheroids assembly with a focus on how these coatings can affect the interactions between two cell populations. It is hypothesized that HEPpep coated spheroids will interact and assemble with heparin coated spheroids to form multi-cell type constructs in dynamic rotary culture. In this study, we have characterized both the HEPpep and heparin coating on MSC spheroid surfaces and their effects on cell viability

through confocal imaging. Additionally, we determined the specificity of these coatings and how investigated how modulating system parameters, such as ratio of cell populations and theoretical binding area, can affect the assembly of HEPpep coated and heparin coated spheroids and their interactions within the system by measuring assembled construct size, composition, and interfacial area between two populations.

5.2 Materials and Methods

5.2.1 MSC expansion

MSCs derived from human bone marrow aspirates were obtained from the Texas A&M Health Sciences Center. Cryopreserved MSCs from three different donors (2 males, 1 female; ages 22, 24 and 37) were thawed and expanded in α-Minimum Essential Medium (Mediatech) containing 16.5% fetal bovine serum (FBS, Atlanta Biological), 2 mM L-glutamine (Mediatech), 100 units/mL penicillin and 100 μg/mL streptomycin (Mediatech) under normoxic conditions (37ºC, 5% CO2 and 20% O2). Media were changed every 2–3 days until 80% confluence and were used at passage 3.

5.2.2 Heparin derivative synthesis and biotin conjugation

To produce biotinylated GAGs, heparin was dissolved in water at 2 mg/mL and conjugated with biotin by reacting N-(3-dimethylaminopropyl)-N′-ethylcarbodiimide (EDC) (Sigma Aldrich), hydroxybenzotriazole (HoBT) (VWR) and biotin-hydrazide (Sigma Aldrich) at a molar excess (compared to heparin) of 0.4 for all reagents for four hours at pH 5. For desulfated heparin, desulfation of heparin was first performed using a previously published protocol [165]. Briefly, heparin was mixed at 5 mg/mL in methanol (VWR) containing 0.5% v/v acetyl chloride (Thermo Fisher Scientific). A methyl ester of

heparin product was synthesized by acidic methanol treatment for 6 days. The product was dissolved in H_2O and precipitated in an excess of 95% ethanol on ice. The methyl ester product was then precipitated in ethyl ether (Thermo Fisher Scientific) and vacuum dried using lyophilization (-40ºC at 0.120 mmHg). Demethylation was performed by 0.1 M potassium hydroxide treatment for 24 hours to produce the final desulfated heparin, which was precipitated in ethanol and ethyl ether and vacuum dried via lyophilization. For biotinylation conjugation, desulfated heparin was dissolved at 2 mg/mL and reacted with EDC, HoBT and biotin-hydrazide at a molar ratio of 3:3:8, respectively, for four hours at pH 5. Each reaction solution was dialyzed for two days in 3500 MWCO dialysis tubing (Spectrum) followed by flash freezing and vacuum drying via lyophilization for two days. All heparin products were stored at -20ºC.

5.2.3 NMR Characterization of biotinylated heparin products

^{1}H NMR was used to assess level of sulfation after solvolytic desulfation of heparin and used to determine conjugation efficiency following biotinylation of heparin derivatives. Approximately 5 mg/mL of each product was dissolved in deuterated water and ^{1}H NMR experimented were conducted on a Bruker Avance III 400 spectrometer at 400MHz. The resulting spectra were analyzed with ACD NMR Processor software (Version 12). Spectra can be seen in Appendix D.

5.2.4 HEPpep/heparin coating and spheroid formation

After lifting with 0.05% trypsin (Mediatech), MSCs were washed in phosphate buffered saline (PBS, Life Technologies) two times and then modified with a glycosaminoglycan or peptide sequence by multilayer assembly of biotin and avidin layers as per [279]. Briefly, cells were first cultured in 4 mM EZ-Link Sulfo-NHS-LC-

Biotin (Pierce) in PBS, followed by 0.5 mg/mL avidin in PBS (Life Technologies), and lastly 5 mg/mL biotin-conjugated heparin (Hep) or 5 mg/mL biotin-conjugated desulfated heparin (Hep-) or 1mg/mL biotinylated heparin binding peptide (HEPpep, Biotin-NH_2-$(CH_2)_4$-GKRTGQYKLG-NH_2, Aapptec) or a scrambled peptide sequence with a similar overall charge as the HEPpep sequence (Scramble, Biotin-NH_2-$(CH_2)_4$-GTYRKKGLQG-NH_2, Aapptec) in PBS (Figure 5.1). Each incubation step with cells was performed in a 24-well Ultra-Low Attachment Surface plate (Corning) for 30 minutes at 37°C on a rotary orbital shaker plate at 65 rpm. Once cells were coated with their respective GAG or peptide layer, 200-cell spheroids were formed via forced aggregation in an array of AggreWells^{TM} inserts made from 3% agarose (Pierce). Inserts were spun down at 200 rcf in serum free media composed of Dulbecco's Modified Eagle Medium, 1% nonessential amino acids, 1% antibiotic/antimycotic, 1% insulin, human transferrin and selenous acid premix (BD Biosciences) and 50 μg/mL ascorbate-2-phosphate (Sigma-Aldrich). After 24 hours, cell spheroids were transferred to 10 cm low attachment petri dishes (Fisher) and cultured on rotary at 65 rpm under normoxic conditions (37ºC, 5% CO_2 and 20% O_2) for further experiments.

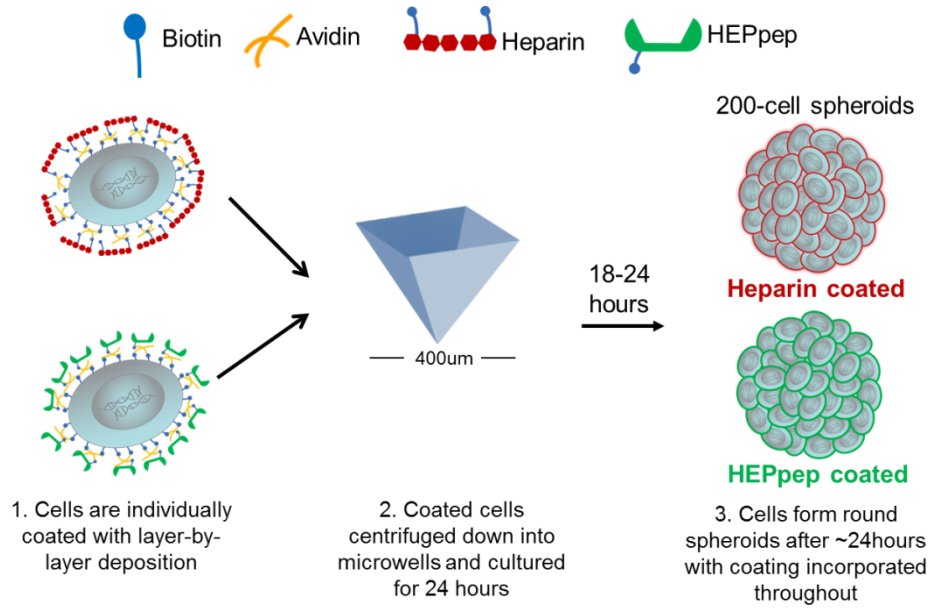

Figure 5.1. Schematic of layer-by-layer coating procedure and spheroid formation.

5.2.5 HEPpep and heparin coating characterization

To image grafted coatings on cell surfaces within the spheroids, HEPpep and heparin were fluorescently tagged with Alexa-Fluor 633. Briefly, this conjugation was performed by EDC coupling in 0.1 M sodium bicarbonate buffer containing 10 mg/mL HEPpep or heparin, 10mM AlexaFluor®-633-hydrazide (Invitrogen), 20 µM EDC. The solution reacted for 1.5 hours at room temperature while protected from light before dialysis in 3500 MWCO tubing for two days and lyophilization for two days. Cells were coated as previously described and formed into 200-cell spheroids (HEPpep coated) or 500-cell spheroids (Hep coated) and serum free media. At days 1 and 3 after coating, spheroids were collected, washed in PBS and stained with LIVE/DEAD staining solution (calcein AM at 1 µM and ethidium homodimer-1 at 1 µM, Invitrogen) and imaged under confocal microscopy at excitation wavelength 633 nm and emission wavelength 647 nm (Zeiss LSM 700 LSM confocal microscope) for the HEPpep or heparin coating and

excitation wavelength 494 nm/517 nm and emission wavelength of 517 nm/617 nm, respectively, for LIVE/DEAD staining (n = 3 plates).

5.2.6 Specificity of coated assembled spheroids

5.2.6.1 Assembly via soluble heparin

Coating specificity was first observed by culturing peptide coated spheroids in media containing GAGs in solution. MSCs were coated with 1 mg/mL HEPpep or 1 mg/mL Scramble using the coating method outlined previously. Coated cells were then formed into 200-cell spheroids through forced aggregation in AggreWells^{TM} and allowed to form spheroids for 24 hours. Coated spheroids were cultured in serum-free media supplemented with 5 mg/mL Hep, 5 mg/mL Hep- or without any additives (basal). Control samples included 200-cell noncoated spheroids cultured in the serum-free media supplemented with 5 mg/mL Hep, 5 mg/mL Hep- or no additives. Each plate was cultured with a total of 900 spheroids and in rotary suspension at 65 rpm for 24 hours under normoxic conditions. After 24 hours, samples were collected, fixed with 10% neutral buffered formalin and imaged under phase microscopy (Inverted Nikon TE 200 microscope) (n = 3 plates with approximately 900 spheroids per plate). For imaging purposes, plates were combined and images taken represented the entire population for that group. All images were analyzed in ImageJ for diameter for the entire population of spheroids in each group.

5.2.6.2 Assembly via coated spheroids

Coating specificity was also observed by culturing peptide coated spheroids with spheroids with GAG molecules that can express binding to those peptides. MSCs that would be coated with 1 mg/mL HEPpep or 1 mg/mL Scramble were stained with

CellTracker Orange (Molecular Probes) prior to coating steps. Other MSCs were coated with 5 mg/mL Hep or 5 mg/mL Hep-. Staining with CellTracker Orange was performed per manufacturer's protocols. In short, after cell expansion and prior to lifting, MSCs were cultured in serum-free media containing α-Minimum Essential Medium, 2 mM L-glutamine, 1% antibiotic/antimycotic and 10 μM of the CellTracker Orange dissolved in dimethyl sulfoxide (DMSO). After 30 minutes, media containing the CellTracker was removed and replaced with serum-free media without CellTracker. After 30 minutes, cells were lifted and coated with either HEPpep or Scramble peptide using layer-by-layer deposition.

Once all cells were coated and formed into 200-cell spheroids using the AggreWell system, 900 total spheroids were cultured together in serum-free media at a ratio of 1:1 (peptide coated spheroids:GAG coated spheroid) on rotary for 24 hours under normoxic conditions (n = 3 plates with approximately 900 total spheroids per plate). Control groups contained HEPpep coated or Scramble coated spheroids with noncoated spheroids at a 1:1 ratio or only noncoated, heparin-coated and desulfated heparin-coated spheroids at a total of 900 spheroids per plate (n = 3 plates). After 24 hours, samples were collected, fixed with 10% neutral buffered formalin, and imaged under phase and fluorescent microscopy. For imaging purposes, plates were combined and images taken represented the entire population for that group. All images were analyzed in ImageJ for diameter for the entire population of spheroids in each group. Peptide coated spheroids can be seen in fluorescent red (via CellTracker dye) in the images shown.

5.2.6.3 Statistical analysis of spheroid assembly

Images were taken of the entire spheroid population and diameters of the spheroids in these images were measured via ImageJ. To statistically compare these populations a cutoff size that represented larger constructs containing assembled spheroids was determined. To calculate cutoff size, the diameter at the upper 5% of the population for each control group was identified. The control groups included populations that contained all noncoated, heparin coated, desulfated heparin coated spheroids, seen in Figure 5.4 and Figure 5.5. The diameters that were determined at the upper 5% of the population for all control groups were averaged and set as the cutoff size. For experimental groups, seen in Figure 5.6 and Figure 5.7, the cutoff size was applied to each population and the percentage of measured diameters above that size was reported. The sub-population of diameters for each group that was larger than the cutoff size was statically compared using a one-way analysis of variance with Tukey's post hoc multiple comparisons test ($p<0.05$) to determine statistical significance between groups in Minitab (v.15.1).

To compare the percentages, the resampling method of bootstrapping was used to produce variance for each population [297, 298]. This was performed because the calculated percentage values represented the entire population of spheroids in that group, therefore only one value was produced and standard deviation could not be determined. When bootstrap resampled was performed in MATLAB (v.7.11), 900 diameters were chosen at random from the original population to create a new set of measurements. This was performed 3 times to create triplicates (as performed in the actual experiment with 3 cultured plates), for each experimental group. Percentage of diameters above the cutoff

size from each resampled population was then determined. Average percentages for each experimental group was calculated and statistically compared using a one-way analysis of variance with Tukey's post hoc multiple comparisons test ($p<0.05$) to determine statistical difference between groups in Minitab (v.15.1).

5.2.7 Assembled spheroid competition assay

To study stability of assembled spheroids, 200-cell HEPpep coated spheroids that were stained with CellTracker Orange and 200-cell Hep coated spheroids were cultured together for 24 hours in serum-free conditions with no additives at 65 rpm on rotary. After 24 hours, an appropriate time to allow for spheroids to assemble, the media was replaced with serum-free media supplemented with 1 mg/mL HEPpep, a concentration that represents a 2X molar excess of the maximum amount of heparin grafted on cell surfaces (See Appendix C.2 for calculations). After 6 hours and 24 hours of culture in rotary suspension culture at 65 rpm, samples were collected, fixed with 10% neutral buffered formalin and imaged with both phase and fluorescent microscopy (n = 2 plates with approximately 900 spheroids).

5.2.8 Assembly of coated spheroids at different ratios

To study assembly of spheroids when populations were cultured at different ratios, HEPpep coated spheroids were stained with CellTracker Orange and Hep coated spheroids were stained with CellTracker Green. Following staining and coating with 1 mg/mL HEPpep or 5 mg/mL Hep, 200-cell spheroids were formed in AggreWells^{TM} and cultured at ratios (HEPpep coated:Hep coated) of 1:1, 2:1, 3:1, 6:1, 10:1 on rotary at 65 rpm (n= 3 plates with approximately 900 spheroids). After 6 hours, 24 hours and 72 hours in culture, groups were collected, fixed with 10% neutral buffered formalin and

imaged under confocal microscopy. ImageJ was used to analyze images for percent assembly, assembled spheroid size, composition, and cell interface area. Aggregate size and composition was measured at the center image of the stack collected and cell interface area was calculated using trapezoidal approximation through the z-stacked images taken at 5 μm apart. ImageJ was also used to construct confocal images of assembled spheroids containing HEPpep coated spheroids that are seen in green and Hep coated spheroids that are seen in red.

5.2.9 Assembly of coated spheroids of different sizes

Spheroids of different sizes were cultured together for 24 hours to represent systems that contained high and low theoretical binding areas between the two populations. This was performed to examine how altering the potential binding area between two different cell populations can affect spheroid assembly. To study the effects of binding area without changing other parameters in the system, total cell number of each population of coated spheroids remained constant between the groups. Size was varied by forming spheroids containing different numbers of cells, ranging from 100 cells/spheroid to 2000 cells/spheroid. Differently sized spheroids were paired together so that each group contained a smaller and larger spheroid. Theoretical binding areas for each pairing were calculated based on the surface area of the larger spheroid and the number of smaller spheroids that could pack tightly on that area. Calculations for binding area can be seen in Appendix C.2.

The first group cultured 100-cell HEPpep coated spheroids with 500-cell Hep coated spheroids at a ratio of 420:560 (HEPpep:Hep) to represent low theoretical binding area in the system (Low BA). The second group cultured 200-cell HEPpep coated

spheroids with 2000-cell Hep coated spheroids at a ratio of 600:400 to represent high theoretical binding area (High BA) (n= 3 plates containing approximately 900 spheroids). HEPpep coated spheroids were stained with CellTracker Orange and Hep coated spheroids were stained with CellTracker Green, as previously described. A total number of 900 spheroids were cultured together for both groups for 6, 24 and 72 hours, at which time, spheroids were collected fixed with 10% neutral buffered formalin and imaged under confocal microscopy. ImageJ was used to analyze images for percent assembly, assembled spheroid size, composition, and cell interface area. Aggregate size and composition was measured at the center image of the stack collected and cell interface area was calculated using trapezoidal approximation through the z-stacked images taken at 5 μm apart. ImageJ was also used to construct confocal images of assembled spheroids containing HEPpep coated spheroids that are seen in green and Hep coated spheroids that are seen in red.

5.2.10 Statistical analysis for area measurements

Measurements collected from images (diameter, assembled spheroid size, composition, cell interface area) were analyzed using a one-way or two-way analysis of variance with Tukey's post hoc multiple comparisons test ($p<0.05$) to determine statistical significance between groups in Minitab (v.15.1). Quantitative data are reported as mean $\pm$ standard deviation.

5.3 Results

5.3.1 Coating characterization

Confocal imaging revealed that, by using a layer-by-layer coating procedure, the biotinylated HEPpep peptide and biotinylated heparin was grafted on cell surfaces and did not disturb spheroid formation. At day 1 and day 3 after coating, both fluorescently tagged HEPpep and Hep were visualized in red on cell surfaces throughout the entire spheroid (Figure 5.2A&B, D&E). Additionally, LIVE/DEAD staining revealed that after 3 days, cells in spheroids remained viable (Figure 5.2C&F). When intermediate layers of biotin and avidin were not present in the coating process, fluorescently tagged HEPpep was not observed on cell surfaces via confocal imaging (Figure 5.3A&B).

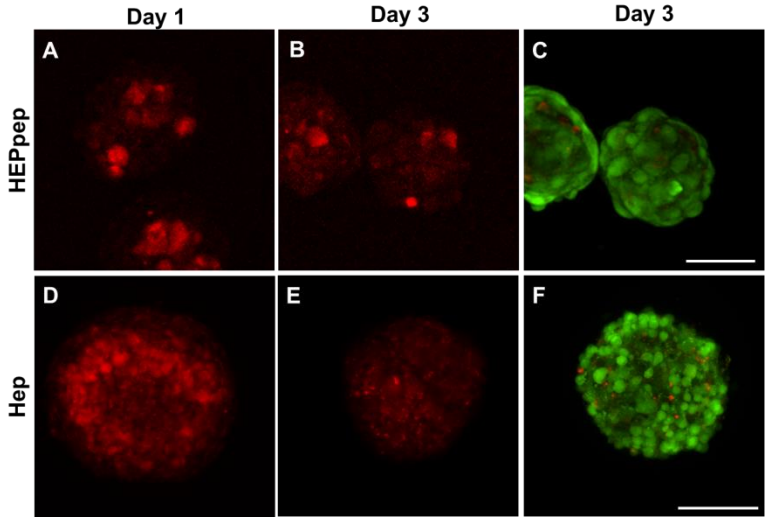

Figure 5.2. HEPpep and Hep coating remains on cell surfaces for up to 3 days and does not negatively affect cell viability. Confocal images of HEPpep coating (red) at (A) day 1, and (B) day 3. (C) LIVE/DEAD of staining HEPpep coated spheroids at day 3. Hep coating (red) at (D) day 1, and (E) day 3. (F) LIVE/DEAD staining of Hep-coated spheroids at day 3. Scale bar = 100μm, n = 100 spheroids.

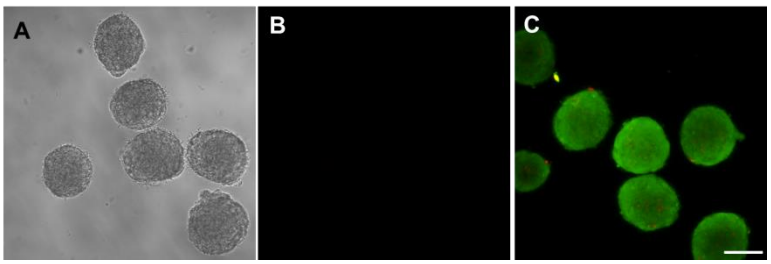

Figure 5.3. HEPpep coating (red) not observed on cell surfaces without intermediate biotin and avidin layer present. (A) Phase image and (B) confocal image of

spheroids coated with HEPpep without biotin and avidin. (C) LIVE/DEAD staining of spheroids at day 3. Scale bar = 100μm, n = 100 spheroids.

5.3.2 Specificity of coating interactions

5.3.2.1 Specificity of coating interactions: Assembly via soluble heparin

To quantify the specificity of the HEPpep coating and its effects on spheroid assembly, coated spheroids were cultured in media containing soluble GAG and after 24 hours, diameter of all spheroids in each population was measured. After 24 hours, none of the control groups exhibit spheroid assembly and the average diameter of each population was not significantly different from each other; thus, the cutoff size was set as the average upper 5% measurement for all control groups at 257.4 μm (Figure 5.4 and 5.5).

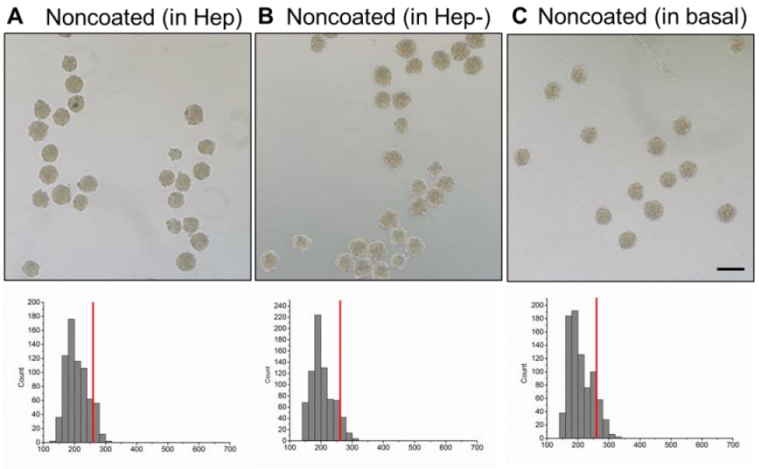

Figure 5.4. Noncoated spheroids did not assemble when cultured for 24 hours in media containing exogenous Hep, Hep- or under basal serum-free conditions. Phase image (top) and histogram of aggregate diameters (bottom) of noncoated aggregates cultured in serum-free media containing (A) 5mg/mL heparin, (B) 5mg/mL desulfated heparin, or (C) in basal conditions. Scale bar = 100μm, n = ~1500 spheroids in total, red line indicates cutoff size.

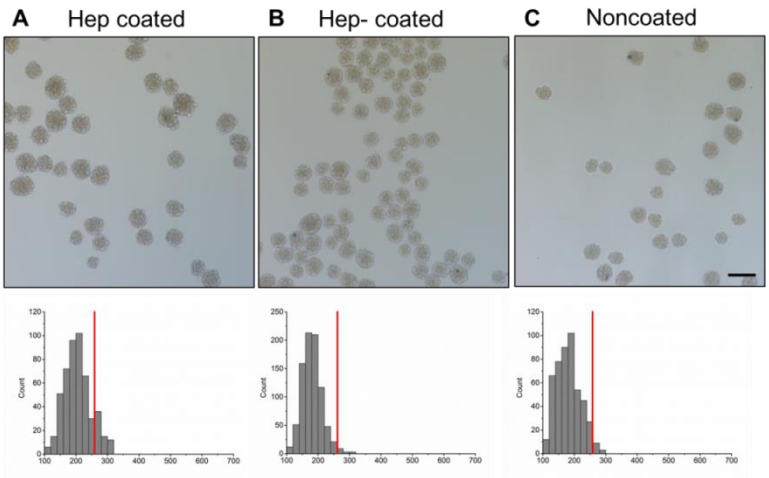

Figure 5.5. Hep coated, Hep- coated and noncoated spheroids cultured by themselves did not assemble after 24 hours in culture. Phase image (top) and histogram of aggregate diameters (bottom) of (A) heparin-coated spheroids, (B) desulfated heparin-coated spheroids, and (C) noncoated spheroids. Scale bar = 100µm, n = ~1500 spheroids in total, red line indicates cutoff size.

Imaging revealed that HEPpep coated spheroids cultured in media containing 5 mg/mL Hep or Hep- resulted in larger spheroids (Figure 5.6A&B). Additionally, 34±6% or 37±5% of the entire population for HEPpep coated spheroids cultured in Hep or Hep- had diameters larger than the cutoff size, respectively, both of which were significantly different when compared to the percentage of spheroids with diameters larger than the cutoff size in the combined control populations (Table 5.1). Percentage of population with spheroids lager than the cutoff size was not significantly different than the control population percentage when HEPpep coated spheroids were cultured in basal serum-free media (6±5%) or when Scramble-coated spheroids were cultured under any conditions (13±7% in Hep, 10±2% in Hep-, and 8±6% in basal) (Table 5.1). Additionally, when the diameter measurements greater than the cutoff size for each group was compared to the measurements from the combined control groups, only HEPpep coated spheroids cultured in Hep or Hep- were significantly different (Figure 5.6.A&B).

Table 5.1 Resampled percentage of spheroids with diameters above cutoff size for HEPpep and Scramble-coated spheroids cultured in media containing GAGs in solution. Resampling produced triplicate (n=3) populations containing 900 spheroids for each group. Statistical analysis was performed on percentages calculated from resampled populations. * indicates significantly different from the percentage calculated from combined control group populations, p<0.05.

Group	Resampled Percentage
HEPpep (in Hep)	34 ± 6% *
HEPPpep (in Hep-)	37 ± 5% *
HEPpep (in basal)	6 ± 5%
Scramble (in Hep)	13 ± 7%
Scramble (in Hep-)	10 ± 2%
Scramble (in basal)	8 ± 6%

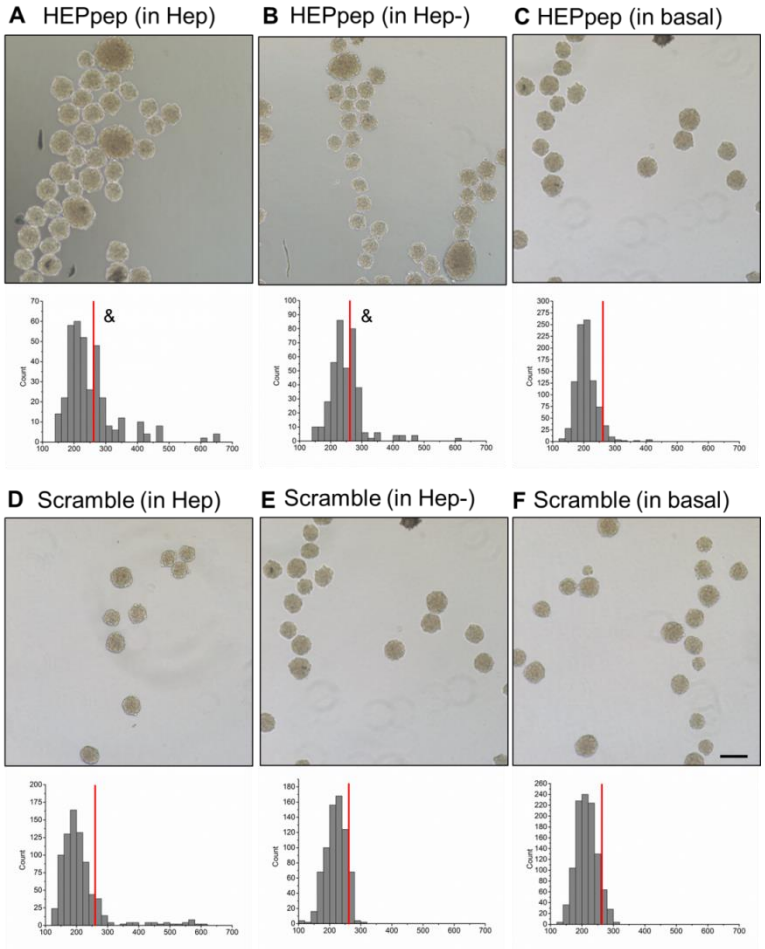

Figure 5.6. HEPpep-coated spheroids increased in diameter when cultured for 24 hours in serum-free media containing soluble Hep or Hep-. Phase image (top) and histogram of aggregate diameters (bottom) of HEPpep-coated aggregates cultured in serum-free media containing (A) 5mg/mL heparin (B) 5mg/mL desulfated heparin or (C) basal conditions. Phase image (above) and histogram of aggregate

diameters (below) of Scramble-coated aggregates cultured in serum-free media containing (D) 5mg/mL heparin, (E) 5mg/mL desulfated heparin, or (F) basal conditions. Scale bar = 100μm, n = ~1500 spheroids in total, red line indicates cutoff size. Statistical analysis performed on measurements above cutoff size. & indicates significantly different from measurements above the cutoff size in the combined control group population, p<0.05.

5.3.2.2 Specificity of coating interactions: Assembly via coated spheroids

The next experiment performed quantified the specificity of the HEPpep coating and its effects on spheroid assembly by culturing peptide-coated spheroids with GAG-coated spheroids for 24 hours. Imaging revealed that after 24 hours, HEPpep coated spheroids cultured with Hep coated or Hep- coated spheroids contained assembled aggregates that were composed of different coated spheroid populations (Figure 5.7.A&B).

Table 5.2 Resampled percentage of spheroids with diameters above cutoff size for peptide-coated spheroids cultured with GAG-coated spheroids. Resampling produced triplicate (n=3) populations containing 900 spheroids for each group. Statistical analysis was performed on percentages calculated from resampled population. * indicates significantly different from the percentage calculated from combined control group populations, p<0.05.

Group	Resampled Percentage
HEPpep:Hep	70 ± 11% *
HEPpep:Hep-	27 ± 4% *
HEPpep:Noncoated	12 ± 5%
Scramble:Hep	10 ± 4%
Scramble:Hep-	9 ± 6%
Scramble:Noncoated	6 ± 2%

When HEPpep coated spheroids were cultured with Hep coated spheroids, the percentage of aggregates with diameters above the cutoff size was 70±11% and was significantly larger than the percentage calculated from the combined control population. Additionally, 27±4% of the spheroids had larger diameters when HEPpep coated spheroids were cultured with Hep- coated, which was also significantly different when compared to the

control groups. However, only 12±5% of the spheroids were larger when HEPpep coated spheroids were cultured with noncoated spheroids (Table 5.2). When Scramble coated spheroids were cultured with the Hep coated, Hep- coated or noncoated spheroids, 10±4%, 9±6%, and 6±2% of each population, respectively, had diameters above the cutoff size (Table 5.2), all of which were not significantly different when compared to the percentage of spheroids with diameters greater than the cutoff size in the combined control populations. When the population of spheroids above the cutoff size for each group was compared to that of the combined control groups, significant difference was observed in the diameters from populations that contained HEPpep coated and Hep coated or HEPpep coated and Hep- coated spheroids.

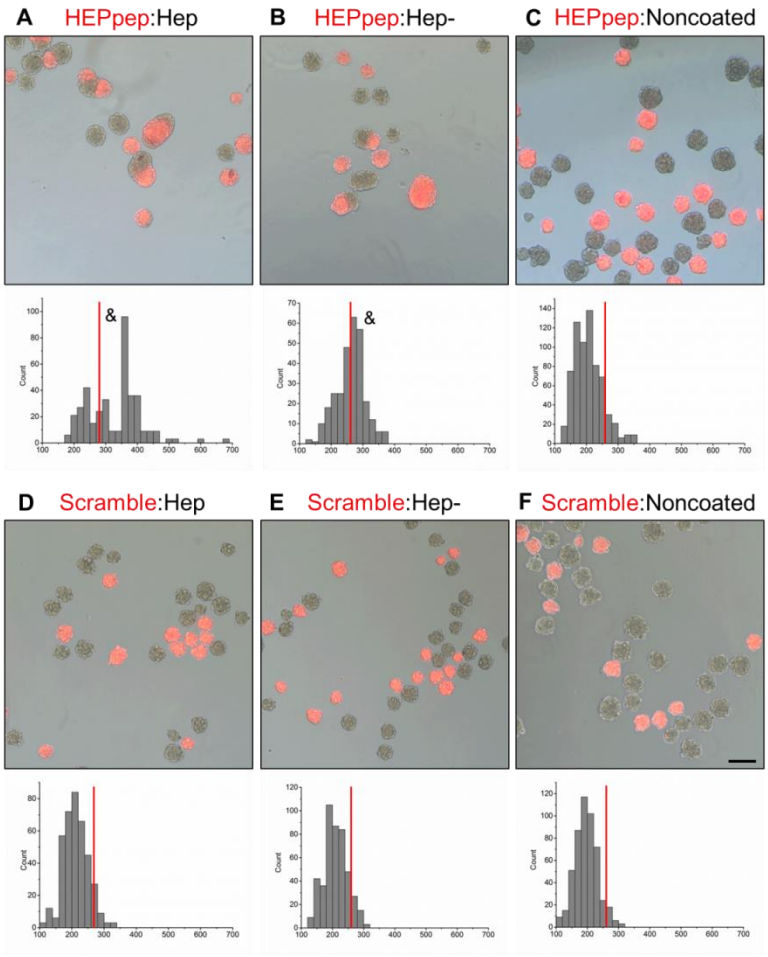

Figure 5.7. HEPpep coated spheroids cultured with Hep coated spheroids exhibit larger assembled aggregates containing both cell populations after 24 hours. Phase image (top) and histogram of aggregate diameters (bottom) of (A) HEPpep coated (red) spheroids cultured with Hep coated spheroids, (B) HEPpep coated with Hep-coated, (C) HEPpep coated with noncoated, (D) Scramble coated (red) with Hep coated, (E) Scramble-coated with desulfated heparin-coated, and (F) Scramble-coated with noncoated. Labels written as peptide-coating:GAG-coating. All groups were cultured at a ratio of 1:1. Scale bar = 100μm, n = ~1500 spheroids in total, red line indicates cutoff size. Statistical analysis performed on measurements above cutoff size. & indicates significantly different from measurements above the cutoff size in the combined control group population, $p<0.05$.

5.3.4 Stability of assembled spheroids

To study the stability of assembled spheroids, assembled HEPpep and Hep coated spheroids were cultured in media containing 1 mg/mL HEPpep competitor in solution. After 6 hours and 24 hours of culture with the soluble HEPpep competitor, imaging revealed that assembled aggregates containing both HEPpep (red) and Hep coated spheroids were still observed (Figure 5.8).

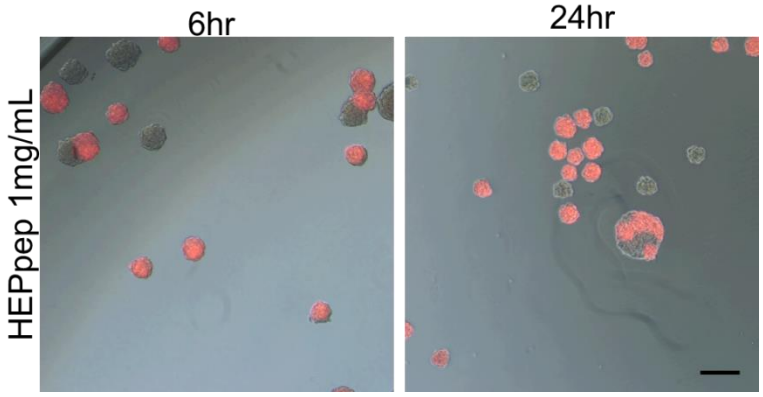

Figure 5.8. HEPpep-coated and Hep-coated aggregates do not disaggregate (once aggregated after 24hr) when cultured in media containing 1mg/mL HEPpep. Images taken at 6hr and 24hr after addition of soluble HEPpep. HEPpep-coated spheroids seen in red. Scale bar = 100μm, n = ~1000 spheroids in total.

5.3.5 Aggregation of spheroids at different ratios

To study how ratio of the two populations can affect coated spheroid assembly, a ratio of 1:1 increasing up to 10:1 of HEPpep coated:Hep coated spheroids were cultured together for over 72 hours. First, we observed that when Hep coated and HEPpep coated spheroids were cultured by themselves, assembly of spheroids did not occur at 6, 24 or 72 hours (Figure 5.9).

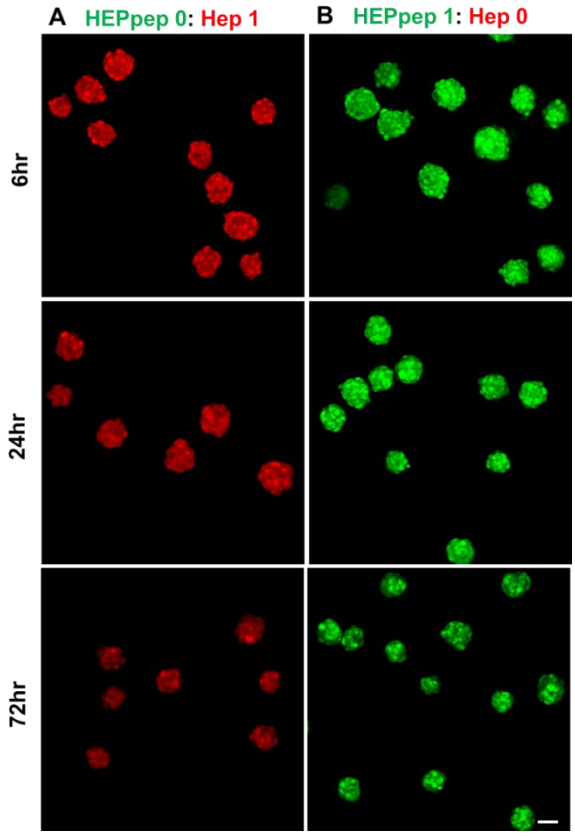

Figure 5.9. HEPpep and Hep coated 200-cell spheroids cultured by themselves do not aggregate over 72hrs. Confocal images of HEPpep coated (green) and heparin coated (red) spheroids cultured at 6hr (top), 24hr (middle) and 72hr (bottom) at ratios (HEPpep:heparin) of (A) 0:1, (B) 1:0, and (C) 10:1. Scale bar = 100μm, n = ~1500 spheroids in total.

For groups cultured at higher ratios, spheroids had not appeared to assemble with each other after 6 hours in rotary culture (Figure 5.10). After 24 hours in dynamic culture, HEPpep coated spheroids (seen in green) assembled with Hep coated spheroids (seen in

red) when cultured at ratios of 1:1, 2:1, 3:1, and 6:1 and formed constructs containing both cell populations.

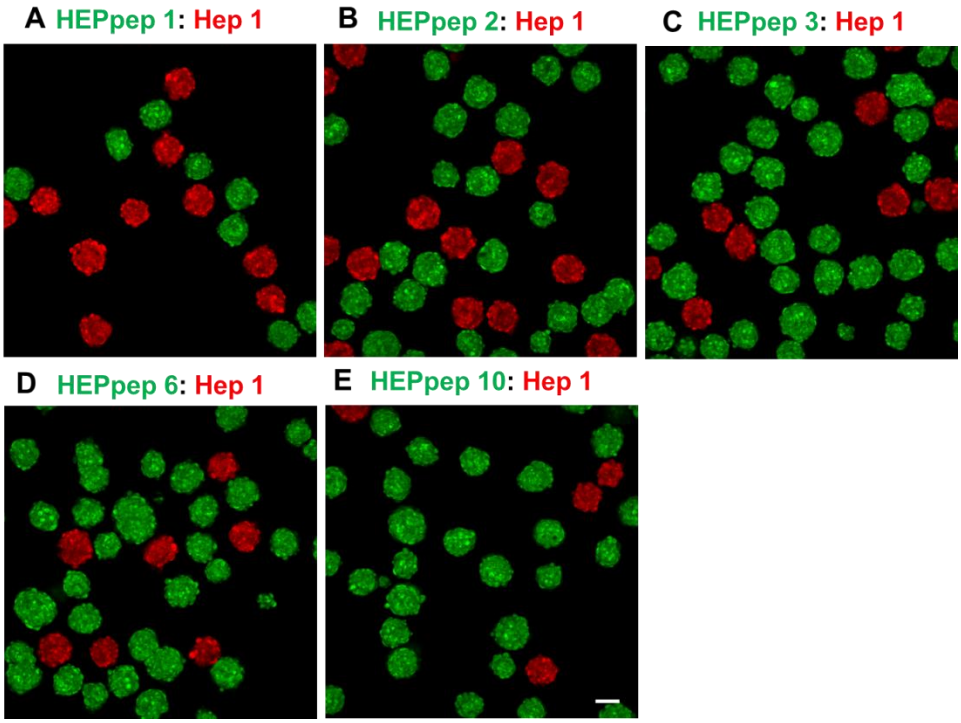

Figure 5.10. HEPpep coated spheroids cultured with Hep coated spheroids at different ratios do not aggregate after 6 hours. Confocal images of HEPpep coated (red) and Hep coated (green) spheroids cultured at ratios (HEPpep:Hep) of (A) 1:1, (B) 2:1, (C) 3:1, (D) 6:1, and (E) 10:1. Scale bar = 100 µm, n=~1500 spheroids in total.

These aggregates containing multiple cell populations were also present at 72 hours (Figure 5.11A). At 24 and 72 hours, assembly of coated spheroids did not occur in the group with 10:1 spheroids (Figure 5.11A). In groups containing cell populations at ratios of 1:1 to 6:1, approximately 9-14% of the imaged spheroids had assembled with different coated spheroids after 24 hours. At 72 hours, approximately 12-19% of spheroids had assembled while in culture (Table 5.1).

Table 5.3. Percentage of assembled spheroids in groups containing different ratios (1:1 – 6:1) of HEPpep coated and Hep coated spheroids at 24 and 72 hours.

Ratio	Time	% Assembled
1:1	24hr	13
	72hr	19
2:1	24hr	14
	72hr	18
3:1	24hr	10
	72hr	13
6:1	24hr	10
	72hr	13

When assembled aggregate size was measured, size of aggregates was not significantly different among any group at both 24 and 72 hours (Figure 5.11B). Additionally, percent composition HEPpep coated within these aggregates was not different among all groups at both timepoints (Figure 5.11C). Lastly, interfacial area between the two populations also was not different among all groups at both timepoints (Figure 5.11D).

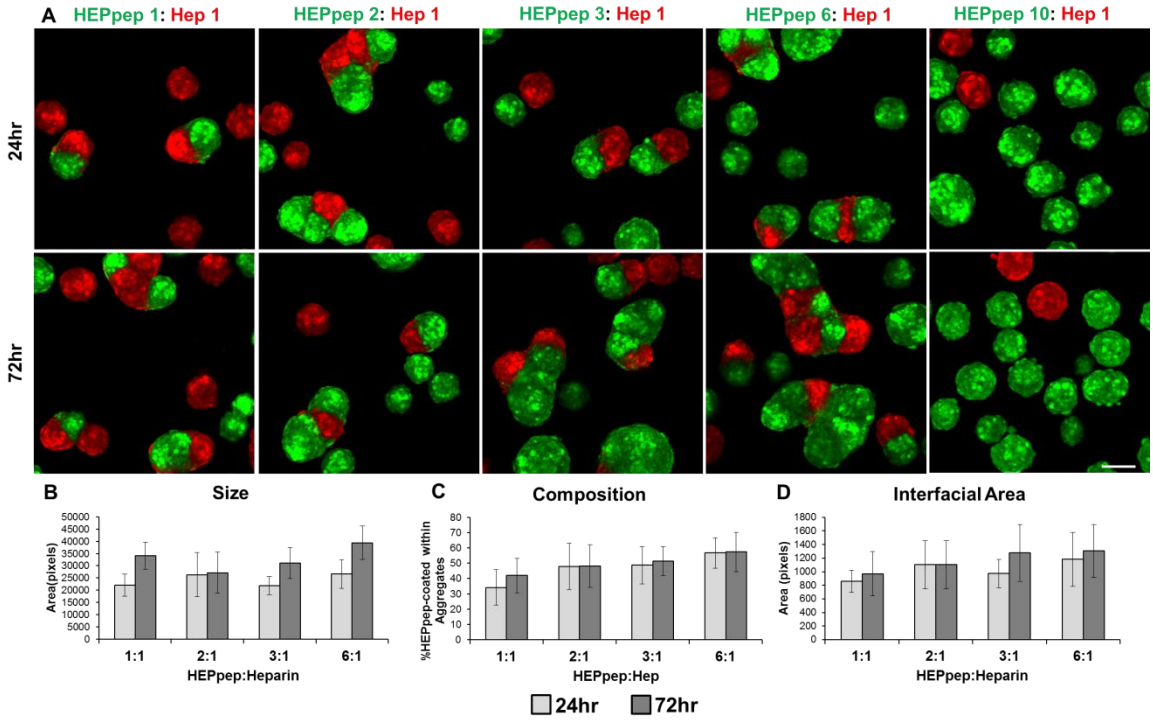

Figure 5.11. HEPpep coated spheroids cultured with Hep coated spheroids at ratios of 1:1, 2:1, 3:1, and 6:1 exhibit assembly at 24 and 72 hours. (A) Confocal images of

HEPpep coated spheroids (green) and Hep coated spheroids (red) cultured at ratios of (from left to right) 1:1, 2:1, 3:1, 6:1, and 10:1 at 24 and 72 hours. Quantified measurements of (B) assembled aggregate size, (C) % HEPpep coated within aggregate, and (D) interfacial area between two populations at 24 and 72 hours. Scale bar = 100 μm, n = ~1500 spheroids imaged, n = 100-200 spheroids analyzed for area measurements.

5.3.6 Aggregation of spheroids of different sizes

To study how binding area in the system affects assembly of coated spheroids, spheroid diameter was altered by changing cell number per spheroid. Assembly of spheroids was observed at both 24 hour and 72 hours, however, at the later timepoint, mixing of the two cell populations was also seen (Figure 5.12A). Percent of assembly in the Low BA group was measured at 11% after 24 hours and increased to 51% after 72 hours. Additionally, it was observed in High BA spheroid culture that percent assembly increased from 17% after 24 hours to 26% after 72 hours (Table 5.2).

Table 5.4. Percentage of assembled spheroids in low and high BA culture conditions at 24 and 72 hours.

Group	Time	% Assembled
Low BA	24hr	11
Low BA	72hr	51
High BA	24hr	17
High BA	72hr	26

When assembled aggregate size was measured, after 24 hours, spheroids cultured with high BA, was significantly higher than the assembled aggregate size measured in spheroids cultured with low BA. Additionally, size of assembled spheroids in the high BA group appeared to decrease significantly compared to both the low BA group at 72 hours and the high SA aggregate size at 24 hours (Figure 5.12B). Composition of these assembled aggregates was not significantly different between both groups at both

timepoints (Figure 5.12C). However, similar to trends observed with assembled spheroid size, interfacial area between the two populations was significantly increased in the high BA group compared to the low BA samples at 24 hours (Figure 5.12D).

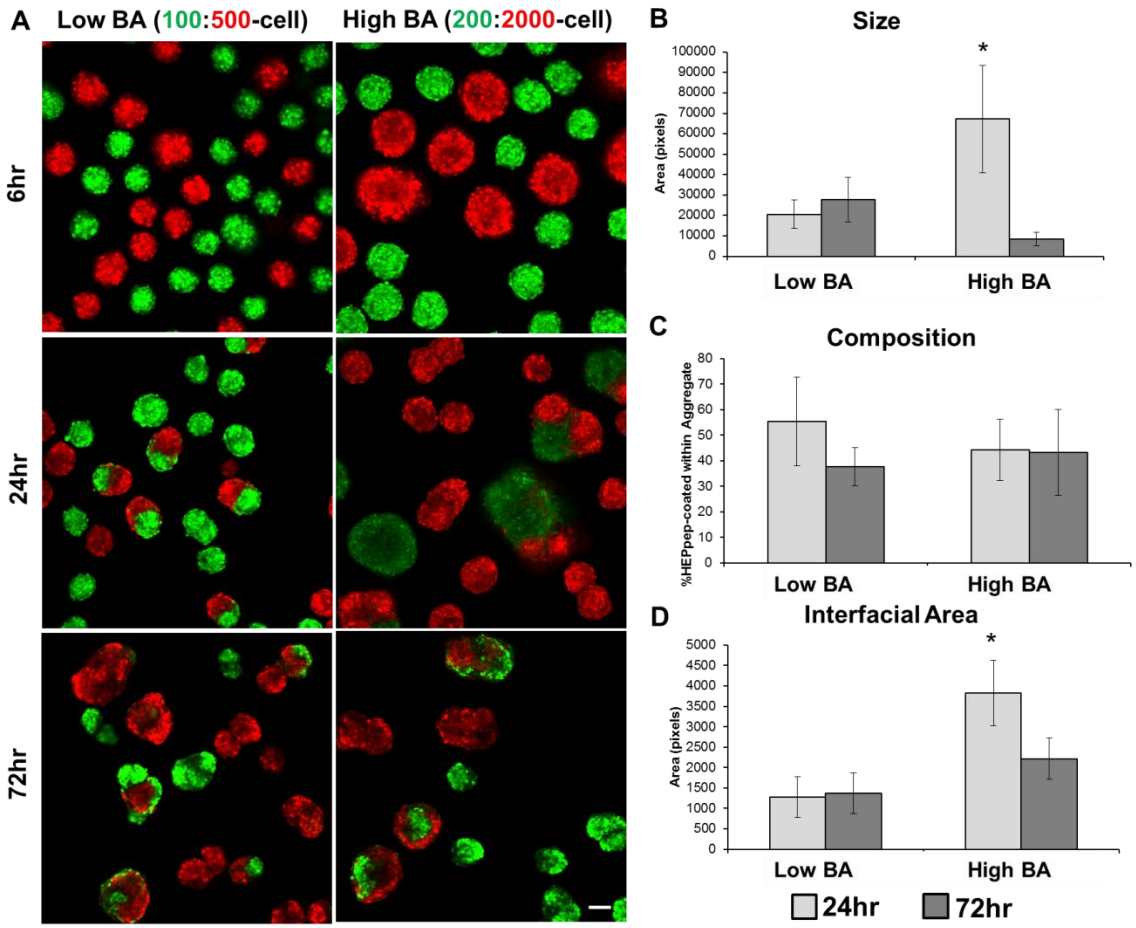

Figure 5.12. HEPpep coated spheroids and Hep coated spheroids in high binding area (BA) culture conditions resulted in larger assembled aggregates and increased interfacial area at 24 hours. (A) Confocal images of HEPpep coated spheroids (green) and Hep coated spheroids (red) cultured in low SA conditions and high SA conditions. Quantified measurements of (B) assembled aggregate size, (C) % HEPpep coated within aggregate, and (D) interfacial area between two populations at 24 and 72 hours. Scale bar = 100 µm, n = ~1500 spheroid in total, n = 100-200 spheroids analyzed for area measurements.

Lastly, to further examine how binding area can affect assembly via coatings, binding area was reduced by culturing spheroids of the same size together at the ratio used for the

high BA group for 72 hours. Over 72 hours, assembly of spheroids was observed, however did not form large constructs that resulted in mixing of cell populations after 72 hours (Figure 5.13).

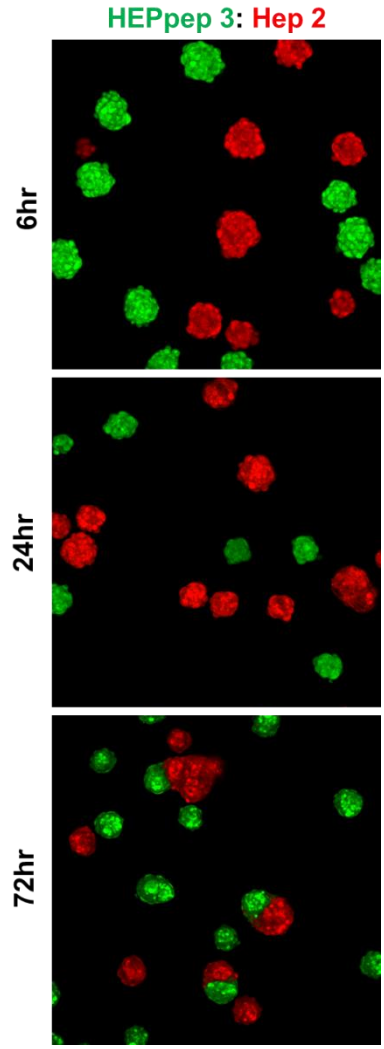

Figure 5.13. HEPpep and Hep coated 200-cell spheroids cultured at a ratio of 3:2 aggregate after 72hrs. Confocal images of HEPpep coated (green) and Hep coated (red) spheroids cultured at 6hr (top), 24hr (middle) and 72hr (bottom). Scale bar = 100µm, n = ~1000 spheroids in total.

5.4 Discussion

In this study, we have examined the effects of HEPpep and Hep coatings on MSC spheroid assembly to form multicellular constructs in a 3D dynamic system. To date, this

is the first reported study of microtissue assembly from smaller MSC building blocks in a dynamic system of culture [74, 130]. Through coating characterization, we first confirmed that using the layer-by-layer technology previously utilized in this laboratory (Figure 5.1), results in grafting of both the peptide sequence HEPpep and the heparin onto cell surfaces. After coating, these cells were able to form into spheroids and after 3 days in culture, the HEPpep and Hep layers were still present and the cells within the spheroids remained viable, indicating that the coating process and the HEPpep and heparin layers do not have detrimental effects on cell viability. While other systems have grafted the HEPpep sequence to 2D surfaces [191], this technology to our knowledge, is the first reported example of grafting this peptide sequence onto cell surfaces.

Assembly of spheroids with a HEPpep coating can occur in two forms: culture in environments containing soluble GAGs or culture with Hep coated spheroids. When cultured in media containing soluble Hep or Hep-, only HEPpep coating spheroids appeared to increase diameter size, indicating that spheroids were assembling to form larger constructs (Figure 5.6A). Because the HEPpep contains a lysine residue, and therefore is positively charged in addition to presenting the sequence specific for heparin binding, we believe that soluble Hep can act as a crosslinker to bring together these HEPpep coated spheroids while in rotary culture. This specific interaction has been observed previous reports that have shown that HEPpep grafted to a 2D surface is able to sequester heparin from culture supplements [191]. While HEPpep and heparin can specifically interact, the similar results observed with Hep- in the media indicates that Hep- may contain an overall negative charge able to bring together the positively-charged HEPpep coated spheroids to form larger assembled spheroids (Figure 5.6B).

Additionally, when using a scrambled peptide that has the same charge as the HEPpep sequence but does not express a specific heparin binding site, Scramble coated spheroids did not appear to assemble when cultured in media containing any soluble GAG (Figure 5.6D-F). This indicates that any nonspecific electrostatic interaction between the Scramble coating and Hep or Hep- was not sufficient to promote spheroid assembly and that there may actually be some degree of specific binding between the HEPpep coating and Hep- in addition to electrostatic interactions.

The specificity of assembled spheroid populations with different coatings was also observed to be specific to HEPpep–Hep interactions. Images confirmed that larger assembled aggregates contained populations of both HEPpep and Hep coated spheroids when assembled (Figure 5.7A). When presented in coating form, the interaction that drives spheroid assembly appears to require the HEPpep and Hep coating that can specifically interact with each other, as all scramble coated groups and HEPpep and Hep- coated spheroids did not result in percentages of aggregates above the cutoff size significantly different than the control group (Table 5.2). The differences observed between the two presentations of GAG, in which both Hep and Hep- in media can direct spheroid assembly while only a Hep coating can drive assembly with HEPpep coated spheroids, may be a result of the availability of the GAG in each form. When soluble Hep and Hep- are in media, they are readily available and surround all HEPpep coated spheroids, and therefore can freely interact with the coating to promote assembly. On the other hand, when HEPpep coated spheroids and Hep coated spheroids are cultured in dynamic rotary culture, random collisions between the two different spheroids are required to then facilitate interactions that result in assembly. The specific interaction that

occurs upon collision between HEPpep coated and Hep coated spheroids enables the binding of the different populations of spheroids to form assembled aggregates.

Once examining the assembly of these spheroid building blocks, we examined the stability of these aggregates by adding a soluble competitor to the media of HEPpep and Hep coated assemblies. After 24 hours of culture in media containing exogenous HEPpep competitor, it was observed that the interaction of HEPpep and Hep that results in assembly is stable and will not disassemble over that period of time (Figure 5.8). This finding is important in applications where cells in the microtissue will secrete proteins that contain heparin binding sites that can interact or compete with the heparin coating to break apart the formed aggregate [128].

After establishing that this coating system can assemble smaller spheroid building blocks when cultured together in a dynamic system, we investigated different parameters in this system that could affect the assembled aggregate properties (size, composition, and interface). We first varied the ratio of HEPpep coated spheroids to Hep coated spheroids in culture from 1:1 to 10:1. At the ratio of 10:1, no assembly of spheroids was observed over 72 hours, indicating that there may be a maximum ratio at which no assembly of different spheroid populations will occur due to the decreased amount of Hep coated spheroids resulting in a lack of available binding site interactions (Figure 5.11A). Percent of assembly in all other groups (1:1-6:1) was maintained approximate around 15% at both time points, demonstrating that once assembly occurs, the overall system does not promote further assembly (Table 5.1). Additionally, assembled aggregate size, composition and interfacial area between the two populations were not significantly different among the groups that aggregated and between 24 and 72 hours (Figure 5.11B-

D). This indicates that altering population ratio in this system may not be a factor in controlling size, composition and binding area of assembled coated spheroids and that other parameters that can affect kinetic collisions within the system can play a role in the observed measurements such as aggregate size. For example, while observed with a different cell type, it has been seen that rotation speed in dynamic rotary suspension can dictate the size of the resulting embryoid bodies formed from single cell embryonic stem cells, indicating that rotation speed is a parameter that can affect aggregate formation size [299, 300].

To further examine this system of coated MSC spheroid assembly, we varied the parameter of available binding area in the system by changing spheroid diameter and spheroid sizes in culture. In comparing these two groups, theoretical binding area was varied, while cell number of each coated populations was constant. This was performed in effort to mimic previous coculture systems that have varied heterotypic interactions between the two cell types, while holding cell number constant to maintain homotypic interactions [148]. As expected, with larger spheroids in culture to provide a higher binding area, larger assembled spheroids and higher interfacial area was observed at 24 hours when compared to the lower surface area group (Figure 5.12B). Similar to the previous study, percent assembly remained around ~15% for both groups at 24 hours, however did appear to increase at 72 hours (Table 5.2). At 72 hours, assembled aggregates exhibited cell population mixing and cell rearrangement, resulting in decreased aggregate size for the larger binding area group (Figure 5.12A&B). This was not observed for smaller aggregates in previous experiments, thus the size of the spheroid, and ultimately the number of cells in each spheroid, may limit the control of

assembly in this coating system. The difference in assembly observed between altering ratio and altering surface area of coated MSC spheroids demonstrate that parameters held constant in these studies, such as rotation speed of rotary culture or total number of spheroids cultured together, alter the kinetics that affects the number of collisions between the two different populations, thus resulting in assembled constructs of different sizes and compositions.

Through these studies, we have also identified certain limitations in this microtissue assembly system of coated MSC spheroids. With the model MSC cell type utilized, it was observed that cellular rearrangement began to occur as early as 72 hours in culture, indicating that we may not have control over the homotypic and heterotypic interactions in long term culture with this adherent cell type. While only one cell type was used in this study, we have shown the ability to initially assemble these coated spheroids, and future usages of this coating technique on different cell types [229, 232, 279], can lead to the development of multicellular microtissues that can be cultured for tissue model or repair applications. Additionally, in these studies, we demonstrated that while assembly can occur between HEPpep and Hep coated spheroids, efficiency of assembly remained consistently below 20%. To increase this assembly efficiency within the population, further examination of this system to determine other factors, such altering rotation speed or altering total number of spheroids, may need to be optimized.

We have ultimately shown in these studies that using a HEPpep and Hep coating system on MSC spheroids can facilitate self-assembly of smaller building blocks to form larger aggregates in a dynamic system. Additionally, harnessing this specific interaction facilitates the aggregation of a population of coated spheroids in one system. These

qualities of this assembly method represent a technology that can be amenable to large scale up bioprocesses, an aspect that has not been studied in the current microtissue field. By exploiting the ability of heparin to bind growth factors, a novel technique to build microtissues from smaller building block aggregates has been developed and has the potential to be implemented in *in vitro* tissue modeling and *in vivo* tissue repair applications.

5.5 Conclusions

These studies demonstrate a novel technique to assemble small building blocks using HEPpep and Hep coatings on MSC spheroids. By using layer-by-layer deposition, biotinylated HEPpep and Hep can be grafted onto MSC surfaces for up to 3 days without having detrimental effects on cell viability. We have shown that the HEPpep coating specifically interacts with the Hep coating to promote assembly of two different spheroid populations and that controlling assembly can be performed by altering available binding area. These results establish a new method that is scalable for large bioprocessing applications to form a population of self-assembled microtissue in dynamic culture by exploiting heparin interactions with growth factor derivatives for future uses of *in vitro* tissue modeling and *in vivo* tissue repair applications.

CHAPTER 6

CONCLUSIONS AND RECOMMENDATIONS[2]

6.1 Summary

Heparin, a highly sulfated GAG, has anti-coagulant activity, plays a role in organizing basement membrane and can act as a co-receptor to bind and sequester positively charged growth factors, cytokines, and chemokines and enhance ligand-receptor signaling [244]. It can be produced by mast cells throughout the entire body or found tethered to cell membrane proteoglycans [157, 166]. Due to its negative charge, heparin can be manipulated as a biomaterial with the ability to sequester and bind positively charged growth factors to cells to guide behavior [16]. In the work presented in this thesis, the unique properties of heparin-protein interaction and binding has been exploited and presented to cells via an engineered coating and the effects of this heparin coating were examined on mesenchymal stem cell (MSC) aggregates and spheroids.

MSCs are multipotent stem cells with the ability to differentiate down bone, cartilage and muscle lineages and secrete trophic factors that promote regeneration and repair of injured tissue [1, 4]. While MSCs are a promising cell source and are currently being used in over 300 clinical trials, an approved therapy using MSC does not exist [5, 6]. To improve MSC-based therapies, biomaterial strategies, such as a heparin cell coating, can be used to provide cues in the surrounding environment to guide cell behavior [16, 17, 103, 209]. Therefore, the combination of using MSCs with heparin

[2] Portions of this chapter were taken from Lei, J., McLane, L., Curtis, J.E., Temenoff, J.S. (2014). "Characterization of a multilayer heparin coating for biomolecule presentation to human mesenchymal stem cell spheroids." *Biomaterials Science*. 2: 666- 673. DOI:10.1039/C3BM60271K

biomaterials can potentially be used in future cell-based therapies for the treatment a wide variety of injuries and pathologies.

The overall goal of this dissertation was to engineer a heparin coating that exploits the interactions with surrounding growth factors or binding peptides to influence MSC behaviors, such as cell proliferation, differentiation and aggregation. To investigate how heparin coatings can modulate cellular response, MSCs were coated using a layer-by-layer method with heparin, desulfated heparin or a heparin binding peptide. Together these studies provide valuable insight into the unique ability of engineered heparin coatings on cell surfaces to promote a desired cell behavior in different environments for future development of MSC-based therapeutics.

In Chapter 3, heparin coatings for MSC cell surfaces were developed for MSC spheroids. A multilayer technology was used to graft a range of 5 μg/mL–5 mg/mL heparin onto the surface of MSC aggregates. Results revealed that heparin coating did not affect cell viability (seen through LIVE/DEAD staining) and cell anti-inflammatory properties (seen through co-culture with activated monocytes) and facilitated sequestration by coated cells of a growth factor (transforming growth factor- β1, TGF-β1) that remained bioactive. Together, these studies provide insight into a system that could potentially maximize the therapeutic potential of MSC-based treatments because the loaded protein can both signal to influence transplanted cell fate and be released into the surrounding environment to help repair injured tissue.

In Chapter 4, the response of heparin-species coatings to positively charged growth factors were studied within an MSC aggregate. Due to the importance of the high negative charge density in the interactions with growth factors, both heparin and

desulfated heparin were grafted onto cell surfaces within the aggregate using the developed coating technology and the following were examined: 1) cell number in response to fibroblast growth factor-2 (FGF-2) and 2) chondrogenic differentiation in response to TGF-β1. Results revealed that in the presence of FGF-2, by day 14, heparin-coated MSC aggregates increased in DNA content 8.5±1.6 fold compared to day 1, which was greater than noncoated and desulfated heparin-coated aggregates. In contrast, when cultured in the presence of TGF-β1, by day 21, desulfated heparin-coated aggregates upregulated gene expression of collagen II by 86.5±7.5 fold and collagen X by 37.1±4.7 fold, which was higher than that recorded in the noncoated and heparin-coated aggregates. These observations indicate that this coating technology represents a versatile platform to design MSC culture systems with pairings of GAGs and growth factors that can be tailored to overcome specific challenges in scale-up and culture for MSC-based therapeutics.

In Chapter 5, the interaction between heparin and a growth factor derived binding sequence (HEPpep) was used to promote assembly of MSC spheroids into small microtissue constructs in a dynamic culture environment. This technology demonstrated a novel method to self-assemble a population of microtissues out of smaller building blocks in suspension culture. The heparin and HEPpep coating interaction was observed to be specific for each other and resulted in assembly of spheroids to form constructs containing multiple cell populations. It was observed that at different cell population ratios and different levels of binding area within the system, the interactions between the heparin and HEPpep coatings resulted in assembly of the two cell populations after 24 hours and remained present up to 72 hours, However, altering these factors did not affect

the interfacial area between the two cell populations and cellular rearrangement within the assembled aggregates was observed at 72 hours. Together, these results present a new method to assemble building blocks in a "bottom-up" approach to form small microtissues with multiple cell populations by exploiting the interaction of GAG and its corresponding binding sequence in a coated presentation.

Together, these findings presented in this dissertation suggest that heparin in a coating form can promote MSC response to growth factors and MSC aggregation. These engineered GAG molecular interactions at the cell surface can be used as a powerful and promising tool to promote a desired cell response or direct cell aggregation in future MSC-based therapies.

6.2 Conclusions

The research presented in this dissertation advances the understanding of how engineered GAG interactions at MSC surfaces can be utilized to direct cell behavior. Based on the native proteoglycan structure seen at cell surfaces, coating cells with heparin is a novel technology to present both native and non-native GAGs to cell to alter the local microenvironment. These studies have examined 1) the effects of the heparin coating on protein loading, inherent MSC anti-inflammatory properties and native pericellular matrix, 2) the effects of heparin on modulate response to positively charged growth factors in the environment, and 3) the effects of heparin interactions on promoting cell aggregation. Together, these results indicate that heparin-based coatings can be used to as a potential tool to promote a desired cell response in MSC-based therapies.

The approach in this dissertation involves engineering the interactions that occur at the cell surface through a coating technology, as developed and characterized in Chapter 3. In this chapter, this approach presented a potential a dual-delivery system, in which a biomolecule of interest can be released from cell surfaces to help regenerate and repair tissue without the use of excess biomaterials. This coating technology exploited growth factor interactions with heparin, as it is the most sulfated native GAG and is known to interact and bind numerous positively charged proteins through electrostatic and sequence specific interactions.

Heparin coating was grafted onto surfaces using layer-by-layer deposition of biotin and avidin. As the outer layer, heparin's high negative charge, resulting from the presence of multiple sulfate groups, facilitated the sequestration of positively charged biomolecules via electrostatic interactions [244]. The amount of heparin grafted on cells was tuned using different initial concentrations in solution. Given a fixed number of cells per spheroid, coating concentrations ranging from 5 μg/mL to 5 mg/mL resulted in an increased amount of heparin visualized on cell surfaces. While it was expected that the amount of heparin grafted would plateau near the theoretical saturation level of the 1 mg/mL concentration, the fact that increased fluorescence was observed at 5 mg/mL suggested that multiple layers of heparin can be deposited onto the surface, perhaps mediated through both the avidin–biotinylated heparin interactions and electrostatic interactions between avidin and heparin. Over time, the removal of the heparin coating from cell surfaces could be attributed to secretion of enzymes that cleave heparin, or cell membrane turnover or non-biotinylated heparin release into surrounding environments

[257]. Overall, characterization of this coating revealed that it was possible to tune and control the amount of heparin that could be grafted on to cell surfaces.

To study the effects of this heparin coating on MSC properties, the pericellular matrix (PCM) and anti-inflammatory properties of MSCs were also examined in Chapter 3. The PCM is composed predominantly of chondroitin sulfate-rich proteoglycans and hyaluronan can play a role in cell interaction with the environment and cell adhesion [250, 258, 259]. It was important to study the presence of the PCM after the coating procedure to better understand what was being presented on the surface of the cells after coating. The decreased PCM thickness and lack of regrowth after 24 hours suggested that the heparin coating procedure removed or collapsed (via crosslinking) the natural PCM found on cell surfaces. This implied that the heparin coating could exist on cell surfaces for at least 1 day without being overwhelmed by the natural matrix. For anti-inflammatory properties, the ability of MSC spheroids to attenuate tumor necrosis factor-α (TNF-α) secretion by activated monocytes was observed [3, 84]. Using a co-culture assay, the highly negatively charged heparin layer did not alter the ability of MSCs to attenuate TNF-α production by monocytes, suggesting that sufficient anti-inflammatory signaling by MSCs was able to occur. These results indicated that the addition and modification of cell surfaces did not alter the inherent ability of MSC spheroids to attenuate monocyte pro-inflammatory cytokine secretion.

Lastly, in Chapter 3, assessment of a loaded protein bioactivity was performed using a reporter mink lung epithelial cell (MLEC) cell line known to express plasminogen activator inhibitor (PAI-1) fused with a luciferase firefly reporter in response to TGF-β1 in a dose dependent manner [255, 268]. After assaying the

supernatant containing any released TGF-β1 that was loaded onto heparin coated cells, it was seen that the presence of the heparin coating could help preserve the bioactivity of the TGF-β1. Based on these results, it was envisioned that the bioactive protein could be able to "signal out" to the neighboring cells and the surrounding environment to encourage regeneration. This multifaceted system could potentially be used in cell-based therapies to both prime cells for cell-mediated tissue regeneration and release biomolecules to modulate the damaged tissue environment.

To characterize the interactions of how this GAG coating could facilitate a bioactive protein's ability to "signal-in" to the cells, in Chapter 4, coated MSCs were cultured in environments containing different growth factors. Because the high negative charge density of heparin is attributed to the sulfation groups found along the GAG backbone [20], desulfation of heparin was performed to study how electrostatic interactions can modulate cell response to growth factors in the surrounding environment. Once heparin was desulfated through solvylytic removal of sulfate groups [165], layer-by-layer deposition was used to graft biotinylated heparin species of native and no sulfation onto cell surfaces. Via chromatography analysis, the amount of heparin and desulfated heparin was measured and confirmed to be approximately the same amount when the same coating concentration was used. Therefore, by using this technique, different species of GAGs were grafted onto cell surfaces at similar amounts, and presented a controlled method to study the effects of GAG interactions with soluble growth factors in coated MSC aggregates.

To potentially overcome the challenge of limited proliferative capacity in MSC aggregates, the addition of the mitogenic protein FGF-2 has been used to improve

proliferation in MSCs [183]. Using the developed technique of grafting heparin species of native and no sulfation, the response of coated MSCs in aggregate form to FGF-2 in the media was observed. Only when both a heparin coating of native sulfation and FGF-2 were present in the system, increased cell number in MSC aggregates occurred. It is known that FGF-2 signals through the dimerization of the growth factor and cell surface receptor, facilitated by heparin interactions between the 2-O and N-sulfate groups and growth factor, occurs [20, 176, 280]. Thus, the presence of the heparin coating could facilitate the sequestration of FGF-2 within the aggregate, as well as could promote signaling through dimerization of the receptor, together resulting in the increased cell number observed. While the desulfated heparin coating may still be able to sequester FGF-2 locally in the aggregate due to an overall negative charge that exists because of the remaining carboxyl groups, it may lack the sulfate groups necessary for signaling of FGF-2 to cause cell proliferation [178], and therefore resulted in DNA content more similar to that of the noncoated controls. Taken together, these results suggested that a heparin coating combined with mitogenic growth factors in the media could help address the reduced proliferation capacity and thus could be used as a system for expansion of MSC aggregates for subsequent administration in cell-based therapies such as treating graft versus host or autoimmune diseases [6, 8].

On the other hand, when cultured with TGF-β1, a growth factor that is commonly used for chondrogenic differentiation, desulfated heparin coated aggregates exhibited more upregulation of the chondrogenic gene marker collagen II and the hypertrophic gene marker collagen X by day 21 compared to noncoated aggregates and heparin coated aggregates. This indicated that a desulfated heparin coating could potentiate the

chondrogenic response of TGF-β1 to promote increased chondrocytic and hypertrophic differentiation in MSC aggregates. In contrast to heparin coatings that were seen to promote proliferation in response to FGF-2 in MSC aggregates, upregulated chondrogenic marker expression was observed in desulfated heparin coated aggregates in response to TGF-β1. It has been shown that the 6-O and N-sulfate groups play a role in the interaction of heparin with TGF-β1, and upon desulfation of those groups, the affinity for the growth factor decreases [186]. However, desulfation did not affect the ability of TGF-β1 to signal to MSCs, indicating that while desulfated forms of different GAGs could have a lower affinity, the effects of TGF-β1 on cellular response is not dictated by that binding interaction [186]. In this coating system, it was speculated that the binding of TGF-β1 to heparin could have prevented growth factor interaction with its receptor, resulting in reduced chondrogenic effects when compared to the desulfated coated MSCs.

While these studies from Chapter 4 support the concept that GAG cell coatings could be used to improve the effect and presentation of growth factors in culture, the results indicated that it is important to consider that a "one GAG fits all" strategy may not be optimal for all MSC culture applications and non-native sulfation patterns may also have the capability to potentiate the activity of specific growth factors. Therefore, this coating technology represents a versatile platform to design MSC culture systems with pairings of GAGs and growth factors that can be tailored to overcome specific challenges for MSC-based therapeutics.

Lastly, MSCs in microtissues can be a promising approach for regeneration of tissue or *in vitro* modeling [7, 135, 136]. By exploiting heparin and growth factor binding interactions presented in coating form, this technology could be used to self-assemble

cells of different populations in a dynamic system to form microtissue constructs. The specific heparin binding site on the growth factor FGF-2 has previously been isolated and synthesized into a short peptide form (HEPpep) [191]. Because this sequence could be produced to include a biotin group, it could also be grafted onto cell surfaces via the layer-by-layer technology used in this dissertation. It was observed that the biotin-avidin layering technique facilitated the grafting of a biotinylated HEPpep sequence onto cell surfaces, without disrupting the MSCs ability to form spheroids or having detrimental effects on cell viability. Additionally, the coating appeared to remain on cell surfaces for up to 3 days. Therefore, these results indicated that this versatile coating method could be used to graft a variety of heparin-based molecules onto cell surfaces.

As observed in Chapter 5, self-assembly occurred when HEPpep coated spheroids were cultured in media containing soluble heparin in solution and when cultured with heparin coated spheroids. The assembly of these HEPpep coated spheroids resulted in larger aggregates when cultured with soluble heparin and aggregates that contained two different cell populations when cultured with heparin coated spheroids. Additionally, this interaction appeared to be specific between the two molecules as assembly of coated MSCs only occurred when heparin coatings were presented to HEPpep coatings, and not a scramble peptide coating. This scramble peptide presented a similar charge density as HEPpep to the spheroids, however did not contain the specific binding sequence for heparin [191]. Together these results presented a potential opportunity to promote assembly of different cell populations by using a coating system that exploited binding between GAGs and its corresponding binding site. This system was advantageous compared to current assembly methods in that assembly to form multiple microtissues

containing multiple cell populations can occur on its own without external direction or manipulation of the cell populations in a dynamic system [23, 134-136]. Additionally, this was believed to be the first report of microtissue assembly in a dynamic system, rather than a static system, and could potentially be implemented in larger scale processing systems.

To further examine the properties of this self-assembled microtissue system, altering cell population ratio and interfacial binding areas was performed in Chapter 5 to study effects on the types of assembly that was occurring in the system. This included examining assembled aggregate size, composition of the assembled aggregate and the interfacial area between the cell populations. After 24 and 72 hours in dynamic culture, aggregate assembly was observed between HEPpep coated and heparin coated spheroids at varying cell population ratios and varying binding area availabilities. However, assembled aggregate size, composition and interfacial area did not appear to be different among the groups varying cell population ratio between 24 and 72 hours and rearrangement of the cells within the assembled aggregate was observed at 72 hours. These results indicated that while optimization of different parameters in the system need to be explored to better characterize assembly of coated spheroids, altering molecular interactions at the cell surface could be used as a method to self-assemble coated spheroids into larger constructs.

This heparin coated-based biomaterials approach presented in this dissertation provides a novel system that exploits GAG interactions in a coated presentation to guide cell behavior for MSC-based therapies. By using the ability of heparin to interact with different positively charged growth factors or its binding sites, cell response to

surrounding growth factors and cell interactions with other coated populations were examined. At the cellular level, harnessing the molecular interactions of heparin species with different sulfation levels at the surface of MSCs allowed this system to potentiate specific growth factor response and direct MSCs to behave in a certain manner for future therapeutic applications. At a larger scale, exploiting heparin and growth factor binding facilitated this system to promote cell aggregation to form tissue constructs for future microtissue applications. Taken together, this coating technology can be a valuable and powerful tool to engineer molecular interactions at cell surfaces that modulate the environment and direct behavior for future cell-based therapies.

6.3 Future Directions

The findings presented in this dissertation provide significant insight into the potential uses of exploiting GAG interactions at cell surfaces to modulate MSC aggregate behavior. A coating system able to graft multiple species of heparin on multiple cell types was developed and its effects on growth factor response and microtissue assembly were examined. The results of these experiments suggest that engineering cell surfaces with exogenous GAG introduces a level of control of what is presented to cells and the subsequent cellular response. The studies in this dissertation represent a broad examination of how these heparin coatings can be used in different MSC behaviors, ranging from proliferation to differentiation to aggregation. However, while this characterized system has shown to be versatile and can potentially be used for a variety of applications in MSC-based therapies, future work can expand on the insights gained

from this dissertation to better understand how the molecular interactions of heparin and growth factors at the cell surface affect cell behavior.

For a thorough investigation of MSC response to growth factors in media, molecular interactions at cell surfaces between the GAG layer and growth factor can be further characterized through depletion or "pull-down" studies. These experiments would culture heparin and desulfated heparin coated cells in the presence of a growth factor, such as FGF-2, and the concentrations of the growth factor would be measured over time to determine the amount of protein remaining in the environment [200]. For pull-down of FGF-2 within coated aggregates, this understanding will provide quantification of heparin coating sequestration of FGF-2 from the environment and ultimately, the contribution of the coating's ability to promote an increase in cell number. To further parse out how heparin coatings can modulate response to FGF-2, visualization of the downstream signal molecules, such as Erk1/2, could provide insight into where signaling is spatially occurring within the aggregate [301], and whether cell proliferation via FGF-2 signaling is observed within the entire aggregate or around simply exterior surface. Together, this information can lead to a better understanding how and where the interaction of GAG coatings on cell surfaces can potentiate a growth factor response.

These studies can also be particularly interesting and informative because of the results observed when heparin coatings of native and no sulfation were cultured with the chondrogenic growth factor TGF-β1. It was observed in Chapter 4 that MSC aggregates coated with desulfated heparin had upregulated gene expression of chondrogenic markers when cultured with TGF-β1 in the environment. It is known that the 6-O and N-sulfate groups on heparin are important for interaction with TGF-β1, therefore, upon desulfation

and removal of those groups, the affinity for the growth factor decreases. However, despite this decreased affinity, there is an increased response to the growth factor in desulfated heparin coated MSCs when compared to heparin coated MSCs. Studying the sequestration profile of TGF-β1 in the presence of a desulfated heparin coating and its subsequent signaling can therefore clarify the how that interaction can result in promoting chondrogenic differentiation in MSC aggregates.

To further develop MSC coated aggregates for purposes of differentiation in cell-based therapies, a different regimen of differentiation cues can be utilized to promote chondrogenic differentiation. For example, often times a cocktail of growth factors is used to promote effect differentiation of MSCs down a chondrogenic lineage for cell-based therapies. Combinations of FGF-2, TGF-β1, BMP-7 and IGF-1 have been reported to all induce chondrogenic differentiation or support cartilage maturation [302]. Although contrasting results were observed with heparin and desulfated heparin coatings when cultured with two separate growth factors, the response of the coated cells when cultured with a cocktail of growth factors could provide insight how these coatings can promote differentiation in MSC aggregates when cultured in a complex environment containing multiple differentiation cues. Overall, this study can examine the effect of GAG coatings in response to different and multiple growth factors can offer novel potential strategies to engineer the environment surrounding cells to guide cell behavior.

In addition to the ability of heparin to sequester positively charged growth factors, heparin also has the ability to act as a delivery vehicle and support controlled release of growth factors [16, 17, 199, 303]. It was observed in Chapter 3 that this heparin coating facilitated loading of TGF-β1 onto cell surfaces and that the released growth factor

remained bioactive. Further studies can be performed to examine the amount of released TGF-β1 and whether it is able to signal to another population of cells to promote chondrogenic differentiation. Additionally, this coating platform establishes an opportunity to explore how altering sulfation pattern can modulate the release of a loaded growth factor from cell surfaces. It has previously been shown that selectively desulfating heparin can tune the release of growth factors, in which increasing desulfation resulted in increased cumulative release of FGF-2 [164]. Thus, by observing the release profiles of growth factors from engineered cell coatings of heparin species with varying sulfation levels, these studies can provide insight into how GAG coatings on cells can be engineered into a dual-delivery system in which both cells and a released biomolecule can act to help regenerate and repair a site of injury.

For translation into *in vivo* studies and eventually clinical settings, a coating that uses minimal manipulation of the cells may be preferred and beneficial. MSCs that have not been subjected to multiple incubations steps that are not performed in the preferred media environment of the cells may reduce cell loss during the coating process. Ultimately, the current layer-by-layer deposition of biotin and avidin, while effective in grafting multiple molecules onto cell surfaces, requires extensive manipulation of cells. Additionally, it has been shown that the use of avidin has the potential to promote an immunogenic response when translated to *in vivo* settings [304]. The removal of this layer combined with development of a method to graft the GAG layer directly to cell surfaces may lead to a coating process that is more efficient in retaining live cells and requires less manipulation, thus is less time consuming.

Two suggested methods to achieve a more optimal coating process are to utilize covalent conjugation to cell surface amino residues or to incorporate amphiphilic polymers into lipid bilayer membranes by hydrophobic interactions [207, 305]. Both methods require chemical modification of the GAG of interest, however there is no longer a necessity of having intermediate layers because of the direct conjugation onto cell surfaces. For covalent conjugation, heparin can be chemically modified with the N-hydroxyl-succinimidyl ester group to form covalent bonds to amino groups of membrane proteins [306, 307]. Poly (ethylene glycol)-conjugated phospholipids (PEG-lipid) or poly (vinyl alcohol) bearing hydrophobic alkyl side chains (PVA-alkyl) have been used due to the spontaneous attachment to cell membranes by anchoring into the lipid bilayer membranes through hydrophobic interactions [308-310]. Both methods require modification of heparin or the GAG of interest with these added side groups that directly target moieties on cell surface membranes. Using these direct coating methods, the removal of layer-by-layer deposition can provide a less manipulative process to coat cells and ultimately can be easily translated for clinical scale up.

Aside from having the ability to potentiate growth factor response, heparin coatings and their interactions with growth factors can be exploited to promote cell aggregation, as observed in Chapter 5. By presenting heparin and HEPpep onto cell surfaces, the interaction can be harnessed to bring together the two differentially coated populations as assembly of small building blocks. This assembly can be used to build microtissues in a self-aggregating manner that does not require manual manipulation of seeding different cell populations around each other. While assembly of coated MSC spheroids was performed in Chapter 5, this coating technology is applicable and

translatable to other cell types, as has been observed in both literature and Chapter 2 [229, 230, 279]. Thus, this coating technology for assembly of microtissues can be used to study complex systems with multiple cell types, such as hepatocyte and fibroblast co-cultures to maintain cell phenotype and function, as well as model complex stem cell environments, such as the bone marrow to understand how MSCs, endothelial cells and osteoblasts can interact to maintain HSC phenotype [96, 148, 149, 294]. Furthermore, HEPpep and heparin coatings can be applied to nonadherent immune cells to promote aggregation of lymphocytes and platelets because it is known that cell-cell contacts between these cell types can enhance adhesion and cell migration of T and B cells [311, 312]. This can be used to study heterotypic interactions and cross talk between lymphocytes and platelets to examine the important regulatory mechanisms from aggregation in thrombosis, inflammation and atherosclerosis processes [311, 312]. Furthermore, by using HEPpep coatings cultured in soluble heparin, homotypic lymphocyte aggregation can also be engineered, as cell-cell interactions play a central role in T and B cell activation as well as migration of cells during the inflammatory response [313-315]. Because of the versatility of this technology, the usage of these coatings is not limited to the forming MSC microtissues in a self-assembled manner, and this platform can be translated to other cellular systems to study behaviors, such as functional phenotype, migration, and immune cell activation.

The studies performed in this dissertation with this coating system were performed in a dynamic system in which MSC spheroids were cultured in suspension. While in this suspension system, heparin coated MSC spheroids were able to interact with HEPpep coated MSC spheroids to form small constructs containing multiple cell

populations. While further parameters of the system should be optimized to control how these coated cells assemble in terms of bringing together two different populations in direct contact with each other, the dynamic platform to promote aggregation of a population of building blocks can be translated to larger scale processes to form large populations of microtissues. This could be useful because many of the proposed MSC-based therapies require high and multiple dosages of cells, therefore, large expansion and culture of these cells are necessary [5]. The assembly of coated MSC spheroids in a dynamic rotational system establishes the basis for a future platform to construct a population of small microtissues in a system that is amenable to large scale production that could be translated into clinical use.

Combined with the results from Chapter 3, this technology has the potential to not only assemble cell populations for microtissue construction, but also deliver growth factors to a specific population. It was shown that the interaction between heparin and FGF-2 can promote a potentiated growth factor response in the coated cells. Therefore, incorporating that aspect with microtissue assembly, this coating technology could be used to not only promote self-assembly within a coated population of cells, but also deliver biomolecules of a specific population of coated cells to promote a subsequent behavior and response. In the case of culturing hepatocytes for the use of liver-assist devices, coated hepatocytes and MSCs could be assembled together using this system to form a population of tissue constructs with controlled homotypic and heterotypic interactions to produce a hepatocyte population that is phenotypically functional (urea and albumin production). Once those parameters are optimized and achieved, a growth factor, such has HGF, can be delivered to the heparin-coated MSC populations in the

constructs to promote differentiation down the hepatic lineage to form hepatic tissue constructs that could be implemented for liver repair or in a liver-assist device [141]. This system exploits both the ability of heparin and HEPpep coatings to promote self-assembly of cells, but also the sequestration properties of heparin. Additionally, because this system is performed in a dynamic setting that supports both the construction and culture of microtissues, this facilitates the ability to temporally introduce different components into the cultured constructs. Therefore, once microtissues have been constructed and cultured, it is possible to continue to build up the construct by introduction of another coated population. In the case of hepatocyte and MSC microtissues, once constructed and cultured to a desired timepoint, the addition of coated endothelial cells can be introduce and self-assembled to represent the *in vivo* sinusoidal structure found in functional liver tissue [316]. This platform represents a modular system that can promote the construction and support the culture of complex tissue structures by exploiting molecular interactions of heparin at cell surfaces.

Future work can expand on the various principles and findings presented in this dissertation to develop a GAG coating that is able to control the immediate microenvironment around a cell to guide cell behavior. The numerous applications and usages of GAG-based coatings establish that this enabling technology can be used to engineer molecular interactions at the cell surface to influence cell and tissue behavior. Taken together, the research presented in this thesis provides valuable insight into the ability to engineer molecular interactions of heparin at cell surfaces to direct the behavior of cells and tissues for a variety of applications.

APPENDIX A

POTENTIAL APPLICATIONS FOR ASSEMBLED AGGREGATES DEVELOPED IN AIM 3

Although the results from Chapter 5 did not reveal a robust system that can be used to control assembly for microtissue formation in a self-assembled manner, the applications of exploiting molecular interactions between heparin and HEPpep coated cells can also be used in other technologies, such as bioprinting. Bioprinting is a recent method to create biologically relevant materials and is defined as a set of techniques that transfer biologically important materials onto a substrate. The result of bioprinting is a complex, well defined three-dimensional structure that recreates multicellular tissues and organs *de novo* [317, 318]. Some examples of bioprinting methods include dip pen lithography and ink jet deposition, both of which place cells onto a substrate and is repeated to build up a hierarchical construct containing different cells in a specific orientation [319, 320]. However, some limitations of these methods include developing a nontoxic and non-damaging technique to assemble constructs rapidly to form a cohesive and mechanically stable tissue while maintaining the integrity of the cells. Additionally, printed constructs must be suitable for perfusion and be able to survive some printing methods that can require high shear environments [317]. Therefore, the application of the coating technology can be incorporated into existing bioprinting methods to help overcome these limitations.

By harnessing the interactions between heparin and HEPpep, these molecules can be coated onto cell surfaces or the substrates to promote rapid cohesion of each component. Because these coatings have been shown to promote assembly and contain a

level of specificity for each other, heparin and HEPpep coatings can essentially be used as a "glue" to keep the printed cells together and promote stable formation of the resulting tissue. These coatings can be incorporated into laser-induced transfer methods in bioprinting that aim to create grafts for wound healing applications that use both fibroblast and mesenchymal stem cells in a graft [321]. Coating these cell types can facilitate the ability to direct the organization of the cell types within the graft by promoting adhesion and aggregation in different orientations through the heparin and HEPpep coating interactions. Additionally, for bioprinting methods such as ink-jet delivery or laser-induced deposition, cell suspensions are often used and methods are often performed in fluid environments to maintain the integrity of the living cells [317]. Shear stresses caused by the transfer and deposition of printing may cause an unstable environment that the results incorrect orientation and formation of the tissue. Therefore, printing layers or sections of a tissue must allow for the printed materials to adhere to each other before proceeding to a subsequent section. Incorporation of the coating technology can be potentially useful because it has been shown to promote assembly between populations under dynamic culture settings. Therefore, it could be used in a shear-containing environment to help stabilize and form a printed tissue in the correct orientation faster by exploiting the heparin and HEPpep interaction and promoting cell adhesion. Overall, the application of incorporating heparin and HEPpep coatings into bioprinting techniques can result in promising and novel methods in bioprinting of tissues and organs.

In addition to incorporating these coating technologies into the bioprinting process to form these constructs, heparin and HEPpep coatings can also be used to direct

the shape and function of the printed tissue over time. This modular system is possible because the heparin coatings can be found on cell surfaces for up to 14 days and HEPpep coatings can be seen for at least 3 days, therefore, by harnessing their interactions to promote assembly, additional coated components can be aggregated onto the tissue construct or different orientations of the overall tissue can be changed after initial construction. Specifically, this can be used in one approach to form microvessels for vascular tissue engineering. Typically, bioprinted capillaries can be formed by using bio-ink particles (cells or cell aggregates) that are deposited on a cylindrical template. However, one limitation is the need for the particles to form adhesion junctions with each other through cell-cell contacts or ECM deposition to form a stable vessel [318]. The use of this coating technology allows bioprinting processes to form the tissue construct in an initial configuration, such as a cell sheet that facilitates a stable formation of the complex microstructure and layers in a vessel [322, 323], followed by the subsequent transformation into a cylindrical vessel by exploiting the interactions with heparin and HEPpep coatings to direct formation of adhesive junctions at the edges of the cell sheet. Therefore, incorporation of this coating technology into bioprinting applications potentially allows for modulating tissue shape and subsequent function over time after initial construction.

While further optimization of the coating system used in Chapter 5 is needed to fully develop a self-assembled microtissue formation technique, the exploitation of the heparin and HEPpep interactions can be used to form microtissue systems that are used to model complex *in vivo* environments. One example includes promoting aggregation via heparin and HEPpep coatings between lymphocytes and platelets to examine the

important regulatory mechanisms in thrombosis, inflammation and atherosclerosis processes [311, 312]. It is known that cell-cell contacts of both homotypic and heterotypic interactions can enhance the adhesion, cell migration and tissue infiltration of T and B cells [311]. Therefore, these coatings can be used as a means to promote and control assembly of these multicellular aggregates to potentially study how the amount (more or less aggregation) or type (homotypic or heterotypic) of interaction can affect lymphocytes and platelet activation in inflammatory responses. While this is a promising application, further optimization still needs to be performed to study the effects of these coatings on different cell types and new parameters, such as ratio, rotation speed and culture time, need to be determined to understand how these coatings can promote and control assembly or aggregation of different cell types.

Finally, this coating technology can potentially be used to form small tissue constructs containing multiple adherent cell types. The exploitation of the heparin and HEPpep coatings can be used to direct the spatial organization of the construct to mimic the in vivo tissue structure. This is particularly applicable for tissues with multiple zones containing different cell types and tissue structures, such as osteochondral constructs that interface between cartilage and bone tissue [324]. By harnessing the interactions of heparin and HEPpep, coated chondrocytes and osteoblasts can be assembled into osteochondral constructs that contain on one end, the cartilage tissue, and on the other end, the bone tissue. To achieve this level of controlled assembly, parameters of how many total cell building blocks are needed in the system, the ratio of the cell populations, and the dynamic and or static culture conditions need to be determined to develop a system that can support assembly in a controlled manner to form tissue constructs with

directed spatial orientations. In this example, the potential application of these coatings can ultimately be used to form constructs for both tissue repair for cartilage injuries and tissue modeling purposes to study the progression of cartilage related pathologies.

APPENDIX B

SUPPLEMENTARY FIGURES

B.1 Alginate bead heparin coating in media

B.1.1 Materials and Methods

Alginate beads were used as an acellular control for MSC spheroids due to their ease of formation and spherical shape. Alginate beads were made using the Nisco electrostatic bead generator, in which 3% alginate formed ~200 μm droplets in 100 mM calcium chloride. Beads were coated with 0.1% poly-L-lysine, followed by 4 mM EZ-Link Sulfo-NHS-LC-Biotin in PBS, followed by 0.5 mg/mL avidin in PBS, and, lastly, 5 mg/mL biotin-conjugated heparin in PBS. Each layer was incubated for 1 hour with washing steps between layers. The volume of 0.1 mL beads was incubated at 37ºC in MSC maintenance media (containing 10% FBS) replaced every other day. The heparin coating was imaged under the same imaging parameters (laser intensity, gain, and exposure time) via confocal microscopy immediately after coating (day 0) and at day 7. Fluorescent quantification was performed in ImageJ.

B.1.2 Results

After alginate beads were formed and coated, confocal imaging was used to image the heparin layer on the surface of the alginate beads. Immediately after coating, heparin was seen around the bead surfaces. After 7 days in MSC maintenance media, beads were imaged and heparin was still observed on the surface of beads with no statistical difference in fluorescence from day 0.

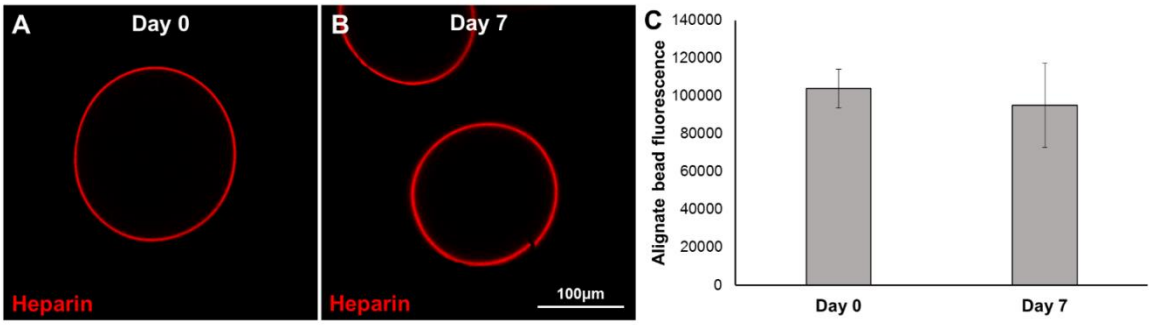

Supplemental Figure B.1. Alginate bead heparin coating in media. A) Heparin seen in red on alginate bead surfaces immediately after coating procedure (day 0). B) Heparin on alginate bead surfaces after being cultured in MSC media for 7 days at 37ºC. C) Quantification of fluorescence on alginate bead surfaces over 7 days, $p < 0.05$, n=4.

B.2. Luminescence of MLEC aggregates without TGF-β1 exposure

B.2.1 Materials and Methods

Noncoated MLECs were cultured with soluble heparin (5 mg/mL or 5 μg/mL) and exposed to TGF-β1 (3 ng/mL) for 30 minutes to mimic the coating procedure used in this study, but using a non-modified heparin that should not attach to cell surfaces. Following the same procedure as outlined for experiments shown in Figure 3.4, cells were then formed into 500-cell aggregates. Subsequently, the aggregates were cultured for 24 hours in media without heparin or with soluble heparin at 5 μg/mL or 5 mg/mL. After 24 hours in culture, cells were lysed with ONE-Glo^{TM} Luciferase Assay buffer and luminescence was measured using a plate reader.

B.2.2 Results

It was observed that soluble heparin at both concentrations without any TGF-β1 stimuli resulted in significantly lower luminescence response when compared to the control group of 3 ng/mL TGF-β1 exposure. With TGF-β1 exposure, there was no

difference observed in cells cultured with soluble heparin at either concentration compared to the control group. The resulting observations reveal that the luminescence response seen in Figure 3.4E is not a result of soluble heparin in solution.

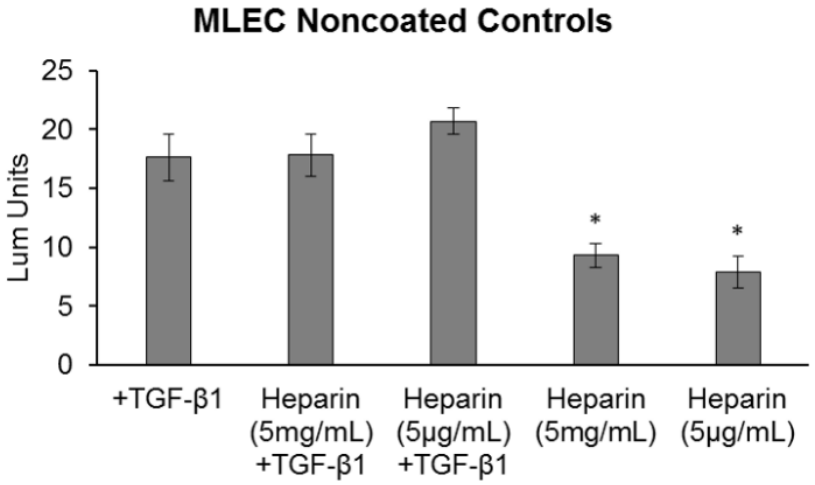

Supplemental Figure B.2. MLEC aggregates without TGF-β1 exposure had significantly less luminescence response compared to control with TGF-β1 exposure. * Statistically different than TGF-β1 only control, $p < 0.05$, n=5.

B.3. Luminescence response to noncoated MLECs with increasing TGF-β1 dosage

B.3.1 Materials and Methods

The MLEC response curve was made by plating MLECs at 50,000 cells/cm^2 in 96-well plates and culturing them in media containing TGF-β1 ranging from 0 pg/mL to 750 pg/mL with or without 5 mg/mL heparin. This concentration was chosen based on the coating concentration of 5 mg/mL, representing the maximum amount of heparin that could be released into the supernatant from the coated surface. After 24 hours in culture, cells were lysed with ONE-Glo^{TM} Luciferase Assay buffer and luminescence was measured using a plate reader.

A.3.2 Results

Higher luminescence levels were observed with higher concentrations of TGF-β1. Additionally, when heparin was is present in the media (5 mg/mL), the luminescence response was significantly lower at higher TGF-β1 concentrations (375 pg/mL and 750 pg/mL) when compared to samples without heparin in solution. These results confirm that the luminescence values reported in Figure 4F are not attributable to soluble heparin released from the cell coatings, even if all of heparin on the coatings was released within the 24 hour assay period.

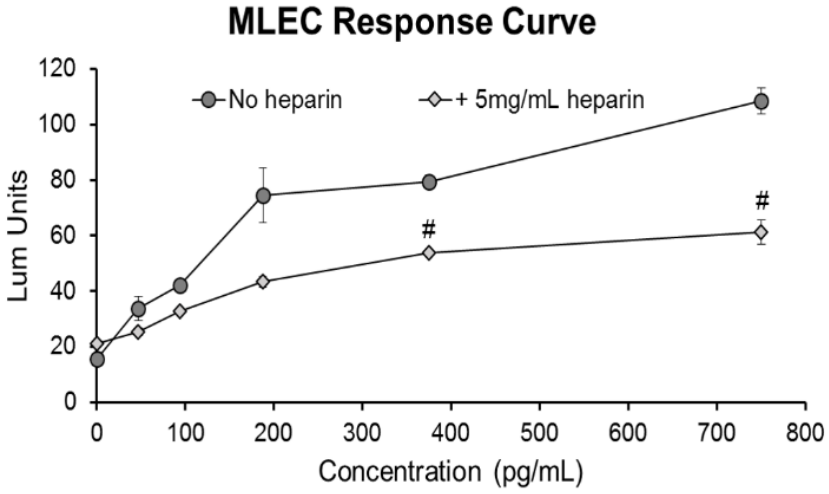

Supplemental Figure A.3. Luminescence response from noncoated plated MLECs when exposed to increasing TGF-β1 concentrations for 24 hours. # Statistically different than sample at same TGF-β1 concentration with no heparin, $p < 0.05$, n=3.

A.4 Fluorescently tagged Hep and Hep- coatings

A.4.1 Materials and Methods

Biotinylated-heparin (Hep) and biotinylated-desulfated heparin (Hep-) species were fluorescently tagged with AlexaFluor®-633 by EDC coupling in 0.1M sodium bicarbonate buffer containing 10 mg/mL GAG, 10mM AlexaFluor®-633-hydrazide,

20μM EDC. The solution reacted for 1.5 hours at room temperature while protected from light before dialysis in 3500MWCO tubing for two days and lyophilization for two days. Cells were coated as described in the Materials and Methods section of Chapter 4 using the fluorescently tagged heparin derivatives, and formed into 2000-cell aggregates in 5% Pluronic-coated 96-well V-bottom plates and cultured in serum-free media containing Dulbecco's Modified Eagle Medium, 1% nonessential amino acids, 1% antibiotic/antimycotic, 1% insulin, human transferrin and selenous acid premix and 50 μg/ml ascorbate-2-phosphate. At days 1,7 and 14, aggregates were collected, washed in PBS, and imaged under confocal microscopy at excitation wavelength 633nm and emission wavelength 647nm (Zeiss LSM 700 LSM confocal microscope). Images taken at the center of the aggregate were extracted and fluorescence observed was quantified using Image J (NIH, Bethesda, MD) (n=9).

A.4.2 Results

The fluorescence signal (seen in red) was observed strongly at day 1, and decreased over the course of 14 days (Supplemental Figure A.4A). Image analysis revealed that by day 14, both Hep and Hep- coated aggregates had decreased ~70% in fluorescence compared to day 1 (Supplemental Figure A.4B).

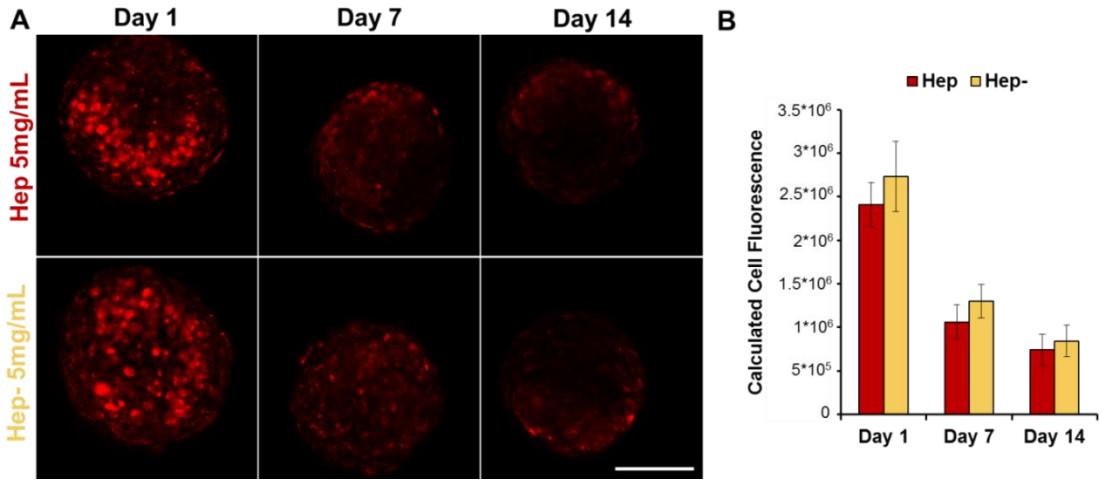

Supplemental Figure A.4. Fluorescently tagged Hep and Hep- coatings decrease in fluorescent intensity over 14 days in culture. A) Confocal images of Hep and Hep- coating (seen in red) at center of aggregate on day 1, day 7 and day 14. B) Image analysis of fluorescently tagged Hep and Hep- coatings quantified with ImageJ revealed that both coatings decreased in fluorescence at similar rates over 14 days. Scale bar = 100um, n=9.

B.5 MSC aggregates coated with biotin and avidin

B.5.1 Materials and Methods

MSCs were coated as described in the Materials and Methods section, but with only the intermediate layers of 4 mM NHS-biotin and 0.5 mg/mL avidin prior to 2000-cell aggregate formation in 5% Pluronic-coated 96-well V-bottom plates and cultured in serum-free media containing Dulbecco's Modified Eagle Medium, 1% nonessential amino acids, 1% antibiotic/antimycotic, 1% insulin, human transferrin and selenous acid premix and 50 μg/ml ascorbate-2-phosphate without growth factor supplements. At days 1, 7 and 14, MSCs were collected and processed for histological staining with H&E as described in the Methods of Chapter 4 (n=8).

B.5.2 Results

When MSCs were coated with only the intermediate layers of biotin and avidin, the rounded cell morphology was not observed, with aggregates at day 14 exhibiting similar morphology to noncoated aggregates (Supplemental Figure B.5).

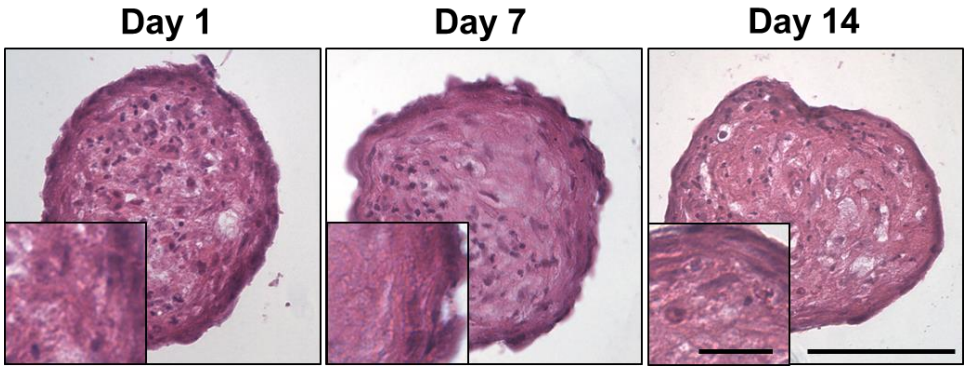

Supplemental Figure B.5. MSC aggregates coated with only biotin and avidin layers (no Hep or Hep- layer) do not exhibit rounded cell morphology over the course of 14 days. H&E stain; Scale bar = 100um, inset scale bar = 25μm, n=8.

B.6 MSC aggregates cultured with heparin supplementedin the media

B.6.1 Materials and Methods

Noncoated MSCs were formed into 2000-cell aggregates in 5% Pluronic-coated 96-well V-bottom plates and cultured in serum-free media composed of Dulbecco's Modified Eagle Medium, 1% nonessential amino acids, 1% antibiotic/antimycotic, 1% insulin, human transferrin and selenous acid premix and 50 μg/ml ascorbate-2-phosphate supplemented with 10 ng/mL FGF-2 (Noncoated + FGF), 5 mg/mL heparin (Noncoated + Soluble Hep), or 5 mg/mL heparin and 10 ng/mL FGF-2 (Noncoated + Soluble Hep + FGF). At day 1, 4 and 7, aggregates were collected and processed for histological staining with H&E (n=16) or DNA content analysis using the CyQUANT® Cell Proliferation Assay (n=8), as described in the Materials and Methods section of Chapter 4.

B.6.2 Results

H&E staining revealed that morphology of these aggregates cultured with soluble heparin did not result in the formation of rounded cell morphology (Supplemental Figure B.6A). Additionally, at day 4, DNA amounts did not increase for aggregates cultured with soluble Hep without FGF-2 (0.42±0.1 fold) and with FGF-2 (0.74±0.1 fold) and did not increase by day 7 (Supplemental Figure B.6B). This suggests that the observed effects are related to the coating and not any heparin released in the system.

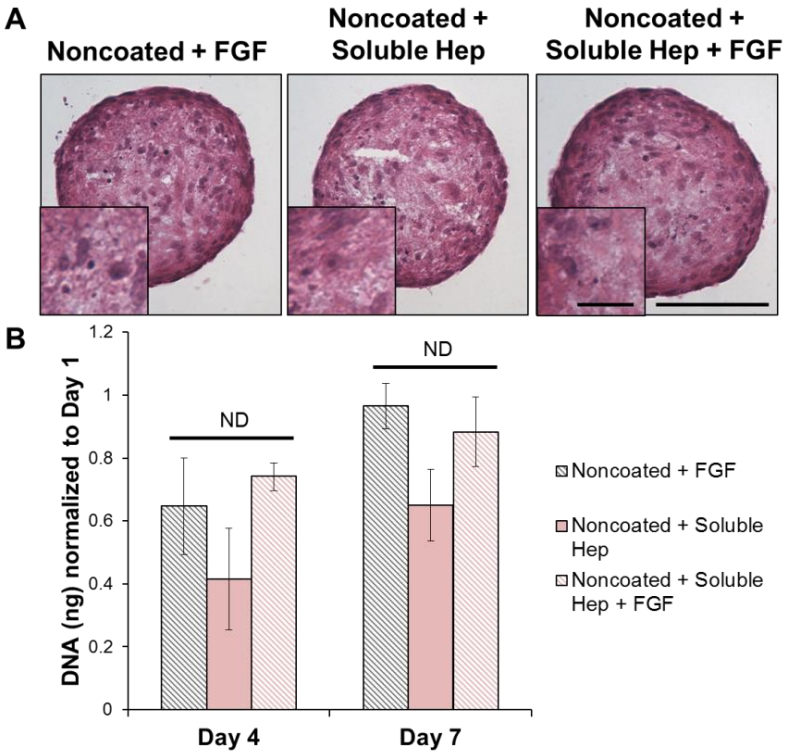

Supplemental Figure B.6. MSC aggregates cultured with heparin supplemented in culture media at 5mg/mL did not exhibit rounded cell morphology at day 1 or increased DNA content over time. A) H&E staining of noncoated aggregates cultured with heparin supplemented in soluble form to culture media with or without FGF-2. Scale bar=100µm, inset scale bar = 25µm, n=16. B) DNA content of MSC aggregates with soluble heparin and FGF-2 compared to noncoated control with FGF-2 and aggregates with soluble heparin (no FGF-2 in media). Data reported as average mean ± standard deviation, $p<0.05$, n=8.

B.7. Safranin-O staining of coated MSC aggregates cultured in TGF-β1

B.7.1 Materials and Methods

MSC aggregates were coated, as described in the Materials and Methods section, formed into 2000-cell aggregates in 5% Pluronic coated 96-well V-bottom plates and cultured in serum-free media containing Dulbecco's Modified Eagle Medium, 1% nonessential amino acids, 1% antibiotic/antimycotic, 1% insulin, human transferrin and selenous acid premix and 50 μg/ml ascorbate-2-phosphate supplemented with 10 ng/mL TGF-β1 and 100nM dexamethasone for 21 days. At days 1 and 21, samples were collected and processed for histological staining with Safranin-O.

B.7.2 Results

Safranin-O staining, typically used to visualize GAG deposition, was detected at day 21 for all groups cultured in TGF-β1 (seen in light purple near cells).

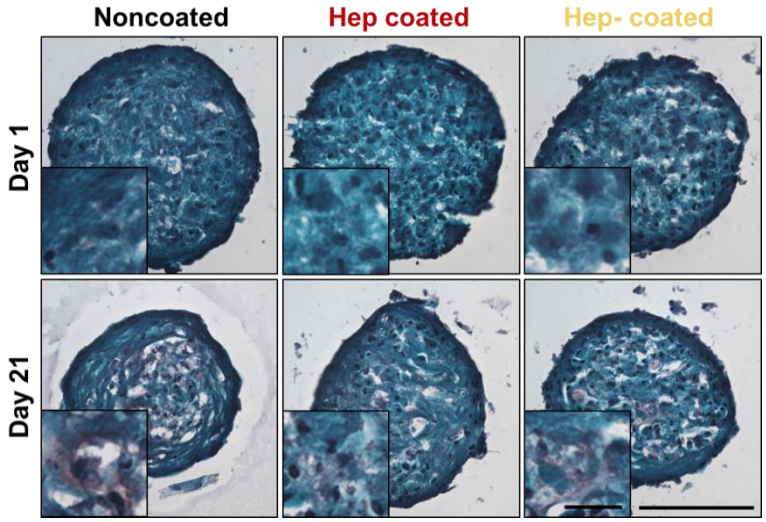

Supplemental Figure B.6. Safranin-O staining reveals that all aggregates cultured with TGF-β1 deposited GAG (light purple) after 21 days in culture. Scale bar = 100um, inset scale bar = 25μm, n=12.

B.8. Collagen I immunostaining of coated MSC aggregates cultured in TGF-β1

B.8.1 Materials and Methods

MSC aggregates were coated, as described in the Materials and Methods section, formed into 2000-cell aggregates in 5% Pluronic-coated 96-well V-bottom plates and

cultured in serum-free media containing Dulbecco's Modified Eagle Medium, 1% nonessential amino acids, 1% antibiotic/antimycotic, 1% insulin, human transferrin and selenous acid premix and 50 μg/ml ascorbate-2-phosphate supplemented with 10 ng/mL TGF-β1 and 100nM dexamethasone for 21 days. At days 1, 14 and 21, samples were collected and processed for immunostaining (specific methods found in Materials and Methods section of Chapter 4) for the ECM molecule collagen I using a 1:60 dilution of the primary antibody and 1:200 dilution of the secondary antibody.

B.8.2 Results

Positive staining for collagen I was observed for all aggregates at the initial day 1 timepoint. However, over the 21 day culture, the staining detected did not appear to change in intensity within each group.

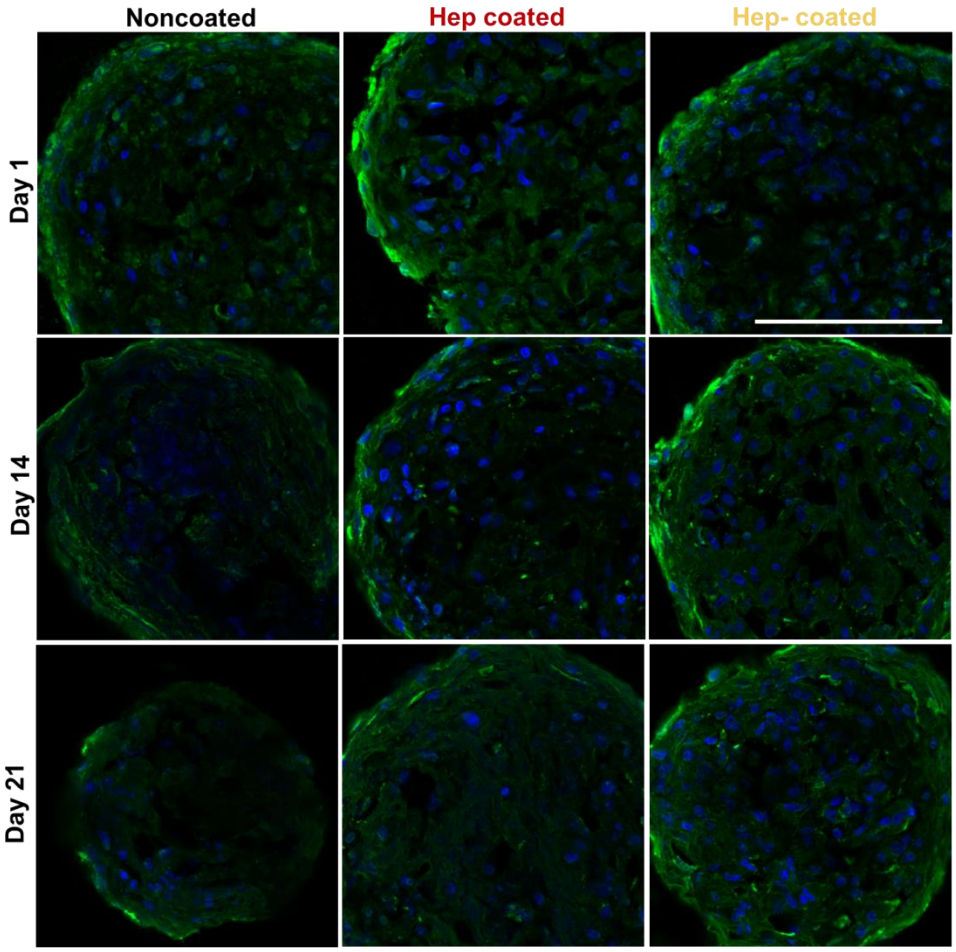

Supplemental Figure B.8. Positive collagen I immunostaining was observed for all groups. Collagen I is seen in green and cell nuclei are stained blue. Scale bar = 100µm, n=12.

APPENDIX C

THEORETICAL CALCULATIONS

C.1 Calculations for Amount of GAG and HEPpep Grafted on Cell Surfaces

C.1.1 Calculation Description

To calculate the maximum amount of heparin that can be grafted onto cell surfaces, calculations were made based on surface area. This means that the amount of maximum surface area present on cell surfaces was the limiting factor in how much heparin could exist on surfaces. Heparin chains were assumed to be cylindrical in shape assembled on cell surfaces in a tightly packed configuration, as has been observed with protein configuration on surfaces [325]. Concentrations of heparin and GAG used in coating steps can be converted to the total amount of heparin molecules present in solution through conversions using molecular weight and Avagadro's number.

To calculate an appropriate concentration of HEPpep for coating experiments, the assumption that the binding of HEPpep to heparin requires one molecule of each. This is based on binding of FGF-2 to heparin, in which one pentasaccharide unit is needed to bind one growth factor molecule [20]. Therefore, the concentration of HEPpep was based on the theoretical number of heparin molecules present at 5 mg/mL coating concentration. The number of molecules for heparin and HEPpep were first matched, and then that number of HEPpep molecules was converted into a concentration. While the final concentration for HEPpep coating was chosen based on this calculation, it was assumed that not all HEPpep molecules get on cell surfaces since some may be lost during coating incubation steps to other surfaces, such as the coating vessel. Therefore,

the final concentration chosen was greater than that of the calculated concentration based on the number of molecules that matched.

C.1.2 Calculation Equations

C.1.2.1 Measurements for calculations

Table B.1.2. Diameter and molecular weight values.

Molecule	Diameter (μm)	Molecular Weight (kDa)	Reference
Mesenchymal stem cell	30	-	[326]
Heparin	0.001	20	[327, 328]
HEPpep	-	1431.76	

C.1.2.2 Calculation for maximum number of heparin molecules grafted on cell surfaces

$$\boldsymbol{Max\ number\ of\ heparin\ molecules}$$

$$= \frac{Surface\ area\ of\ cell}{Area\ of\ base\ of\ heparin\ cylinder} * 100{,}000\ cells$$

$$= \frac{4\pi r_{cell}^2}{\pi r_{hep}^2} * 100{,}000\ cells$$

Note: 100,000 cells were used as an approximate amount that would be coated with 1 mL of the GAG coating solution.

C.1.2.3 Calculation for number of heparin molecules available at a given concentration

$$\boldsymbol{Number\ of\ heparin\ molecules}$$

$$= \frac{Concentration\ (\frac{g}{mL})}{Heparin\ molecular\ weight\ (\frac{g}{mole})} * Avagadro's\ Number$$

C.1.2.4 Calculation for HEPpep coating concentration

$$Number\ of\ heparin\ molecules\ at \frac{5mg}{mL} = Number\ of\ HEPpep\ molecules$$

$$\boldsymbol{HEPpep\ concentration} = \frac{Number\ of\ HEPpep\ molecules}{Avagadro's\ number} * HEPpep\ molecular\ weight$$

C.1.2.5 Calculation results

Table C.1.2. Concentration and number of molecule values for heparin and HEPpep coating solutions

	Concentration	# of Molecules
Maximum heparin molecules per 100,000 cells	-	$3.6*10^{14}$
Number of heparin molecules per mL	5mg/mL	$1.67*10^{17}$
	1mg/mL	$3.34*10^{16}$
	5µg/mL	$1.67*10^{14}$
Number of HEPpep molecules per mL	0.4mg/mL	$1.5*10^{17}$
	1mg/mL	$4.2*10^{17}$

C.2 Calculations for Theoretical Binding Area

C.2.1 Calculation Description

To alter binding area (BA) in Chapter 5, different sized spheroid paired with each other was used to represent high and low theoretical binding area between two populations. To calculate theoretical surface area in the system, different sized spheroids were paired together while holding total number of cell type constant within the system. This was performed first by determining how cell number per spheroid can affect the diameter (Table C.2.1). Once different size spheroids were established, surface area for each spheroid size was calculated and different pairs of spheroids of different sizes were matched up. To calculate the number of smaller spheroids can bind and interface with larger spheroids, the assumption that the smaller spheroids would organize to pack tightly on larger spheroid surfaces was made. To calculate the number of small spheroids that would pack onto a large spheroid, the ratio of the surface area of the larger spheroid was compared to the projected area of the smaller spheroid. These numbers were then used to calculate the theoretical binding area between the two populations and the total cell numbers of each population. The resulting groups were referred to as low and high SA groups based on their resulting total binding area values.

C.2.2 Spheroid Size Quantification

Spheroid size can be altered by changing the number of single cells formed into a spheroid. Spheroids containing cell numbers ranging from 100 to 2000 were formed and after 24 hours, their diameters were measured using phase microscopy and ImageJ analysis (n = 5 images containing approximately 30 spheroids). Table C.2.1 summarizes the approximate size of spheroids with increasing cell numbers.

Table C.2.1 Size of spheroids with increasing cell numbers

Cell Number per Spheroid	Approximate Diameter (d) (μm)
100	98
200	109
500	149
2000	240

C.2.3 Calculation Equations

C.2.3.1 Calculation for surface area

$$Spheroid\ Surface\ Area = 4\pi(\frac{d_{sph}}{2})^2$$

C.2.3.2 Calculation for projected area

Projected area was calculated as the projected area that a sphere would cover, ultimately resulting in a square shadow.

$$Projected\ Area = (d_{sph})^2$$

C.2.3.3 Calculation for packing of smaller spheroids

To calculate packing of smaller spheroids, the projected area of the smaller spheroid was compared to the spheroid surface area of the larger spheroid. The number of Population A spheroids packed onto Population B spheroid surfaces is summarized in Table B.2.3.

$$Ratio\ B{:}A = \frac{Larger\ Spheroid\ Surface\ Area\ (Population\ B)}{Smaller\ Sperhoid\ Projected\ Area\ (Population\ A)}$$

C.2.3.4 Calculation for theoretical binding area between two populations

To calculate theoretical binding area between the two populations, the assumption that 80% of the area of the spheroid at its diameter was interfaced and bound to the surface was used for each smaller spheroid (Population A) that was bound to the surface

of the larger spheroid. To calculate total binding area, the binding area for one spheroid was multiplied by the ratio of smaller spheroids that could pack onto the larger spheroid surface (Ratio B:A). Total theoretical binding areas for two groups are seen in Table C.2.3.

$$Total\ Binding\ Area = (0.8) * \pi(\frac{d_{sph\ A}}{2})^2 * (Ratio\ B{:}A)$$

C.2.3.5 Cell number calculations

The purpose of this calculation was to ensure that the number of cells in each population was approximately the same for the different experimental groups with different sized spheroids paired together in the orientation that the smaller Population A spheroids are packed tightly on the larger Population B spheroids. To do so, the cell number for Population B (larger spheroids) were matched between the two groups and the smaller spheroid number was then recalculated based on the Ratio of B:A number. For example, the 100:500 group, the Final Cell Number for Population B was multiplied by 4 to match the Final Cell Number of Population B in the 200:2000 group. Final Cell Number of A for the 100:500 group was then multiplied by 4 and the Ratio of B:A for that group resulting. Resulting cell numbers are summarized in Table C.2.4.

C.2.3.6 Calculation results

Table C.2.2. Surface area and projected area of spheroids of different sizes.

Cell Number per Spheroid	Approximate Diameter (μm)	Surface Area (μm^2)	Projected Area (μm^2)
100	98	30156.6	9604
200	109	37306.3	11881
500	149	69711.1	22201
2000	240	180864.0	57600

Table C.2.3. Number of Population A spheroids packed onto Population B spheroid surface (Ratio B:A) and resulting binding area.

Cell number - Population A (smaller)	Cell number - Population B (larger)	Ratio of B:A	Total Binding Area (μm^2)
100	500	7.3	43778.596
200	2000	15.2	113582.59

Table C.2.4. Final cell numbers for spheroids in Population A and B for the two experimental groups.

Cell number - Population A (smaller)	Cell number - Population B (larger)	Final Cell Number A	Final Cell Number B
100	500	2903.4	2000
200	2000	3044.6	2000

APPENDIX D

^{1}H NMR SPECTRA

D.1 Conjugation efficiency calculations

To calculate conjugation efficiency, ^{1}H NMR analysis was utilized to identify relative amounts of heparin or desulfated heparin and biotin in each synthesized product. Using NMR, unique hydrogen groups on heparin, desulfated heparin and biotin were identified and peaks were integrated to provide relative amounts of how much each group is present in the sample. Using this method of analysis, the amount of biotin conjugated to heparin or desulfated heparin was measured after synthesis of these biotinylated GAGs.

Heparin and desulfated heparin were identified with the hydrogen group that exists on the hydroxyl group (-OH) of the saccharide unit [329]. The peaks were observed within the range of 5.1-5.6 ppm. This integration was normalized to 1 to represent a single heparin or desulfated heparin unit that exists in the sample. The following integration for other peaks is then relative to that initial normalization. To identify the amount of biotin present, the 2 hydrogen groups found on the carbon groups next to the amine group in the chain linker portion is integrated at 2.5-3.0 ppm. There are typically 2 peaks included within this integration and the resulting integration value is measured. That value is then divided by 2 to determine the amount of biotin present. This is performed because there are 2 hydrogens contributing to that integration value. The resulting value is the percentage of biotin found per one unit of heparin, and referred to in this thesis as the biotin conjugation efficiency. Table D.1.1 summarizes the integration

values and conjugation efficiencies calculated for the biotinylated products used throughout this thesis.

Table D.1.1 Biotinylation Conjugation Efficiency

Date	Sample	Peak	Integration	Biotinylation Efficiency
1/21/2014	Desulfated heparin	5.1-5.6	1	
		2.5-3.0	0.32	16.0%
2/7/2014	Heparin	5.1-5.6	1	
		2.5-3.0	0.28	14.0%
11/4/2014	Heparin	5.1-5.6	1	
		2.5-3.0	0.42	21.0%
11/4/2014	Desulfated heparin	5.1-5.6	1	
		2.5-3.0	0.48	24.0%
4/24/2015	Heparin	5.1-5.6	1	
		2.5-3.0	0.45	22.5%
4/24/2015	Desulfated heparin	5.1-5.6	1	
		2.5-3.0	0.41	20.5%
8/24/2015	Heparin	5.1-5.6	1	
		2.5-3.0	0.33	16.5%

D.2 Biotinylated desulfated heparin – 01/21/2014

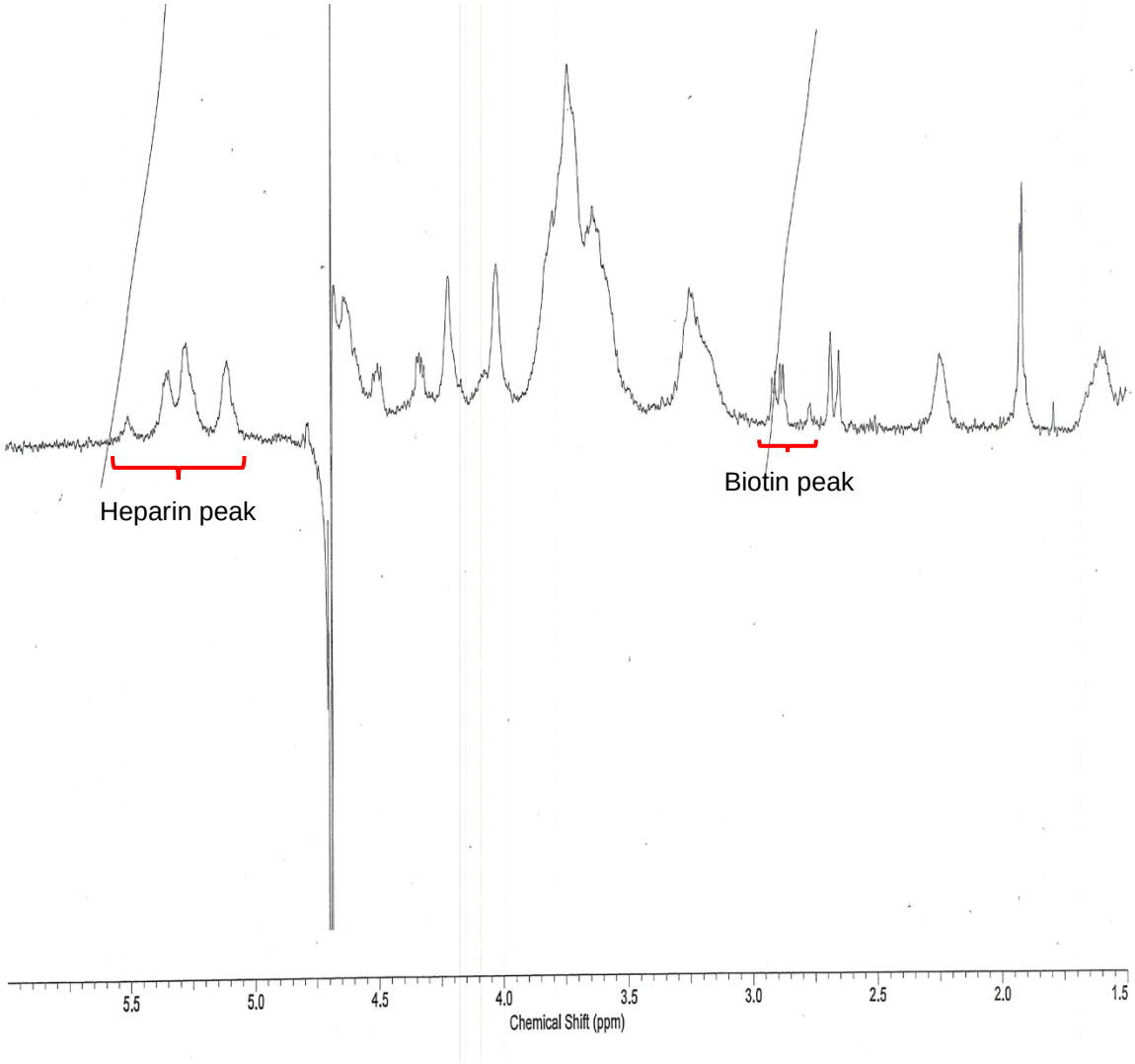

D.3 Biotinylated heparin – 02/07/2014

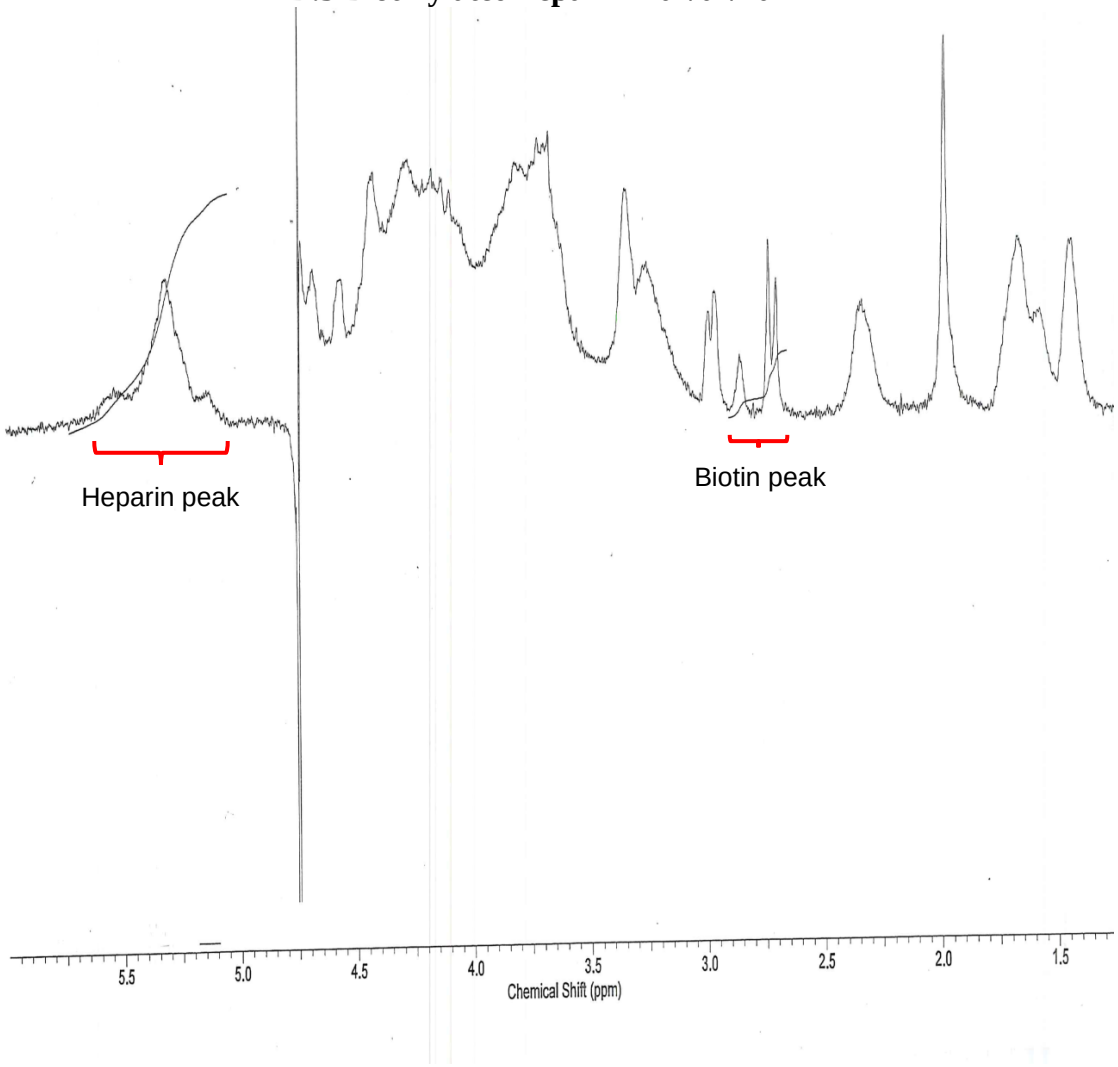

D.4 Biotinylated heparin – 11/04/2014

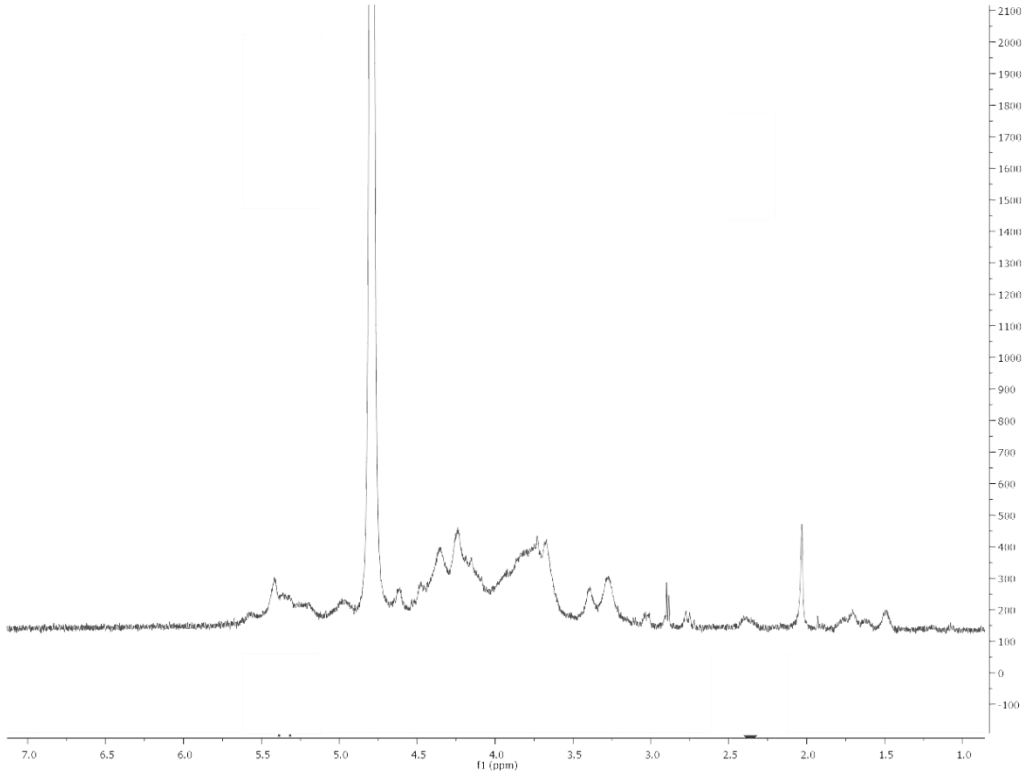

D.5 Biotinylated desulfated heparin – 11/04/2014

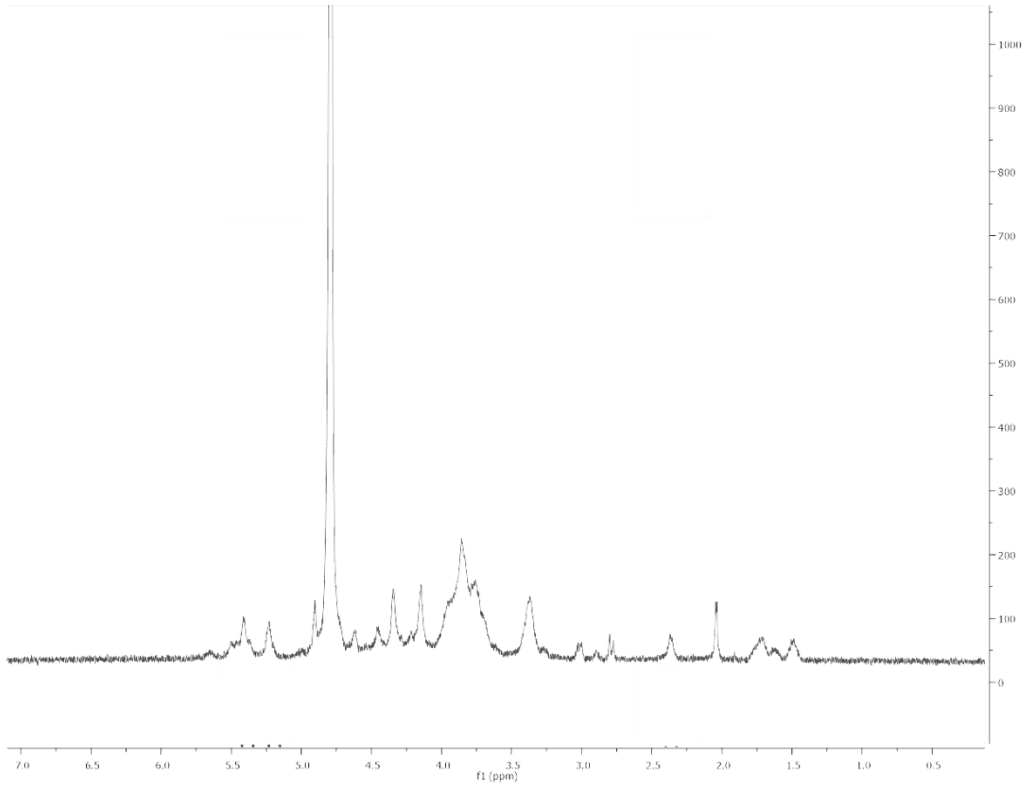

D.6 Biotinylated heparin – 04/24/2015

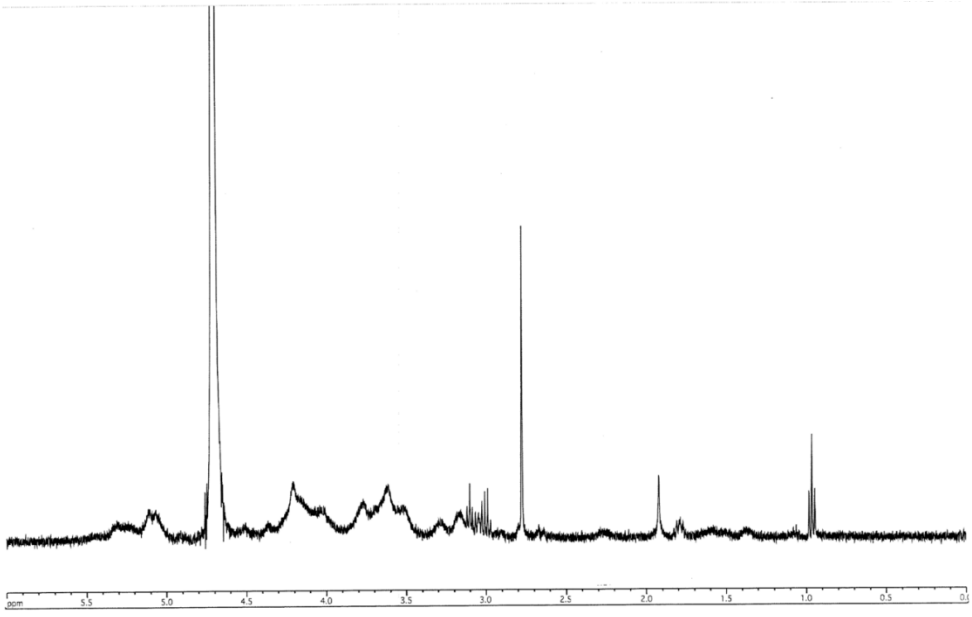

D.7 Biotinylated desulfated heparin – 04/24/2015

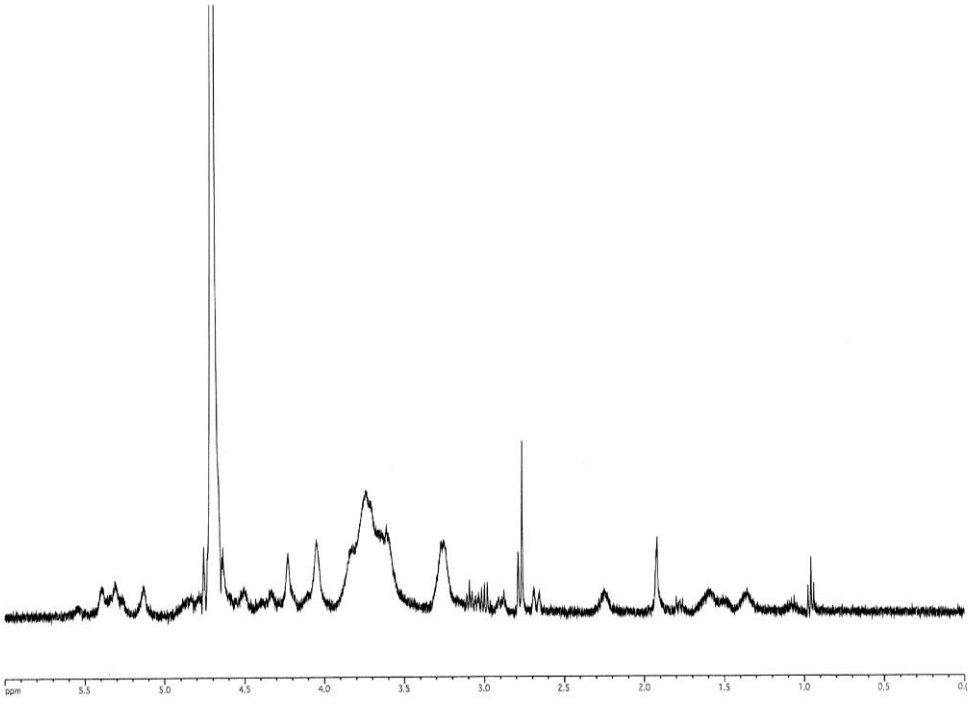

D.8 Biotinylated heparin – 08/24/2015

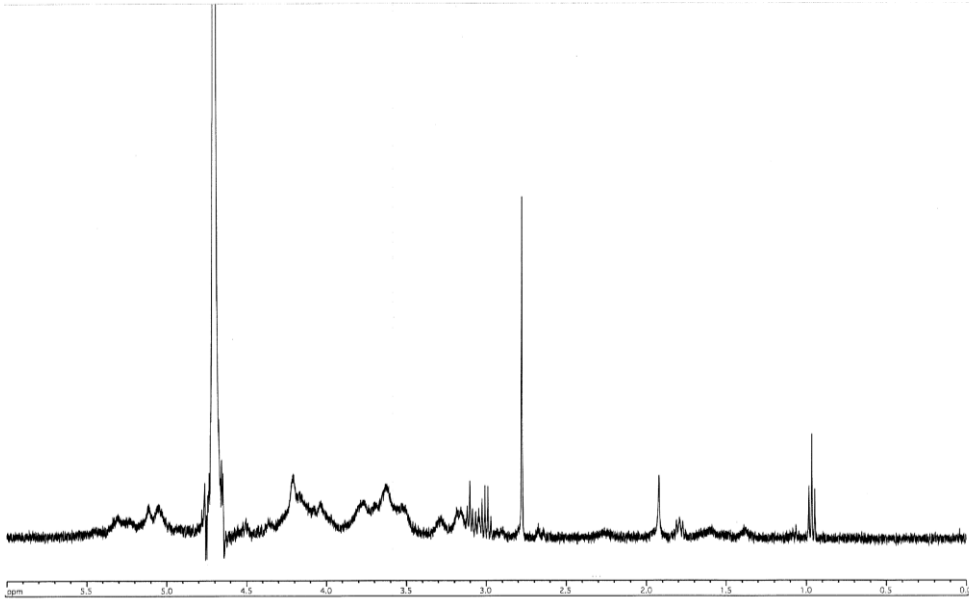

References

1. Caplan, A.I. and J.E. Dennis, *Mesenchymal stem cells as trophic mediators.* J Cell Biochem, 2006. **98**(5): p. 1076-84.

2. Ankrum, J. and J.M. Karp, *Mesenchymal stem cell therapy: Two steps forward, one step back.* Trends Mol Med, 2010. **16**(5): p. 203-9.

3. Bernardo, M.E. and W.E. Fibbe, *Mesenchymal stromal cells: sensors and switchers of inflammation.* Cell Stem Cell, 2013. **13**(4): p. 392-402.

4. Dimarino, A.M., A.I. Caplan, and T.L. Bonfield, *Mesenchymal Stem Cells in Tissue Repair.* Front Immunol, 2013. **4**: p. 201.

5. Mendicino, M., et al., *MSC-based product characterization for clinical trials: an FDA perspective.* Cell Stem Cell, 2014. **14**(2): p. 141-5.

6. Trounson, A. and C. McDonald, *Stem Cell Therapies in Clinical Trials: Progress and Challenges.* Cell Stem Cell, 2015. **17**(1): p. 11-22.

7. Emmert, M.Y., et al., *Human stem cell-based three-dimensional microtissues for advanced cardiac cell therapies.* Biomaterials, 2013. **34**(27): p. 6339-54.

8. Sart, S., et al., *Three-dimensional aggregates of mesenchymal stem cells: cellular mechanisms, biological properties, and applications.* Tissue Eng Part B Rev, 2014. **20**(5): p. 365-80.

9. Kelm, J.M. and M. Fussenegger, *Microscale tissue engineering using gravity-enforced cell assembly.* Trends Biotechnol, 2004. **22**(4): p. 195-202.

10. Kelm, J.M. and M. Fussenegger, *Scaffold-free cell delivery for use in regenerative medicine.* Adv Drug Deliv Rev, 2010. **62**(7-8): p. 753-64.

11. Baraniak, P.R. and T.C. McDevitt, *Scaffold-free culture of mesenchymal stem cell spheroids in suspension preserves multilineage potential.* Cell Tissue Res, 2012. **347**(3): p. 701-11.

12. Hildebrandt, C., H. Buth, and H. Thielecke, *A scaffold-free in vitro model for osteogenesis of human mesenchymal stem cells.* Tissue Cell, 2011. **43**(2): p. 91-100.

13. Kapur, S.K., et al., *Human adipose stem cells maintain proliferative, synthetic and multipotential properties when suspension cultured as self-assembling spheroids.* Biofabrication, 2012. **4**(2): p. 025004.

14. Hayashi, K. and Y. Tabata, *Preparation of stem cell aggregates with gelatin microspheres to enhance biological functions.* Acta Biomater, 2011. **7**(7): p. 2797-803.

15. Van Winkle, A., I. Gates, and M. Kallos, *Mass Transfer Limitations in Embryoid Bodies during Human Embryonic Stem Cell Differentiation.* Cell Tissue Organs 2012. **196**(1): p. 34-47.

16. Liang, Y. and K.L. Kiick, *Heparin-functionalized polymeric biomaterials in tissue engineering and drug delivery applications.* Acta Biomater, 2014. **10**(4): p. 1588-600.

17. Sakiyama-Elbert, S., *Incorporation of heparin into biomaterials.* Acta Biomaterialia, 2014. **10**(4): p. 1581-1587.

18. Bernfield, M., et al., *Functions of cell surface heparan sulfate proteoglycans.* Annual Review of Biochemistry, 1999. **68**(1): p. 729-777.

19. Bishop, J.R., M. Schuksz, and J.D. Esko, *Heparan sulphate proteoglycans fine-tune mammalian physiology.* Nature, 2007. **446**(7139): p. 1030-7.

20. Esko, J.D. and R.J. Linhardt, *Proteins that Bind Sulfated Glycosaminoglycans*, in *Essentials of Glycobiology*, A. Varki, R.D. Cummings, and J.D. Esko, Editors. 2009, Cold Spring Harbor Laboratory Press: Cold Spring Harbor, NY.

21. Bartosh, T.J., et al., *Aggregation of human mesenchymal stromal cells into 3D spheroids enhances their antiinflammatory properties.* Proceedings of the National Academy of Science, 2010. **107**(31): p. 13724-12729.

22. Klumpers, D.D., D.J. Mooney, and T.H. Smit, *From Skeletal Development to Tissue Engineering: Lessons from the Micromass Assay.* Tissue Eng Part B Rev, 2015.

23. Kelm, J.M., et al., *Design of Custom-Shaped Vascularized Tissues Using Microtissue Spheroids as Minimal Building Units.* Tissue Engineering, 2006. **12**(8): p. 2151-2160.

24. Gallego-Perez, D., et al., *High throughput assembly of spatially controlled 3D cell clusters on a micro/nanoplatform.* Lab Chip, 2010. **10**(6): p. 775-82.

25. Gneechi, M. and L.G. Melo, *Bone marrow-derived mesenchymal stem cells: isolation, expansion, characterization, viral transduction, and production of conditioned medium.* Methods in Molecular Biology, 2009. **482**: p. 281-294.

26. Caplan, A.I., *Adult mesenchymal stem cells for tissue engineering versus regenerative medicine.* Journal of Cellular Physiology, 2007. **213**: p. 341-347.

27. Hong, H.S., Y.H. Kim, and Y. Son, *Perspectives on mesenchymal stem cells: tissue repair, immune modulation, and tumor homing.* Arch Pharm Res, 2012. **35**(2): p. 201-11.

28. Prockop, D.J., *Concise review: two negative feedback loops place mesenchymal stem/stromal cells at the center of early regulators of inflammation.* Stem Cells, 2013. **31**(10): p. 2042-6.

29. Strauer, B.E., *Stem cell therapy in perspective.* Circulation, 2003. **107**(7): p. 929-934.

30. Yagi, H., et al., *Mesenchymal stem cells: Mechanisms of immunomodulation and homing.* Cell Transplant, 2010. **19**(6): p. 667-79.

31. Phinney, D.G. and D.J. Prockop, *Concise review: mesenchymal stem/multipotent stromal cells: the state of transdifferentiation and modes of tissue repair-Current views.* Stem Cells, 2007. **25**(11): p. 2896-902.

32. Nombela-Arrieta, C., J. Ritz, and L.E. Silberstein, *The elusive nature and function of mesenchymal stem cells.* Nat Rev Mol Cell Biol, 2011. **12**(2): p. 126-31.

33. Russell, K.C., et al., *In vitro high-capacity assay to quantify the clonal heterogeneity in trilineage potential of mesenchymal stem cells reveals a complex hierarchy of lineage commitment.* Stem Cells, 2010. **28**(4): p. 788-98.

34. Zuk, P.A., et al., *Human adipose tissue is a source of multipotent stem cells.* Mol Biol Cell, 2002. **13**(12): p. 4279-95.

35. Xie, L., et al., *In vitro mesenchymal trilineage differentiation and extracellular matrix production by adipose and bone marrow derived adult equine multipotent stromal cells on a collagen scaffold.* Stem Cell Rev, 2013. **9**(6): p. 858-72.

36. Jiang, Y., et al., *Pluripotency of mesenchymal stem cells derived from adult marrow.* Nature, 2002. **418**: p. 41-49.

37. Birmingham, E., et al., *Osteogenic differentiation of mesenchymal stem cells is regulated by osteocyte and osteoblast cells in simplified bone niche.* European Cells and Materials, 2012. **23**: p. 13-27.

38. Krause, U., A. Seckinger, and C.A. Gregory, *Assays of osteogenic differentiation by cultured human mesenchymal stem cells* Methods in Molecular Biology, 2011. **698**: p. 215-230.

39. Lee, K.S., H.J. Kim, and Q.L. Li, *Runx2 is a common target of transforming growth factor β1 and bone morphogenetic protein 2, and cooperation between*

Runx2 and Smad5 induces osteoblast-specific gene expression in the pluripotent mesenchymal precursor cell line C2C12. Molecular and Cellular Biology, 2000. **20**(23): p. 8783-8792.

40. Komori, T., *Regulation of osteoblast differentiation by runx.* Advances in Experimental Medicine and Biology, 2010. **658**: p. 43-49.

41. Pratap, J., J. Wixted, and T. Gaur, *Runx2 transcriptional activation of Indian Hedgehog and a downstream bone metastatic pathway in breast cancer cells.* Cancer Research, 2008. **68**(19): p. 7795-7802.

42. James, A.W., *Review of Signaling Pathways Governing MSC Osteogenic and Adipogenic Differentiation.* Scientifica (Cairo), 2013. **2013**: p. 684736.

43. Mauney, J.R., V. Volloch, and D.L. Kaplan, *Matrix-mediated retention of adipogenic differentiation potential by human adult bone marrow-derived mesenchymal stem cells during ex vivo expansion.* Biomaterials, 2005. **26**(31): p. 6167-75.

44. Sekiya, I., et al., *Adipogenic differentiation of human adult stem cells from bone marrow stroma (MSCs).* J Bone Miner Res, 2004. **19**(2): p. 256-64.

45. Valorani, M.G., et al., *Hypoxia increases Sca-1/CD44 co-expression in murine mesenchymal stem cells and enhances their adipogenic differentiation potential.* Cell Tissue Res, 2010. **341**(1): p. 111-20.

46. Kolf, C.M., E. Cho, and R.S. Tuan, *Biology of adult stem cells: Regulation of niche, self-renewal and differentiation.* Arthrutus Research and Therapy, 2007. **9**: p. 204.

47. Tzameli, I., et al., *Regulated production of a peroxisome proliferator-activated receptor-gamma ligand during an early phase of adipocyte differentiation in 3T3-L1 adipocytes.* J Biol Chem, 2004. **279**(34): p. 36093-102.

48. Bosnakovski, D., et al., *Chondrogenic differentiation of bovine bone marrow mesenchymal stem cells in pellet cultural system.* Exp Hematol, 2004. **32**(5): p. 502-9.

49. Mauck, R.L., X. Yuan, and R.S. Tuan, *Chondrogenic differentiation and functional maturation of bovine mesenchymal stem cells in long-term agarose culture.* Osteoarthritis Cartilage, 2006. **14**(2): p. 179-89.

50. Solchaga, L.A., K.J. Penick, and J.F. Welter, *Chondrogenic differentiation of bone marrow-derived mesenchymal stem cells: tips and tricks.* Methods Mol Biol, 2011. **698**: p. 253-78.

51. Bosnakovski, D., et al., *Chondrogenic differentiation of bovine bone marrow mesenchymal stem cells (MSCs) in different hydrogels: influence of collagen type II extracellular matrix on MSC chondrogenesis.* Biotechnol Bioeng, 2006. **93**(6): p. 1152-63.

52. Chichester, C.O., et al., *Chondrogenic differentiation of cultured human mesenchymal stem cells from marrow.* Tissue Engineering, 1998. **4**(4): p. 415.

53. Goessler, U.R., et al., *In-vitro analysis of the expression of TGF-b-superfamily members during chondrogenic differentation of mesenchymal stem cells and chondrocytes during dedifferentation in cell culture.* Cellular and Molecular Biology Letters, 2005. **10**: p. 345-362.

54. Indrawattana, N., et al., *Growth factor combination for chondrogenic induction from human mesenchymal stem cell.* Biochem Biophys Res Commun, 2004. **320**(3): p. 914-9.

55. O'Conor, C.J., N. Case, and F. Guilak, *Mechanical regulation of chondrogenesis.* Stem Cell Res Ther, 2013. **4**: p. 61.

56. Barry, F., et al., *Chondrogenic differentiation of mesenchymal stem cells from bone marrow: differentiation-dependent gene expression of matrix components.* Exp Cell Res, 2001. **268**(2): p. 189-200.

57. Furumatsu, T., et al., *Smad3 induces chondrogenesis through the activation of SOX9 via CREB-binding protein/p300 recruitment.* J Biol Chem, 2005. **280**(9): p. 8343-50.

58. Wu, R., et al., *Isolation and myogenic differentiation of mesenchymal stem cells for urologic tissue engineering.* Organ Regeneration, 2013. **1001**: p. 65-80.

59. Tian, H., et al., *Myogenic differentiation of human bone marrow mesenchymal stem cells on a 3D nano fibrous scaffold for bladder tissue engineering.* Biomaterials, 2010. **31**(5): p. 870-7.

60. Burk, J., et al., *Gene expression of tendon markers in mesenchymal stromal cells derived from different sources.* BMC Research, 2014. **7**: p. 826.

61. Kuo, C.K. and R.S. Tuan, *Mechanoactive tenogenic differentiation of human mesenchymal stem cells.* Tissue Eng Part A, 2008. **14**(10): p. 1615-27.

62. Uysal, A.C. and H. Mizuno, *Differentiation of Adipose-Derived Stem Cells for Tendon Repair.* Methods in Molecular Biology, 2011. **702**(443-451).

63. Phinney, D.G. and D.J. Prockop, *Concise review: mesenchymal stem/multipotent stromal cells: the state of transdifferentiation and modes of tissue repair--current views.* Stem Cells, 2007. **25**(11): p. 2896-902.

64. Meisel, R., et al., *Human bone marrow stromal cells inhibit allogeneic T-cell responses by indoleamine 2,3-dioxygenase-mediated tryptophan degradation.* Blood, 2004. **103**(12): p. 4619-21.

65. Sato, K., et al., *Nitric oxide plays a critical role in suppression ofT-cell proliferation by mesenchymal stem cells.* Immunobiology, 2007. **109**(1): p. 228-234.

66. Tse, W.T., et al., *Suppression of allogeneic T-cell proliferation by human marrow stromal cells: implications in transplantation.* Immunobiology, 2003. **75**(3): p. 389-397.

67. Shi, Y., et al., *Mesenchymal stem cells: a new strategy for immunosuppression and tissue repair.* Cell Res, 2010. **20**(5): p. 510-8.

68. Waterman, R.S., et al., *A new mesenchymal stem cell (MSC) paradigm: polarization into a pro-inflammatory MSC1 or an Immunosuppressive MSC2 phenotype.* PLoS One, 2010. **5**(4): p. e10088.

69. Tasso, R., et al., *Mesenchymal stem cells induce functionally active T-regulatory lymphocytes in a paracrine fashion and ameliorate experimental autoimmune uveitis.* Invest Ophthalmol Vis Sci, 2012. **53**(2): p. 786-93.

70. Oh, S.K., et al., *A phase III clinical trial showing limited efficacy of autologous mesenchymal stem cell therapy for spinal cord injury.* Neurosurgery, 2015.

71. Samsonraj, R.M., et al., *Establishing criteria for human mesenchymal stem cell potency.* Stem Cells, 2015. **33**(6): p. 1878-91.

72. Lee, K.S., et al., *Effects of serial passage on the characteristics and chondrogenic differentiation of canine umbilical cord matrix derived mesenchymal stem cells.* Asian-Australas J Anim Sci, 2013. **26**(4): p. 588-95.

73. Bonab, M.M., et al., *Aging of mesenchymal stem cell in vitro.* BMC Cell Biol, 2006. **7**: p. 14.

74. Fennema, E., et al., *Spheroid culture as a tool for creating 3D complex tissues.* Trends Biotechnol, 2013. **31**(2): p. 108-15.

75. Alimperti, S., et al., *Serum-free spheroid suspension culture maintains mesenchymal stem cell proliferation and differentiation potential.* Biotechnol Prog, 2014. **30**(4): p. 974-83.

76. Suzuki, S., et al., *Properties and usefulness of aggregates of synovial mesenchymal stem cells as a source for cartilage regeneration.* Arthritis Res Ther, 2012. **14**(3): p. R136.

77. Wang, W., et al., *3D spheroid culture system on micropatterned substrates for improved differentiation efficiency of multipotent mesenchymal stem cells.* Biomaterials, 2009. **30**(14): p. 2705-15.

78. Yamaguchi, Y., et al., *Mesenchymal stem cell spheroids exhibit enhanced in-vitro and in-vivo osteoregenerative potential.* BMC Biotechnol, 2014. **14**: p. 105.

79. Winter, A., et al., *Cartilage-like gene expression in differentiated human stem cell spheroids: a comparison of bone marrow-derived and adipose tissue-derived stromal cells.* Arthritis Rheum, 2003. **48**(2): p. 418-29.

80. Zhao, X., et al., *Three-Dimensional Aggregates Enhance the Therapeutic Effects of Adipose Mesenchymal Stem Cells for Ischemia-Reperfusion Induced Kidney Injury in Rats.* Stem Cells Int, 2016. **2016**: p. 9062638.

81. Santos, J.M., et al., *Three-dimensional spheroid cell culture of umbilical cord tissue-derived mesenchymal stromal cells leads to enhanced paracrine induction of wound healing.* Stem Cell Res Ther, 2015. **6**: p. 90.

82. Ylostalo, J.H., et al., *Human mesenchymal stem/stromal cells cultured as spheroids are self-activated to produce prostaglandin E2 that directs stimulated macrophages into an anti-inflammatory phenotype.* Stem Cells, 2012. **30**(10): p. 2283-96.

83. Bartosh, T.J., et al., *Dynamic compaction of human mesenchymal stem/precursor cells into spheres self-activates caspase-dependent IL1 signaling to enhance secretion of modulators of inflammation and immunity (PGE2, TSG6, and STC1).* Stem Cells, 2013. **31**(11): p. 2443-56.

84. Bartosh, T.J., et al., *Aggregation of human mesenchymal stromal cells (MSCs) into 3D spheroids enhances their antiinflammatory properties.* PNAS, 2010. **107**(31): p. 13724-13729.

85. Zimmermann, J.A. and T.C. McDevitt, *Pre-conditioning mesenchymal stromal cell spheroids for immunomodulatory paracrine factor secretion.* Cytotherapy, 2014. **16**(3): p. 331-45.

86. Madrigal, M., K.R. Rao, and N.H. Riordan, *A review of therapeutic effects of mesenchymal stem cell secretions and induction of secretory modification by different culture methods.* Journal of Translational Medicine, 2014. **12**: p. 260.

87. Kim, H.S., et al., *Preparation and Characterization of Genetically Engineered Mesenchymal Stem Cell Aggregates for Regenerative Medicine.* Journal of Pharmaceutical Investigation, 2010. **40**(6): p. 333-337.

88. An, Y., et al., *Bone marrow mesenchymal stem cell aggregate: an optimal cell therapy for full-layer cutaneous wound vascularization and regeneration.* Sci Rep, 2015. **5**: p. 17036.

89. Lee, E.J., et al., *Spherical bullet formation via E-cadherin promotes therapeutic potency of mesenchymal stem cells derived from human umbilical cord blood for myocardial infarction.* Mol Ther, 2012. **20**(7): p. 1424-33.

90. Cheng, N.C., S. Wang, and T.H. Young, *The influence of spheroid formation of human adipose-derived stem cells on chitosan films on stemness and differentiation capabilities.* Biomaterials, 2012. **33**(6): p. 1748-58.

91. Huang, G.S., et al., *Spheroid formation of mesenchymal stem cells on chitosan and chitosan-hyaluronan membranes.* Biomaterials, 2011. **32**(29): p. 6929-45.

92. Bartosh, T.J. and J.H. Ylostalo, *Preparation of anti-inflammatory mesenchymal stem/precursor cells (MSCs) through sphere formation using hanging-drop culture technique.* Curr Protoc Stem Cell Biol, 2014. **28**: p. Unit 2B 6.

93. Langenbach, F., et al., *Generation and differentiation of microtissues from multipotent precursor cells for use in tissue engineering.* Nat Protoc, 2011. **6**(11): p. 1726-35.

94. Miyagawa, Y., et al., *A microfabricated scaffold induces the spheroid formation of human bone marrow-derived mesenchymal progenitor cells and promotes efficient adipogenic differentiation.* Tissue Eng Part A, 2011. **17**(3-4): p. 513-21.

95. Ungrin, M.D., et al., *Reproducible, ultra-high throughput formation of multicellular organization from single cell suspension-derived human embryonic stem cell aggregates* PloS One, 2008. **3**(2): p. e1565.

96. Cook, M.M., et al., *Micromarrows - Three-dimensional coculture of hematopoietic stem cells and mesenchymal stromal cells.* Tissue Eng Part C Methods, 2012. **18**(5): p. 319-28.

97. Bhang, S.H., et al., *Angiogenesis in ischemic tissue produced by spheroid grafting of human adipose-derived stromal cells.* Biomaterials, 2011. **32**(11): p. 2734-47.

98. Frith, J.E., B. Thomson, and P.G. Genever, *Dynamic three-dimensional culture methods enhance mesenchymal stem cell properties and increase therapeutic potential.* Tissue Eng Part C Methods, 2010. **16**(4): p. 735-749.

99. De Francesco, F., et al., *Human CD34/CD90 ASCs are capable of growing as sphere clusters, producing high levels of VEGF and forming capillaries.* PLoS One, 2009. **4**(8): p. e6537.

100. Firth, J.E., B. Thomson, and P.G. Genever, *Dynamic three-dimensional culture methods enhance mesenchymal stem cell properties and icnrease therapeutic potential.* Tissue Engineering: Part C, 2010. **16**(4): p. 735.

101. Mylotte, L.A., et al., *Metabolic flexibility permits mesenchymal stem cell survival in an iischemic environment.* Stem Cells, 2008. **26**: p. 1325-1336.

102. Sart, S., T. Ma, and Y. Li, *Cryopreservation of pluripotent stem cell aggregates in defined protein-free formulation.* Biotechnol Prog, 2013. **29**(1): p. 143-53.

103. Temenoff, J.S. and A.G. Mikos, *Reivew: Tissue engineering for regeneration of articular cartilage.* Biomaterials, 2000. **21**: p. 431-440.

104. Shu, K., H. Thatte, and M. Spector, *Chondrogenic differentiation of adult mesenchymal stem cells and embryonic stem cells.* 2009: p. 1-2.

105. Fischer, J., et al., *Human articular chondrocytes secrete parathyroid hormone-related protein and inhibit hypertrophy of mesenchymal stem cells in coculture during chondrogenesis.* Arthritis Rheum, 2010. **62**(9): p. 2696-706.

106. Markway, B.D., et al., *Enhanced chondrogenic differentiation of human bone marrow-derived mesenchymal stem cells in low oxygen environment micropellet cultures.* Cell Transplant, 2010. **19**(1): p. 29-42.

107. Zhang, L., et al., *Chondrogenic differentiation of human mesenchymal stem cells: a comparison between micromass and pellet culture systems.* Biotechnol Lett, 2010. **32**(9): p. 1339-46.

108. Kramer, J., et al., *Embryonic stem cell-derived chondrogenic differentiation in vitro: activation by BMP-2 and BMP-4.* Mech Dev, 2000. **92**(2): p. 193-205.

109. Lefebvre, V., et al., *SOX9 is a potent activator of the chondrocyte-specific enhancer of the pro alpha1(II) collagen gene.* Mol Cell Biol, 1997. **17**(4): p. 2336-46.

110. Vidal, M.A., et al., *Comparison of chondrogenic potential in equine mesenchymal stromal cells derived from adipose tissue and bone marrow.* Vet Surg, 2008. **37**(8): p. 713-24.

111. Goude, M.C., T.C. McDevitt, and J.S. Temenoff, *Chondroitin sulfate microparticles modulate transforming growth factor-beta1-induced*

chondrogenesis of human mesenchymal stem cell spheroids. Cells Tissues Organs, 2014. **199**(2-3): p. 117-30.

112. Bhardwaj, N. and S.C. Kundu, *Chondrogenic differentiation of rat MSCs on porous scaffolds of silk fibroin/chitosan blends.* Biomaterials, 2012. **33**(10): p. 2848-57.

113. Kim, H.J., J.H. Lee, and G.I. Im, *Chondrogenesis using mesenchymal stem cells and PCL scaffolds.* J Biomed Mater Res A, 2010. **92**(2): p. 659-66.

114. Zhu, M., Q. Feng, and L. Bian, *Differential effect of hypoxia on human mesenchymal stem cell chondrogenesis and hypertrophy in hyaluronic acid hydrogels.* Acta Biomater, 2014. **10**(3): p. 1333-40.

115. Im, G.I., H.J. Kim, and J.H. Lee, *Chondrogenesis of adipose stem cells in a porous PLGA scaffold impregnated with plasmid DNA containing SOX trio (SOX-5,-6 and -9) genes.* Biomaterials, 2011. **32**(19): p. 4385-92.

116. Murphy, J.M., et al., *Stem cell therapy in a caprine model of osteoarthritis.* Arthritis Rheum, 2003. **48**(12): p. 3464-74.

117. Hwang, N.S., et al., *Regulation of osteogenic and chondrogenic differentiation of mesenchymal stem cells in PEG-ECM hydrogels.* Cell Tissue Res, 2011. **344**(3): p. 499-509.

118. Liu, S.Q., et al., *Biomimetic hydrogels for chondrogenic differentiation of human mesenchymal stem cells to neocartilage.* Biomaterials, 2010. **31**(28): p. 7298-307.

119. Noth, U., et al., *Chondrogenic differentiation of human mesenchymal stem cells in collagen type I hydrogels.* J Biomed Mater Res A, 2007. **83**(3): p. 626-35.

120. Varghese, S., et al., *Chondroitin sulfate based niches for chondrogenic differentiation of mesenchymal stem cells.* Matrix Biol, 2008. **27**(1): p. 12-21.

121. Huang, A.H., et al., *Long-term dynamic loading improves the mechanical properties of chondrogenic mesenchymal stem cell-laden hydrogels.* European Cells and Materials, 2008. **17**: p. 72-85.

122. Kisiday, J.D., et al., *Dynamic Compression Stimulates Proteoglycan Synthesis by Mesenchymal Stem Cells in the Absence of Chondrogenic Cytokines.* Tissue Eng Part A, 2009. **15**(10): p. 2817.

123. Thorpe, S.D., et al., *The response of bone marrow-derived mesenchymal stem cells to dynamic compression following TGF-beta3 induced chondrogenic differentiation.* Ann Biomed Eng, 2010. **38**(9): p. 2896-909.

124. Bian, L., et al., *Dynamic compressive loading enhances cartilage matrix synthesis and distribution and suppresses hypertrophy in hMSC-laden hyaluronic acid hydrogels.* Tissue Eng Part A, 2012. **18**(7-8): p. 715-24.

125. Kanichai, M., et al., *Hypoxia promotes chondrogenesis in rat mesenchymal stem cells: a role for AKT and hypoxia-inducible factor (HIF)-1alpha.* J Cell Physiol, 2008. **216**(3): p. 708-15.

126. Munir, S., et al., *Hypoxia enhances chondrogenic differentiation of human adipose tissue-derived stromal cells in scaffold-free and scaffold systems.* Cell Tissue Res, 2014. **355**(1): p. 89-102.

127. Schipani, E., *Hypoxia and HIF-1 alpha in chondrogenesis.* Semin Cell Dev Biol, 2005. **16**(4-5): p. 539-46.

128. Kelm, J.M., et al., *VEGF profiling and angiogenesis in human microtissues.* J Biotechnol, 2005. **118**(2): p. 213-29.

129. Kim, J.Y., et al., *3D spherical microtissues and microfluidic technology for multi-tissue experiments and analysis.* J Biotechnol, 2015. **205**: p. 24-35.

130. Lin, R.Z. and H.Y. Chang, *Recent advances in three-dimensional multicellular spheroid culture for biomedical research.* Biotechnol J, 2008. **3**(9-10): p. 1172-84.

131. Gartner, Z.J. and C.R. Bertozzi, *Programmed assembly of 3-dimensional microtissues with defined cellular connectivity.* Proc Natl Acad Sci U S A, 2009. **106**(12): p. 4606-10.

132. Grutzmann, R., et al., *Meta-analysis of microarray data on pancreatic cancer defines a set of commonly dysregulated genes.* Oncogene, 2005. **24**(32): p. 5079-88.

133. Yoon No, D., et al., *3D liver models on a microplatform: well-defined culture, engineering of liver tissue and liver-on-a-chip.* Lab Chip, 2015. **15**(19): p. 3822-3837.

134. Beachley, V.Z., et al., *Tissue matrix arrays for high-throughput screening and systems analysis of cell function.* Nat Methods, 2015.

135. Kelm, J.M., et al., *3D microtissue formation of undifferentiated bone marrow mesenchymal stem cells leads to elevated apoptosis.* Tissue Eng Part A, 2012. **18**(7-8): p. 692-702.

136. Futrega, K., et al., *The microwell-mesh: A novel device and protocol for the high throughput manufacturing of cartilage microtissues.* Biomaterials, 2015. **62**: p. 1-12.

137. Zhao, F., *Manipulation mesenchymal stem cells for vascular tissue engineering.* JSM Biotechnology and Biomedical Engineering, 2013. **1**(2): p. 1012-1015.

138. Chen, S., et al., *Strategies to minimize hypertrophy in cartilage engineering and regeneration.* Genes & Diseases, 2015. **2**(1): p. 76-95.

139. Gu, J., et al., *Establishment of a three-dimensional co-culture system by porcine hepatocytes and bone marrow mesenchymal stem cells in vitro.* Hepatol Res, 2009. **39**(4): p. 398-407.

140. Lu, H.F., et al., *Three-dimensional co-culture of rat hepatocyte spheroids and NIH/3T3 fibroblasts enhances hepatocyte functional maintenance.* Acta Biomater, 2005. **1**(4): p. 399-410.

141. Qihao, Z., et al., *Spheroid formation and differentiation into hepatocyte-like cells of rat mesenchymal stem cell induced by co-culture with liver cells.* DNA Cell Biol, 2007. **26**(7): p. 497-503.

142. Gu, J., et al., *Heterotypic interactions in the preservation of morphology and functionality of porcine hepatocytes by bone marrow mesenchymal stem cells in vitro.* J Cell Physiol, 2009. **219**(1): p. 100-8.

143. Nyberg, S.L., et al., *Rapid, large-scale formation of porcine hepatocyte spheroids in a novel spheroid reservoir bioartificial liver.* Liver Transpl, 2005. **11**(8): p. 901-10.

144. Hammoudi, T.M., et al., *Three-dimensional in vitro tri-culture platform to investigate effects of crosstalk between mesenchymal stem cells, osteoblasts, and adipocytes.* Tissue Eng Part A, 2012. **18**(15-16): p. 1686-97.

145. Rinker, T.E., et al., *Interactions between mesenchymal stem cells, adipocytes, and osteoblasts in a 3D tri-culture model of hyperglycemic conditions in the bone marrow microenvironment.* Integr Biol (Camb), 2014. **6**(3): p. 324-37.

146. Maia, F.R., et al., *Matrix-driven formation of mesenchymal stem cell-extracellular matrix microtissues on soft alginate hydrogels.* Acta Biomater, 2014. **10**(7): p. 3197-208.

147. Khanarian, N.T., et al., *A hydrogel-mineral composite scaffold for osteochondral interface tissue engineering.* Tissue Eng Part A, 2012. **18**(5-6): p. 533-45.

148. Bhatia, S.N., et al., *Probing heterotypic cell interactions: Hepatocyte function in microfabricated co-cultures.* Journal of Biomaterials Science, Polymer Edition, 1998. **9**(11): p. 1137-1160.

149. Bhatia, S.N., M.L. Yarmush, and M. Toner, *Controlling cell interactions by micropatterning in co-cultures: Hepatocytes and 3T3 fibroblast.* Journal of Biomedical Materials Researh, 1997. **34**: p. 187-199.

150. Bratt-Leal, A.M., et al., *Magnetic manipulation and spatial patterning of multi-cellular stem cell aggregates.* Integr Biol (Camb), 2011. **3**(12): p. 1224-32.

151. Khademhosseini, A., et al., *Microscale technologies for tissue engineering and biology.* Proc Natl Acad Sci U S A, 2006. **103**(8): p. 2480-7.

152. Koepsel, J.T. and W.L. Murphy, *Patterned self-assembled monolayers: efficient, chemically defined tools for cell biology.* Chembiochem, 2012. **13**(12): p. 1717-24.

153. Toh, Y.C., et al., *A microfluidic 3D hepatocyte chip for drug toxicity testing.* Lab Chip, 2009. **9**(14): p. 2026-35.

154. van Midwoud, P.M., E. Verpoorte, and G.M. Groothuis, *Microfluidic devices for in vitro studies on liver drug metabolism and toxicity.* Integr Biol (Camb), 2011. **3**(5): p. 509-21.

155. Otsuka, H., *Nanofabrication of nonfouling surfaces for micropatterning of cell and microtissue.* Molecules, 2010. **15**(8): p. 5525-46.

156. Legant, W.R., et al., *Microfabricated tissue gauges to measure and manipulate forces from 3D microtissues.* Proc Natl Acad Sci U S A, 2009. **106**(25): p. 10097-102.

157. Lamberg, S. and A. Stoolmiller, *Glycosaminoglycans, a biochemical and clinical review.* The Journal of Investigative Dermatology, 1974. **61**: p. 433-449.

158. Miller, T., et al., *Molecular engineering of glycosaminoglycan chemistry for biomolecule delivery.* Acta Biomater, 2014. **10**(4): p. 1705-19.

159. Esko, J.D., H. Kido, and U. Lindahl, *Proteoglycans and sulfated glycosaminoglycans*, in *Essentials of Glycobiology*, J.D. Esko, Editor. 2009, Cold Spring Harbor Laboratory Press: Cold Spring Harbor, NY.

160. Kogan, G., et al., *Hyaluronic acid: a natural biopolymer with a broad range of biomedical and industrial applications.* Biotechnol Lett, 2007. **29**(1): p. 17-25.

161. Seyrek, E. and P. Dubin, *Glycosaminoglycans as polyelectrolytes.* Adv Colloid Interface Sci, 2010. **158**(1-2): p. 119-29.

162. Ayerst, Bethanie I., et al., *New strategies for cartilage regeneration exploiting selected glycosaminoglycans to enhance cell fate determination.* Biochemical Society Transactions, 2014. **42**(3): p. 703-709.

163. Hintze, V., et al., *Sulfated hyaluronan and chondroitin sulfate derivatives interact differently with human transforming growth factor-beta1 (TGF-beta1).* Acta Biomater, 2012. **8**(6): p. 2144-52.

164. Zieris, A., et al., *Biohybrid networks of selectively desulfated glycosaminoglycans for tunable growth factor delivery.* Biomacromolecules, 2014. **15**(12): p. 4439-46.

165. Seto, S.P., T. Miller, and J.S. Temenoff, *Effect of selective heparin desulfation on preservation of bone morphogenetic protein-2 bioactivity after thermal stress.* Bioconjug Chem, 2015. **26**(2): p. 286-93.

166. Sarrazin, S., W.C. Lamanna, and J.D. Esko, *Heparan sulfate proteoglycans.* Cold Spring Harb Perspect Biol, 2011. **3**(7).

167. Groffen, A.J., et al., *Primary structure and high expression of human agrin in basement membranes of adult lung and kidney.* European Journal of Biochemistry, 1998. **254**: p. 123-128.

168. Knox, S.M. and J.M. Whitelock, *Perlecan: how does one molecule do so many things?* Cell Mol Life Sci, 2006. **63**(21): p. 2435-45.

169. B, M., K. S, and P. SJ, *Molecular architecture of heparin and heparan sulfate: Recent developments in solution structural studies.* Pure Appl Chem, 2012. **84**: p. 66-76.

170. Linhardt, R.J., et al., *Enzymatic synthesis of glycosaminoglycan heparin.* Semin Thromb Hemost, 2007. **33**(5): p. 453-65.

171. Jin, L., et al., *The anticoagulant activation of antithrombin by heparin.* PNAS, 1997. **94**: p. 14683-14688.

172. Tyler-Cross, R., et al., *Structure-function relations of antithrombin III-heparin interactions as assessed by biophysical and biolgical assays and molecular modeling of peptide-pentasaccharide docked complexes.* Archives of Biochemistry and Biophysics, 1996. **334**(2): p. 206-213.

173. Gospodarowicz, D., et al., *Isolation of brain fibroblast growth factor by heparin-Sepharose affinity chromatography: Identity with pituitary fibroblast growth factor.* PNAS, 1984. **81**(6963-6967).

174. Spivak-Kroizman, T., et al., *Heparin-induced oligomerization of FGF molecules is responsible for FGF receptor dimerization, activation, and cell proliferation.* Cell, 1994. **79**(6): p. 1015-1024.

175. Ostrovsky, O., et al., *Differential effects of heparin saccharides on the formation of specific fibroblast growth factor (FGF) and FGF receptor complexes.* J Biol Chem, 2002. **277**(4): p. 2444-53.

176. Baird, A., et al., *Receptor- and heparin-binding domains of basic fibroblast growth factor.* PNAS 1988. **85**: p. 2324-2328.

177. Yuguchi, Y., et al., *Structural observation of complexes of FGF-2 and regioselectively desulfated heparin in aqueous solutions.* Int J Biol Macromol, 2005. **35**(1-2): p. 19-25.

178. Lundin, L., et al., *Selectively desulfated heparin inhibits fibroblast growth factor-induced mitogenicity and angiogenesis.* J Biol Chem, 2000. **275**(32): p. 24653-60.

179. Chu, H., et al., *A [polycation:heparin] complex releases growth factors with enhanced bioactivity.* J Control Release, 2011. **150**(2): p. 157-63.

180. Gospodarowicz, D. and J. Cheng, *Heparin protects basic and acidic FGF from inactivation.* Journal of Cellular Physiology, 2005. **128**(3): p. 475-484.

181. Mori, Y., et al., *Preparation and characterization of low-molecular-weight heparin/protamine nanoparticles as FGF-2 carrier* Internation Journal of Medicine, 2010. **5**: p. 147-155.

182. Zomer Volpato, F., et al., *Preservation of FGF-2 bioactivity using heparin-based nanoparticles, and their delivery from electrospun chitosan fibers.* Acta Biomater, 2012. **8**(4): p. 1551-9.

183. Solchaga, L.A., et al., *Fibroblast frowth factor-2 enhances proliferation and delays loss of chondrogenic potential in human adult bone-marrow-derived mesenchymal stem cells.* Tissue Engineering: Part A, 2010. **16**: p. 1009-1019.

184. Zhuo, F.Y., et al., *Heparin-dependent fibroblast growth factor activities: Effects of defined heparin oligosaccharides.* European Journal of Cell Biology, 1997. **73**: p. 71-80.

185. Huegel, J., et al., *Heparanase stimulates chondrogenesis and is up-regulated in human ectopic cartilage: a mechanism possibly involved in hereditary multiple exostoses.* Am J Pathol, 2015. **185**(6): p. 1676-85.

186. Lee, J., et al., *Structural determinants of heparin–transforming growth factor-β1 interactions and their effects on signaling.* Glycobiology, 2015: p. 1-14.

187. Lee, M.J., *Heparin inhibits activation of latent transforming growth factor-β1.* Pharmacology, 2013. **92**(5-6): p. 238-244.

188. McCaffrey, T.A., D.J. Falcone, and B. Du, *Transforming growth factor-beta 1 is a heparin-binding protein: identification of putative heparin-binding regions and isolation of heparins with varying affinity for TGF-beta 1.* Journal of Cellular Physiology, 1992. **1152**(2): p. 430-440.

189. Burgess, W.H. and T. Maciag, *The heparin-binding (fibroblast) growth factor family of proteins.* Annual Review Biochemistry, 1989. **58**: p. 575-606.

190. Yaylon, A., et al., *Isolation of peptides that inhibit FGF to its receptor from random phage epitode library* PNAS, 1993. **90**: p. 10643-10647.

191. Hudalla, G.A., J.T. Koepsel, and W.L. Murphy, *Surfaces that sequester serum-borne heparin amplify growth factor activity.* Adv Mater, 2011. **23**(45): p. 5415-8.

192. Hudalla, G.A., et al., *Harnessing endogenous growth factor activity modulates stem cell behavior.* Integr Biol (Camb), 2011. **3**(8): p. 832-42.

193. Thompson, L.D., M.W. Pantoliano, and B.A. Springer, *Energetic characterization of the basic fibroblast growth factor-heparin interaction: Identification of the heparin binding domain.* Biochemistry, 1994. **33**: p. 3831-3840.

194. Koepsel, J.T., et al., *Combinatorial screening of chemically defined human mesenchymal stem cell culture substrates.* Journal of Material Chemistry, 2012. **22**(37): p. 19474-19481.

195. Hudalla, G.A. and W.L. Murphy, *Immobilization of peptides with distinct biological activities onto stem cell culture substrates using orthogonal chemistries.* Langmuir, 2010. **26**(9): p. 6449-56.

196. Tsurkan, M.V., et al., *Growth factor delivery from hydrogel particle aggregates to promote tubular regeneration after acute kidney injury.* J Control Release, 2013. **167**(3): p. 248-55.

197. Wu, J.M., et al., *Heparin-functionalized collagen matrices with controlled release of basic fibroblast growth factor.* J Mater Sci Mater Med, 2011. **22**(1): p. 107-14.

198. Zieris, A., et al., *Dual independent delivery of pro-angiogenic growth factors from starPEG-heparin hydrogels.* Journal of Controlled Release, 2011. **156**(1): p. 28-36.

199. Nakamura, S., et al., *Controlled release of fibroblast growth factor-2 from an injectable 6-O-desulfated heparin hydrogel and subsequent effect on in vivo vascularization.* J Biomed Mater Res A, 2006. **78**(2): p. 364-71.

200. Lim, J.J. and J.S. Temenoff, *The effect of desulfation of chondroitin sulfate on interactions with positively charged growth factors and upregulation of cartilaginous markers in encapsulated MSCs.* Biomaterials, 2013. **34**(21): p. 5007-18.

201. Bjornsson, T., D.E. Schneider, and A.R. Hetch, *Effect of N-desulfation and N-deactylation of heparin on its anticoagulant activity and in vivo disposition.* Journal of Pharmacology and Experimental Therapeutics, 1988. **245**(3): p. 804.

202. Freudenberg, U., et al., *Heparin desulfation modulates VEGF release and angiogenesis in diabetic wounds.* J Control Release, 2015. **220**(Pt A): p. 79-88.

203. Ai, H., S.A. Jones, and Y.M. Lvov, *Biomedical applications of electrostatic layer-by-layer nano-assembly of polymers, enzymes, and nanoparticles.* Cell Biochemistry and Biophysics, 2003. **39**.

204. Shu, Y., et al., *Layer by layer assembly of heparin/layered double hydroxide completely renewable ultrathin films with enhanced strength and blood compatibility.* Journal of Materials Chemistry, 2012. **22**(40): p. 21667.

205. Wang, H.G., et al., *Biofunctionalization of titanium surface with multilayer films modified by heparin-VEGF-fibronectin complex to improve endothelial cell proliferation and blood compatibility.* J Biomed Mater Res A, 2013. **101**(2): p. 413-20.

206. Meng, S., et al., *The effect of a layer-by-layer chitosan heparin coating on the endothelization and coagulation properties of a coronary stent system.* Biomaterials, 2009. **20**(12): p. 2276-2283.

207. Teramura, Y. and H. Iwata, *Cell surface modification with polymers for biomedical studies.* Soft Matter, 2010. **6**(6): p. 1081.

208. Seto, S.P., M.E. Casas, and J.S. Temenoff, *Differentiation of mesenchymal stem cells in heparin-containing hydrogels via coculture with osteoblasts.* Cell Tissue Res, 2012. **347**(3): p. 589-601.

209. Benoit, D.S., A.R. Durney, and K.S. Anseth, *The effect of heparin-functionalized PEG hydrogels on three-dimensional human mesenchymal stem cell osteogenic differentiation.* Biomaterials, 2007. **28**(1): p. 66-77.

210. Nie, T., et al., *Production of heparin-functionalized hydrogels for the development of responsive and controlled growth factor delivery systems.* J Control Release, 2007. **122**(3): p. 287-96.

211. N, Y., et al., *Growth factor mediated assembly of cell receptor-responsive hydrogels.* J Am Chem Soc, 2007. **129**(11): p. 3040-3041.

212. O, J., et al., *Affinity-based growth factor delivery using biodegradable, photocrosslinked heparin-alginate hydrogels.* Journal of Controlled Release, 2011. **154**: p. 158.

213. M, K., et al., *The use of de-differentiated chondrocytes delivered by a heparin-based hydrogel to regenerate cartilage in partial-thickness defects.* Biomaterials, 2011. **32**(31): p. 7883.

214. Baraniak, P.R., et al., *Stiffening of human mesenchymal stem cell spheroid microenvironments induced by incorporation of gelatin microparticles.* J Mech Behav Biomed Mater, 2012. **11**: p. 63-71.

215. Bratt-Leal, A.M., et al., *Incorporation of biomaterials in multicellular aggregates modulates pluripotent stem cell differentiation.* Biomaterials, 2011. **32**(1): p. 48-56.

216. Hettiaratchi, M.H., et al., *Heparin microparticle effects on presentation and bioactivity of bone morphogenetic protein-2.* Biomaterials, 2014. **35**(25): p. 7228-38.

217. Sarkar, D., et al., *Cell surface engineering of mesenchymal stem cells.* Methods Mol Biol, 2011. **698**: p. 505-23.

218. Sarkar, D., et al., *Engineered mesenchymal stem cells with self-assembled vesicles for systemic cell targeting.* Biomaterials, 2010. **31**(19): p. 5266-74.

219. Schmidt, R.C. and K.E. Healy, *Effect of avidin-like proteins and biotin modification on mesenchymal stem cell adhesion.* Biomaterials, 2013. **34**(15): p. 3758-62.

220. Wilson, J.T., W. Cui, and E.L. Chaikof, *Layer-by-layer assembly of a conformal nanothin PEG coating for intraportal islet transplantation.* Nano Letters, 2008. **8**(7): p. 1940-1948.

221. Teramura, Y. and H. Iwata, *Islets surface modification prevents blood-mediated inflammatory responses.* Bioconjug Chem, 2008. **19**: p. 1389-1395.

222. Teramura, Y. and H. Iwata, *Islet encapsulation with living cells for improvement of biocompatibility.* Biomaterials, 2009. **30**(12): p. 2270-5.

223. Teramura, Y., et al., *Behavior of synthetic polymers immobilized on a cell membrane.* Biomaterials, 2008. **29**(10): p. 1345-55.

224. Totani, T., Y. Teramura, and H. Iwata, *Immobilization of urokinase on the islet surface by amphiphilic poly(vinyl alcohol) that carries alkyl side chains.* Biomaterials, 2008. **29**(19): p. 2878-83.

225. Elbert, D.L., C.B. Herbert, and J.A. Hubbell, *Thin polymer layers formed by polyelectrolyte myltilayer tehcniques on biological surfaces.* Langmuir, 1999. **15**(5355-5362).

226. Krol, S., et al., *Multilayer nanoencapsulation. New approach for immune protection of human pancreatic islets.* Nanoletters, 2006. **6**(9): p. 1933-1939.

227. Germain, M., et al., *Protection of mammalian cell used in biosensors by coating with a polyelectrolyte shell.* Biosens Bioelectron, 2006. **21**(8): p. 1566-73.

228. Veerabadran, N.G., et al., *Nanoencapsulation of stem cells within polyelectrolyte multilayer shells.* Macromol Biosci, 2007. **7**(7): p. 877-82.

229. Cabric, S., et al., *Anchoring of vascular endothelial growth factor to surface-immobilized heparin on pancreatic islets: Implications for stimulating islet angiogenesis.* Tissue Engineering: Part A, 2010. **16**(3): p. 961-970.

230. Cabric, S., et al., *Islet surface heparinization prevents the instant blood-mediated inflammatory reaction in islet transplantation.* Diabetes, 2007. **56**(8): p. 2008-15.

231. Wilson, J.T., et al., *Cell surface engineering with polyelectrolyte multilayer thin films.* J Am Chem Soc, 2011. **133**(18): p. 7054-64.

232. Wilson, J.T., et al., *Biomolecular surface engineering of pancreatic islets with thrombomodulin.* Acta Biomater, 2010. **6**(6): p. 1895-903.

233. Murua, A., et al., *Cell microencapsulation technology: towards clinical application.* J Control Release, 2008. **132**(2): p. 76-83.

234. Wilson, J.T., et al., *Biomolecular surface engineering of pancreatic islets with thrombomodulin.* Acta Biomaterialia, 2010. **6**(6): p. 1895-903.

235. Papadopoulou, A., et al., *Mesenchymal stem cells are conditionally therapeutic in preclinical models of rheumatoid arthritis.* Annals of the Rheumatic Diseases, 2012. **71**(10): p. 1733-40.

236. Li, W.J., et al., *Multilineage differentiation of human mesenchymal stem cells in a three-dimensional nanofibrous scaffold.* Biomaterials, 2005. **26**: p. 25.

237. Grad, S., et al., *The use of biodegradable polyurethane scaffolds for cartilage tissue engineering: potential and limitations.* Biomaterials, 2003. **24**(28): p. 5163-5171.

238. Farell, E., et al., *A collagen-glycosaminoglycan scaffold supports adult rat mesenchymal stme cell differentiation along osteogenic and chondrogenic routes.* Tissue Engineering, 2006. **12**(3): p. 459-468.

239. Lin, C.C. and K.S. Anseth, *PEG hydrogels for the controlled release of biomolecules in regenerative medicine.* Pharm Res, 2009. **26**(3): p. 631-43.

240. Williams, C.G., et al., *In vitro chondrogenesis of bone marrow-derived mesenchymal stem cells in a photopolymerizing hydrogel.* Tissue Engineering, 2004. **9**(4).

241. Salinas, C.N. and K.S. Anseth, *Mesenchymal stem cells for craniofacial tissue gegeneration: Designing hydrogel delivery vehicles.* Journal of Dental Research, 2009. **88**(8): p. 681-692.

242. Cool, S.M. and V. Nurcombe, *Heparan sulfate regulation of progenitor cell fate.* Journal of Cellular Biochemistry, 2006. **99**(4): p. 1040-51.

243. Benoit, D.S. and K.S. Anseth, *Heparin functionalized PEG gels that modulate protein adsorption for hMSC adhesion and differentiation.* Acta Biomater, 2005. **1**(4): p. 461-70.

244. Capila, I. and R.J. Linhardt, *Heparin and protein interactions.* Angewandte Chemie International Edition, 2002. **41**: p. 390-412.

245. Liang, Y. and K.L. Kiick, *Heparin-functionalized polymeric biomaterials in tissue engineering and drug delivery applications.* Acta Biomaterialia, 2013.

246. Hammond, P.T., *Form and function in multilayer asembly: New applications at the nanscale* Advance Materials, 2004. **16**(15): p. 1271-1293.

247. Kinnane, C.R., et al., *Low-fouling poly(n-vinyl pyrrolidone) capsules with engineered degradabe properties.* Biomacromolecules, 2009. **10**: p. 2839-2846.

248. Quinn, J.F., et al., *Next generation, sequentially assembled ultrathin films: beyond electrostatics.* Chem Soc Rev, 2007. **36**(5): p. 707-18.

249. Bratt-Leal, A.M., et al., *A microparticle approach to morphogen delivery within pluripotent stem cell aggregates.* Biomaterials, 2013. **34**(30): p. 7227-35.

250. McLane, L.T., et al., *Spatial organization and mechanical properties of the pericellular matrix on chondrocytes.* Biophysical Journal, 2013. **104**(5): p. 986-96.

251. Tanaka, F., et al., *Exogenous administration of mesenchymal stem cells ameliorates dextran sulfate sodium-induced colitis via anti-inflammatory action in damaged tissue in rats.* Life Sciences, 2008. **83**(23-24): p. 771-9.

252. Ylostalo, J., et al., *Human mesenchymal stem/stromal cells cultured as spheroids are self-activated to produce prostaglandin E2 that directs stimulated macrophages into an anti-inflammatory phenotype.* Stem Cells, 2012. **30**(10): p. 2283-2296.

253. Cohen, M., et al., *Organization and adhesive properties of the hyaluronan pericellular coat of chondrocytes and epithelial cells.* Biophysical Journal, 2003. **85**: p. 1996-2005.

254. Knudson, W. and C.B. Knudson, *Assembly of a chondrocyte-like pericellular matrix on non-chondrogenic cells.* Journal of Cell Science, 1991. **99**: p. 227-235.

255. Abe, M., et al., *An assay for transforming growth factor-beta using cells transfected with a plasminogen activator inhibitor-1 promoter-luciferase construct.* Analytical Biochemistry, 1994. **216**: p. 276-284.

256. Pavlov, G., et al., *Conformation of heparin studied with macromolecular hydrodynamic methods and X-ray scattering.* European Biophysics Journal, 2003. **32**(5): p. 437-49.

257. Miller, T., et al., *Molecular engineering of glycosaminoglycan chemistry for biomolecule delivery.* Acta Biomater, 2013.

258. Goldberg, F.L. and B.P. Toole, *Pericellular coat of chick embryo chondrocytes: Structural role of Hyaluronate* The Journal of Cell Biology, 1984. **99**: p. 2114-2122.

259. Rilla, K., et al., *Pericellular hyaluronan coat visualized in live cells with a fluorescent probe is scaffolded by plasma membrane protrusions.* Journal of Histochemistry & Cytochemistry, 2008. **56**(10): p. 901-10.

260. Amelia, B., et al., *Mesenchymal stem cells suppress lymphocyte proliferation in vitro and prolong skin graft survival in vivo.* Experimental Hematology, 2002. **30**: p. 42-48.

261. Bartosh, T.J., et al., *Dynamic compaction of human mesenchymal stem/precursor cells (MSC) into spheres self-activates caspase-dependent IL1 signaling to*

enhance secretion of modulators of inflammation and immunity (PGE2, TSG6 and STC1). Stem Cells, 2013.

262. Lee, T.H., H.G. Wisniewski, and J. Vilcek, *A novel secretory tumor necrosis factor-inducible protein (TGS-6) is a member of the family of hyaluronate binding proteins, closely related to the adhesion receptor CD44.* The Journal of Cell Biology, 1992. **116**(2): p. 545-557.

263. Kalinski, P., *Regulation of immune responses by prostaglandin E2.* J Immunol, 2012. **188**(1): p. 21-8.

264. Kanellis, J., et al., *Stanniocalcin-1, an inhibitor of macrophage chemotaxis and chemokinesis.* Am J Physiol Renal Physiol, 2004. **286**(F356-F362).

265. Gorski, A., et al., *Immunomodulating activity of heparin.* FASEB J, 1991. **5**: p. 2287-2291.

266. Young, E., *The anti-inflammatory effects of heparin and related compounds.* Thrombosis Research, 2008. **122**(6): p. 743-52.

267. Hochart, H., et al., *Low-molecular weight and unfractionated heparins induce a downregulation of inflammation: decreased levels of proinflammatory cytokines and nuclear factor-kappaB in LPS-stimulated human monocytes.* British Journal of Haematology, 2006. **133**(1): p. 62-7.

268. Amatayakul-Chantler, S., et al., *Transforming growth factor-b1: Selective biological activity and receptor binding in mink lung epithelial cells.* The Journal of Biological Chemistry, 1994. **269**(44): p. 27687-27691.

269. Balamurugan, K., A. Ortiz, and H.M. Said, *Biotin uptake by human intestinal and liver epithelial cells: role of the SMVT system.* American Journal of Physiology-Gastrointestinal and Liver Physiology, 2003. **285**(1): p. G73-7.

270. Said, H.M., et al., *Biotin uptake by human colonic epithelial NCM460 cells: A carrier-mediated process shared with panththenic acid.* American Journal of Physiology-Cell Physiology, 1998. **275**: p. 1365-1371.

271. Bramono, D.S., et al., *Bone marrow-derived heparan sulfate potentiates the osteogenic activity of bone morphogenetic protein-2 (BMP-2).* Bone, 2012. **50**(4): p. 954-64.

272. Mitsi, M., et al., *A catalytic role of heparin within the extracellular matrix.* The Journal of Biological Chemistry, 2008. **283**(50): p. 34796-807.

273. Kottakis, F., et al., *FGF-2 regulates cell proliferation, migration, and angiogenesis through an NDY1/KDM2B-miR-101-EZH2 pathway.* Mol Cell, 2011. **43**(2): p. 285-98.

274. Tsutsumi, S., et al., *Retention of multilineage differentiation potential of mesenchymal cells during proliferation in response to FGF.* Biochem Biophys Res Commun, 2001. **288**(2): p. 413-9.

275. Grazul-Bilska, A., et al., *Effects of basic fibroblast growth factor (FGF-2) on proliferation of human skin fibroblasts in type II diabetes mellitus.* Exp Clin Endocrinol Diabetes, 2002. **110**(4): p. 176-181.

276. Romo, P., et al., *Differential effects of TGF-beta and FGF-2 on in vitro proliferation and migration of primate retinal endothelial and Muller cells.* Acta Ophthalmol, 2011. **89**(3): p. e263-8.

277. Carlsberg, A., et al., *Efficient chondrogenic differentiation of mesenchymal cells in micromass culture by retroviral gene transfer of BMP-2.* Differentiation, 2000. **67**: p. 128-138.

278. Hortensius, R.A., et al., *The effect of glycosaminoglycan content on polyethylenimine-based gene delivery within three-dimensional collagen-GAG scaffolds.* Biomater Sci, 2015. **3**(4): p. 645-54.

279. Lei, J., et al., *Characterization of a multilayer heparin coating for biomolecule presentation to human mesenchymal stem cell spheroids.* Biomater Sci, 2014. **2**(5): p. 666-673.

280. Bellosta, P., et al., *Identification of Receptor and Heparin Binding Sites in Fibroblast Growth Factor 4 by Structure-Based Mutagenesis.* Molecular and Cellular Biology, 2001. **21**(17): p. 5946-5957.

281. Zieris, A., et al., *FGF-2 and VEGF functionalization of starPEG-heparin hydrogels to modulate biomolecular and physical cues of angiogenesis.* Biomaterials, 2010. **31**(31): p. 7985-94.

282. Orth, P., et al., *Current perspectives in stem cell research for knee cartilage repair.* Stem Cells Cloning, 2014. **7**: p. 1-17.

283. Lodish, H., *Post-translational modification of proteins.* Enzyme and Microbial Technology, 1981. **3**(3): p. 178-188.

284. Aigner, T., et al., *SOX9 expression does not correlate with type II collagen expression in adult articular chondrocytes.* Matrix Biology, 2003. **22**(4): p. 363-372.

285. Akiyama, H., *Control of chondrogenesis by the transcription factor Sox9.* Modern Rheumatology, 2008. **18**(3): p. 213-219.

286. Marlovits, S., et al., *Changes in the ratio of type-I and type-II collagen expression during monolayer culture of human chondrocytes.* Journal of Bone and Joint Surgery, 2004. **86**(B): p. 286-295.

287. Steinmetz, N. and S. Bryant, *Chondroitin sulfate and dynamic loading alter chondrogenesis of human MSCs in PEG hydrogels.* Biotechnology and Bioengineering, 2012. **109**(10): p. 2671-2682.

288. Fischer, J., et al., *Intermittent PTHrP(1-34) exposure augments chondrogenesis and reduces hypertrophy of mesenchymal stromal cells.* Stem Cells Dev, 2014. **23**(20): p. 2513-23.

289. Bourguignon, L.Y., et al., *Hyaluronan promotes signaling interaction between CD44 and the transforming growth factor beta receptor I in metastatic breast tumor cells.* J Biol Chem, 2002. **277**(42): p. 39703-12.

290. Hascall, V. and J.D. Esko, *Hyaluronan*, in *Essentials of Glycobiology*, R.D. Cummings and J.D. Esko, Editors. 2009, Cold Spring Harbor Laboratory Press: Cold Spring Harbor, NY.

291. Lo, Y.L., et al., *Chemically conjugating polyethylenimine with chondroitin sulfate to promote CD44-mediated endocytosis for gene delivery.* Mol Pharm, 2013. **10**(2): p. 664-76.

292. Bertram, K. and R. Krawetz, *Osmolarity regulates chondrogenic differentiation potential of synovial fluid derived mesenchymal progenitor cells.* Biochem Biophys Res Commun, 2012. **422**(3): p. 455-461.

293. Caron, M., et al., *Osmolarity determines the in vitro chondrogenic differentiation capacity of progenitor cells via nuclear factor of activated T-cells 5.* Bone, 2013. **53**(1): p. 94-102.

294. Morrison, S.J. and D.T. Scadden, *The bone marrow niche for haematopoietic stem cells.* Nature, 2014. **505**(7483): p. 327-34.

295. Walenda, T., et al., *Co-culture with mesenchymal stromal cells increases proliferation and maintenance of haematopoietic progenitor cells.* J Cell Mol Med, 2010. **14**(1-2): p. 337-50.

296. Bhatia, S.N., et al., *Microfabrication of hepatocyte/fibroblast co-cultures: role of homotypic cell interactions.* Biotechnol Prog, 1998. **14**(3): p. 378-87.

297. Anselme, K. and M. Bigerelle, *Modelling approach in cell/material interaction studies.* Biomaterials, 2006. **27**: p. 1187-1199.

298. Bigerelle, M. and K. Anselme, *Bootstrap analysis of the relation between initial adhesive events and long-term cellular functions of human osteoblasts cultured on biocompatible metallic substrates.* Acta Biomaterialia, 2005. **1**: p. 499-510.

299. Carpenedo, R., C. Sargent, and T. McDevitt, *Rotary suspension culture enhances the efficiency, yield, and homogeneity of embryoid body differentiation.* Stem Cells, 2007. **25**(9): p. 2224-2234.

300. Sargent, C., et al., *Hydrodynamic modulation of embryonic stem cell differentiation by rotary orbital suspension culture.* Biotechnology and Bioengineering, 2010. **105**(3): p. 611-626.

301. Lanner, F. and J. Rossant, *The role of FGF/Erk signaling in pluripotent cells.* Development, 2010. **137**(20): p. 3351-60.

302. Danisovic, L., I. Varga, and S. Polak, *Growth factors and chondrogenic differentiation of mesenchymal stem cells.* Tissue and Cell, 2012. **44**(2): p. 69-73.

303. Chen, W.C., et al., *Controlled dual delivery of fibroblast growth factor-2 and Interleukin-10 by heparin-based coacervate synergistically enhances ischemic heart repair.* Biomaterials, 2015. **72**: p. 138-51.

304. Scott, D., et al., *Immunogenicity of biotinylated Hapten-Avidin complexes* Molecular Immunology, 1994. **21**(11): p. 1055-1060.

305. Kim, J.C. and G. Tae, *The modulation of biodistribution of stem cells by anchoring lipid-conjugated heparin on the cell surface.* J Control Release, 2015. **217**: p. 128-37.

306. Lee, D., et al., *Highly poly(ethylene) glycolylated islets improve long-term islet allograft survival without immunosuppressive medication.* Tissue Engineering, 2007. **13**(8): p. 2133-2141.

307. Jang, J.Y., et al., *Immune reactions of lymphocytes and macrophages against PEG-grafted pancreatic islets.* Biomaterials, 2004. **25**(17): p. 3663-9.

308. Miura, S., Y. Teramura, and H. Iwata, *Encapsulation of islets with ultra-thin polyion complex membrane through poly(ethylene glycol)-phospholipids anchored to cell membrane.* Biomaterials, 2006. **27**(34): p. 5828-35.

309. Tatsumi, K., et al., *The non-invasive cell surface modification of hepatocytes with PEG-lipid derivatives.* Biomaterials, 2012. **33**(3): p. 821-8.

310. Teramura, Y., Y. Kaneda, and H. Iwata, *Islet-encapsulation in ultra-thin layer-by-layer membranes of poly(vinyl alcohol) anchored to poly(ethylene glycol)-lipids in the cell membrane.* Biomaterials, 2007. **28**(32): p. 4818-25.

311. Li, N., *Platelet-lymphocyte cross-talk.* Journal of Leukocyte Biology, 2008. **83**(5): p. 1069-1078.

312. Marquardt, L., et al., *Leukocyte-Platelet Aggregates in Acute and Subacute Ischemic Stroke.* Cerebrovascular Diseases, 2009. **28**: p. 276-282.

313. Petruzzelli, L., L. Maduzia, and T.A. Springer, *Differential requirements for LFA-1 binding to ICAM-1 and LFA-1-mediated cella ggregation.* The Journal of Immunology, 1998. **160**: p. 4208-4216.

314. Hammerschmidt, D.E., et al., *Lymphocyte aggregation in response to adrenergic stimulation.* Blood, 1988. **71**(5): p. 1470-1774.

315. Bednarczyk, J.L. and B.W. McIntyre, *A monoclonal antibody to VLA-4 alpha-chain (CDw49d) induces homotypic lymphocyte aggregation.* The Journal of Immunology, 1990. **144**(3): p. 777-784.

316. Kasuya, J., et al., *Reconstruction of hepatic stellate cell-incorporated liver capillary structures in small hepatocyte tri-culture using microporous membranes.* J Tissue Eng Regen Med, 2015. **9**(3): p. 247-56.

317. Mironov, V., N. Reis, and B. Derby, *Bioprinting: A Beginning.* Tissue Engineering 2006. **12**(4): p. 631-634.

318. Jakab, K., et al., *Tissue engineering by self-assembly and bio-printing of living cells.* Biofabrication, 2010. **2**(2): p. 022001.

319. Guillotin, B., et al., *Laser assisted bioprinting of engineered tissue with high cell density and microscale organization.* Biomaterials, 2010. **31**(28): p. 7250-6.

320. Mironov, V., G. Prestwich, and G. Forgacs, *Bioprinting living structures.* Journal of Materials Chemistry, 2007. **17**(20): p. 2054.

321. Lee, V., et al., *Design and fabrication of human skin by three-dimensional bioprinting.* Tissue Engineering: Part C, 2014. **20**(6): p. 473-484.

322. Murphy, S. and A. Atala, *3D bioprinting of tissues and organs.* Nature Biotechnology, 2014. **32**: p. 773-785.

323. Norotte, C., et al., *Scaffold-free vascular tissue engineering using bioprinting.* Biomaterials, 2009. **30**(30): p. 5910-7.

324. Lozito, T., et al., *Three-dimensional osteochondral microtissue to model pathogenesis of osteoarthritis* Stem Cell Research and Therapy, 2013. **4**(1): p. 56.

325. Bello, J., *Tight packing of protein cores and interfaces.* International Journal of Peptide and Protein Research, 1978. **12**(1): p. 38-41.

326. Ge, J., et al., *The size of mesenchymal stem cells is a significant cause of vascular obstructions and stroke.* Stem Cell Reviews, 2014. **10**(2): p. 295-303.

327. Pavlov, G., et al., *Conformation of heparin studied with macromolecular hydrodynamic methods and X-ray scattering.* Eur Biophys J, 2003. **32**(5): p. 437-49.

328. Hirsh, J., et al., *Heparin and low-molecular weight heparin: Mechanisms of action, pharmacokinetics, dosing, monitoring, efficacy and safety* CHEST, 2001. **119**(64S-94S).

329. Gatti, G., et al., *Studies on the conformation of heparin by 1H and 13C NMR spectroscopy.* Macromolecules, 1979. **12**(5): p. 1001-1007.